UNI
BASEL

Synthesis and investigations of
(6-hydroxy-3-oxo-3*H*-xanthen-9-yl)methyl derivatives.
A new photoremovable protecting group

Inauguraldissertation

zur

Erlangung der Würde eines

Doktors der Philosophie

vorgelegt der

Philosophisch-Naturwissenschaftlichen Fakultät

der Universität Basel

von

Dipl. - Ing. Wintner Jürgen

aus Laakirchen (Österreich)

Basel, 2007

Genehmigt von der Philosophischen-Naturwissenschaftlichen Fakultät der Universität Basel auf Antrag der Herren

Prof. Dr. Bernd Giese

Prof. Dr. Hans-Jakob Wirz

Basel, den 27.03.2007

Prof. Dr. Hans-Peter Hauri
(Dekan)

Dedicated to my parents

Acknowledgments

I declare that I wrote this thesis "Synthesis and investigations of (6-hydroxy-3-oxo-3*H*-xanthen-9-yl)methyl derivatives. A new photoremovable protecting group" with help indicated and only handed it in to the faculty of science of the University of Basel and no other faculty and no other university.

Basel, 27.03.2007   Dipl. - Ing. Wintner Jürgen

The work presented here was initiated and supervised by Prof. Dr. Hans-Jakob Wirz at the Chemistry Department of the University of Basel.

Like all things of the mind, science is a brittle thing: it becomes absurd when you look at it too closely. It is designed for few at a time, not as a mass profession. But now we have megascience: an immense apparatus discharging in a minute more bursts of knowledge than humanity is able to assimilate in a lifetime. Each of us has two eyes, two ears, and, I hope one brain. We cannot even listen to two symphonies at the same time. How do we get out of the horrible cacophony that assails our minds day and night? We have to learn, as others did, that if science is a machine to make more science, a machine to grind out so-called facts of nature, not all facts are equally worth knowing. Students, in other words, will have to learn to forget most of what they have learned. This process of forgetting must begin after each exam, but never before. The Ph.D. is essentially a license to start unlearning.

Erwin Chargaff 1905-2002

A thesis has to presentable…but don't attach too much importance to it. If you do succeed in the sciences, you will do later on better things and then it will be of little moment, if you don't succeed in the sciences, it doesn't matter at all.

Paul Ehrenfest 1880-1933

Table of Contents

1. Introduction

1.1. Protecting Groups

The chemistry of protecting groups plays an important role in organic chemistry. As chemical applications become more sophisticated, it is essential to have maximum control and selectivity in chemical reactions. Protecting groups permit such selectivity in organic molecules having more than one functionality (Figure 1). During a synthetic sequence, most of these functionalities must be blocked and released when a selective chemical manipulation needs to be performed. The choice of a set of protecting groups[1, 2] is one of the important factors in the successful synthesis of a target compound, and the following issues need to be considered. The reaction conditions required to introduce a protecting group should be compatible with the other functionalities in the molecule. A protecting group must be stable under all the conditions used during subsequent synthetic steps and must be capable of being cleaved under mild conditions in a highly selective manner and high yield. The selective removal of protective groups is accomplished by chemical, electrolytic or photolytic methods.
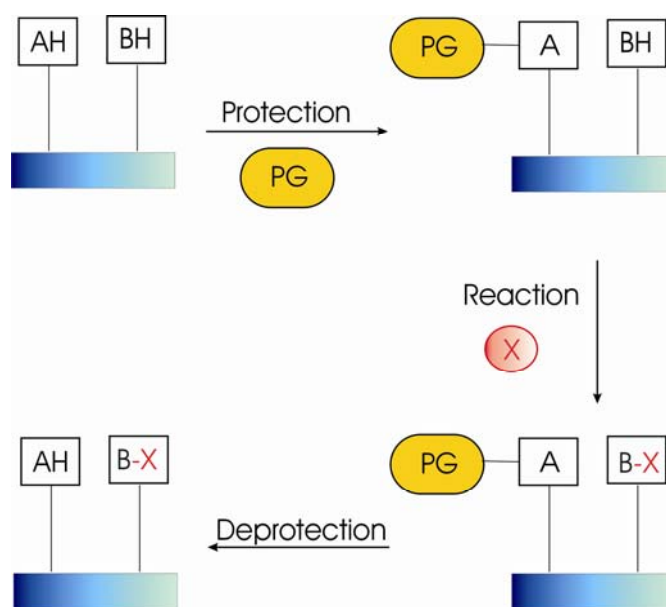
Scheme

Figure 1: Protecting groups (PG) in organic synthesis

Moreover, a protecting group should be easily available and cheap and it should keep in mind that some protecting groups may influence the reactivity of other functionalities. Protecting groups can be distinguished as either permanent or temporary. Persistent protecting groups are used to block reactive sites that do not need functionalisation and so are present during the synthesis. Ideally, all permanent protecting groups will be removed at the end of a synthetic sequence in one chemical step. Some functional groups need to be protected in such a way that they can be made available for derivatisation at some point in a synthesis. These functionalities are typically protected with temporary protecting groups.

1.2. Photoremovable Protecting Groups

A photoremovable protecting group (PPG) functions much as any other protecting group, except that its release step is triggered by irradiation with light. Thos offers more control and specificity as the light beam can be turned on and off as desired (temporal control) and light can be directed at particular sites (spatial control). Furthermore the energy of the beam can be modified by using light of different wavelengths. There is the additional advantage of mild and neutral reaction conditions. Traditional protecting groups usually require rigorous acidic or basic conditions for their removal which restricts their application to robust molecules. For more sensitive compounds photoremovable protecting groups provide an attractive alternative.

The first report of a successful development of a photoremovable protecting group dates back to 1962, where Barltrop and Schofield[3] observed that benzyloxycarbonylglycine is readily converted to the free amino acid by irradiation with light of 254 nm in basic solution (Scheme 1).
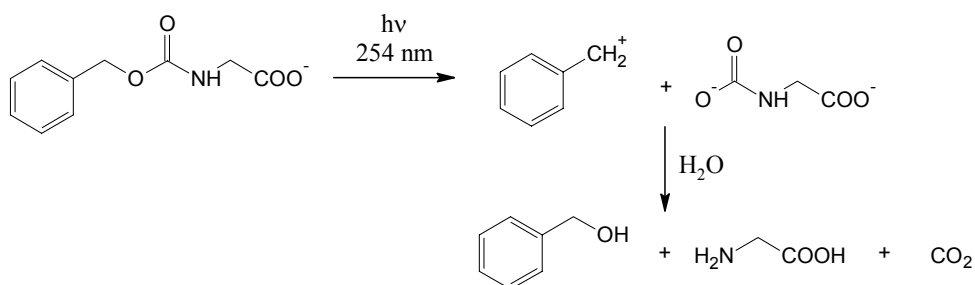
Scheme 1: Photoremoval of the benzyloxycarbonyl group

Since that time, diverse PPGs have been developed for different functional groups and for miscellaneous requirements and applications. Several terms can be found in the literature for PPGs like "caging group" and "photolabile protecting group". They are synonyms for all practical purposes, because the main difference is the intention behind the photorelease. The term "caging" which originated with caged ATP, was coined in 1978 by J. F. Kaplan *et al.*[4] to describe photosensitive precursors in which the effectors are normally rendered inert via a covalent bond to the photoremovable protecting group. Photochemical cleavage of this bond unleashes the active species rapidly. Unfortunately the term "cage" is not unproblematic for several reasons. Unless a person is already knowledgeable in the field it will inevitably think that the molecules in question are in fact inside of a cage in the topological sense. The PPGs have led to recent advances in areas and technologies as diverse as organic synthesis, photoactive precursors of neurotransmitters, photolabile calcium chelators and time-resolved studies in disciplines ranging from cell biology to x-ray crystallography. PPGs are also key to the novel techniques of light-directed synthesis. Since the beginnings over 30 years ago the field has been reviewed quite a few times, covering a wide range of applications in biology and related fields[5-13] and also dedicated to synthetic[1,2,14,15] and mechanistic aspects[5,15].

The following criteria have to be considered for the design of new photoremovable protecting group:

- Generally, the photoreaction should be clean, occur with sufficiently high quantum yield Φ and with fast kinetics to ensure that the caged molecule is rapidly released.

- The chromophore should absorb light strongly (that is, with a high extinction coefficient ε) above 340 nm in order to avoid cell damage.

- The by-products of the photorelease should be biologically inert and should not absorb light at the wavelength of irradiation of the PPGs in order to avoid competitive absorption of the incident light.

- The caged compound should be soluble in the media that are required for the specific application. For biological systems this is mostly water or buffered aqueous solutions, pH~7.

- The PPG should be attached to the substrate easily, quickly, in high yields and with readily separated by-products

- The PPG should not generate any stereogenic centres upon photolysis.

Currently, there is no PPG that satisfies all of these requirements in an ideal sense. In fact it is doubtful that any one "universal" PPG will be discovered. Nevertheless several PPGs have been demonstrated to be effective in several applications, but at the same time the number of available PPGs is still small.

The properties and photochemistry of these PPGs will be discussed in detail in the following sections.

1.2.1. The 2-Nitrobenzyl Group (2-NB)

In 1966 Barltrop *et al.*[16] reported the release of benzoic acid from its nitrobenzyl ester upon photolysis (Scheme 2). Since then, the 2-nitrobenzyl group with all its derivatives (Figure 2) has found a variety of applications in biology and is by now the most commonly applied photolabile protecting group, but it has a few shortcomings.

R´ = H, Ph or

2-C$_6$H$_5$NO$_2$
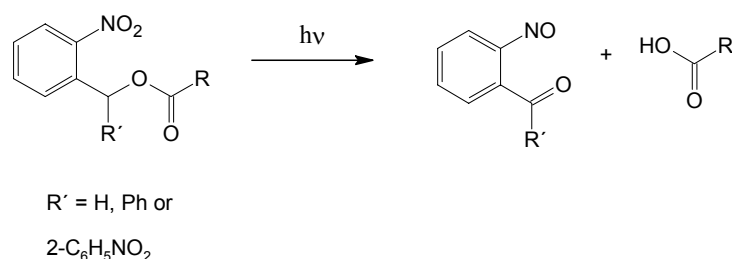
Scheme 2: Photoremoval from the 2-nitrobenzyl group

First, a reactive *o*-nitrosoaldehyde is formed as by-product of the photolysis reaction which can be harmful, e.g. in a biological environment[5,17]. Furthermore, the 2-nitrosoaldehyde forms a secondary photoproduct, the azobenzene-2,2´-dicarboxylic acid which absorbs even more in the same region as 2-nitrobenzyl group (2-NB) and thus acts as internal light filter (Scheme 3). Second, after the initial photochemical excitation, the molecule undergoes a series of steps before the bioactive substrate is released. This makes the 2-nitrobenzyl group inapt for studying reactions that occur on the sub-millisecond time scale. The rate of release varies depending on many factors (the leaving group ability, nature of substituent R, pH and solvent) and in aqueous solution it is slowest around physiological pH values. Third, short-wavelength UV light is required for deprotection.
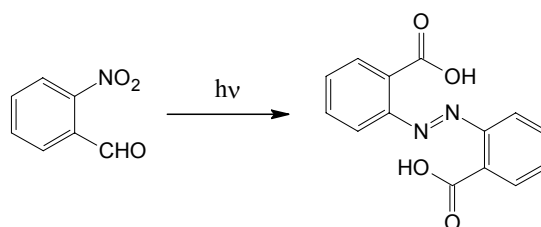
Scheme 3: Formation of secondary photoproduct

It seems that the popularity of the 2-NB is due to several advantages such as ease of protection and removal, quantitative yields upon deprotection and the use of light above 320 nm for deprotection, at which even the most light-sensitive amino acid, tryptophan is unaffected.

The mechanism of the 2-NB group can be divided into five major steps (Scheme 4): excitation, photoredox to the aci-nitro intermediate, cyclization to the benzisoxazole, ring-opening to the hemiacetal, and collapse of the hemiacetal with release of the substrate.
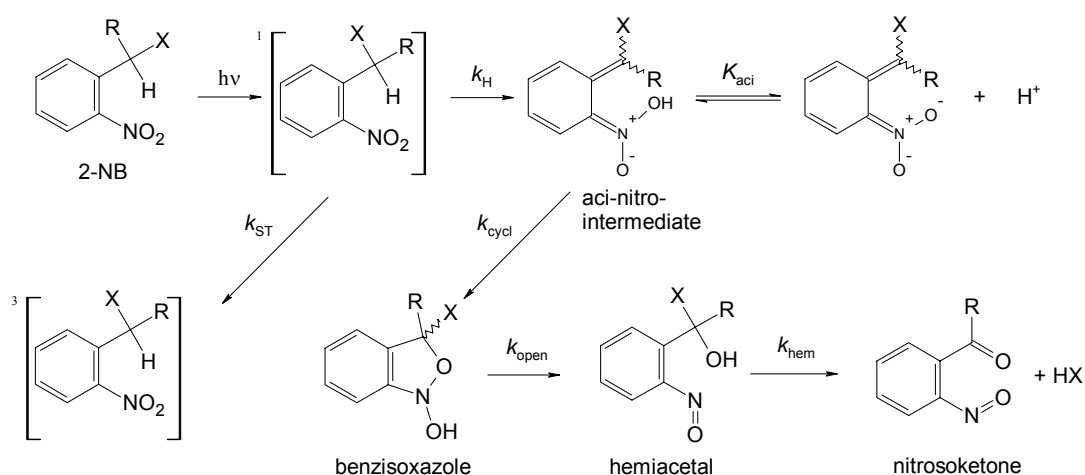
Scheme 4: Reaction mechanism of the 2-nitrobenzyl group

Upon absorption of a photon the 2-NB is excited to the singlet state where it can either go through intersystem crossing to the triplet excited state (k_{ST}) or undergo intramolecular hydrogen abstraction (k_H). Presumably both the triplet and the singlet excited state could undergo photoredox hydrogen abstraction. It is generally assumed that the rate constants of the hydrogen abstraction (k_H) are rapid enough to be competitive with the singlet-triplet crossing rate constants (k_{ST}). The [1,5]-shift of hydrogen to oxygen results in the formation of an aci-nitro intermediate, which is stable enough to be detected by laser-flash photolysis (LFP). The decay of the transient was often assumed to be the rate of release of HX.

Wirz *et al.*[17] has shown that the *E,E*-aci nitro isomer cyclises directly to benzisoxazole, which does not absorb in the near UV-VIS and its presence, was discovered mainly by time-resolved infrared spectroscopy (TRIR). The decay of benzisoxazole generates new signals in the IR spectrum, which were attributed to the hemiacetal. Its IR spectrum shows a strong nitroso absorption band but no signal for a carbonyl group. In the last step, the signal of the carbonyl group absorption appears, which establishes the hydrolysis of the hemi-acetal to the nitrosobenzaldehyde and the release rate of the substrate **X**. This seems to be one reliable measure for the release rates of the members of the 2-NB group. Corrie *et al.* [18] determined the rate of release of 1-(2-nitrophenyl)ethyl sulphate (caged sulphate) by time-resolved absorbance and photoacoustic methods and Trentham *et al.*[19] of 2-NB caged ATP by monitoring the kinetics of ATP-induced dissociation of actomyosin, a reaction of known kinetic characteristics.

Quite a few modifications of the 2-NB group were developed to improve its usability. The nitrophenylethyl (NPE) group (**A**, R = Me) can be deprotected and results in the formation of a nitrosoketone. On the other hand, a new stereogenic centre is introduced in the caged molecule. The wavelength of the absorption can be tuned, for instance, by introducing of dimethoxy substituents (DMNB)[20]. Bochet *et al.*[21] developed a variant for the protection of carbonyl groups **B**. Another modification which traps the resulting nitroso species in an intramolecular hetero Diels–Alder reaction **C** was introduced by Pirrung and co-workers[22]. Pfleiderer *et al.*[21] established an interesting alternative, the 2-(2-nitrophenyl)propyl group (NPP) **D** which upon irradiation yields a less harmful nitrostyryl species.
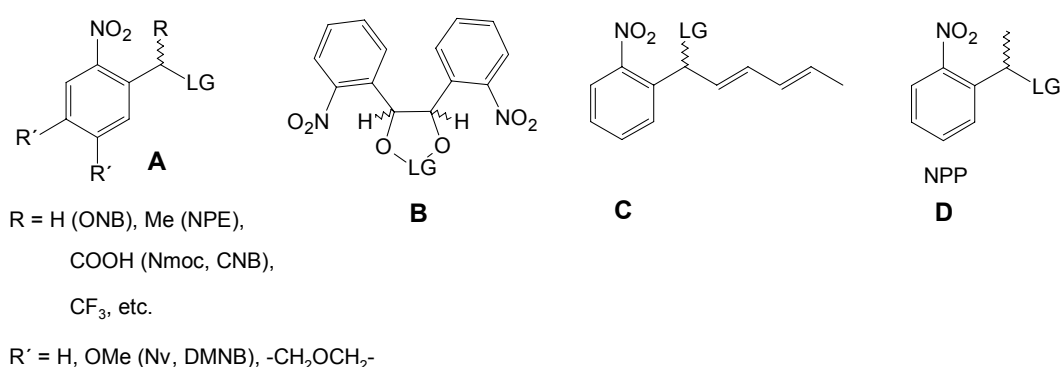
Figure 2: Several variants of the 2-nitrobenzyl group.
(LG = Leaving group, in some cases this includes a carbonate or carbamate linker)

1.2.2. The Benzoin Group (Bnz, Desyl)

Sheehan *et al.*[23] introduced the benzoin group as PPG for carboxylic acids in 1971. They discovered that irradiation of benzoin esters results in a photocyclization reaction yielding the free acids and 2-phenylbenzofuran. The reaction was found to be highly dependent on the nature and position of ring substituents, with methoxy groups providing the best yields. Optimum results were achieved with 3',5'-dimethoxybenzoin (DMB) esters (Scheme 5).

R = H, OMe (DMB)
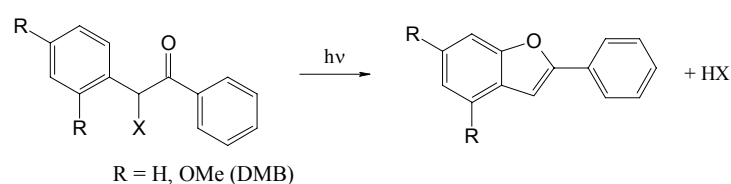
Scheme 5: Photoremoval from the benzoin group

The advantages of the benzoin PPG are high chemical and quantum yields. Furthermore rapid release rates, which makes benzoin cages ideal phototriggers for fast reactions and formation of a benzofuran by-product (Scheme 5), which is apolar and inert and thus easily separated from polar or acidic components. Its maximum absorption centred on 300 nm allows efficient irradiation.

Various research groups proposed different mechanisms for the deprotection of the benzoin protecting group. It was shown that substituents on the aromatic ring, the nature of the leaving group, and the solvent all exert an influence on the mechanism as well as on the deprotection yields of the benzoin cage. Sheehan *et al.*[23] proposed for the 3′,5′-DMB ester a Paterno-Büchi reaction forming a strained oxetane intermediate, which undergoes ring opening and loss of the acetate leaving group to give the benzofuran. Shi *et al.*[24] performed nanosecond laser flash photolysis (LFP) studies of various 3',5'-dimethoxy benzoin esters and proposed a singlet mechanism involving interaction of the dimethoxybenzene ring with the singlet n, π^* excited state of acetophenone via a singlet exciplex. They observed a short-lived cyclohexadienyl cation intermediate as the precursor to the benzofuran product. One of the major shortcomings of benzoin cages is their poor solubility. Rock *et al.*[25] developed a water soluble cage based on 3',5'-DMB esters. They improved the solubility by the introduction of carboxymethoxy functionalities into the DMB group to give 3',5'-bis(carboxymethoxy)benzoin (BCMB, Scheme 5, R = -OCH$_2$-COOH) acetate. They observed that release of the acetate leaving group was accompanied

by formation of BCMB as the major photoproduct in lieu of benzofuran. To interpret this result, they proposed a mechanism involving a biradical intermediate which undergoes an acetoxy migration to give a cyclic intermediate which can undergo attack by water to give BCMB or rearomatize to give benzofuran.

Rajesh, Givens and Wirz[26] provided information on the mechanism of phosphate photorelease from unsubstituted benzoin diethyl phosphate (Scheme 6). In accordance with their mechanism, two competing reaction paths of diethyl phosphate release proceed from the triplet state of the benzoin diethyl phosphate, depending on the solvent. In most solvents, reaction path (a) predominates, and forms 2-phenylbenzofuran and diethyl phosphoric acid rapidly. In water and fluorinated alcohols, reaction path (b) dominates, and forms trifluoroethyl benzoin ether as the major product.
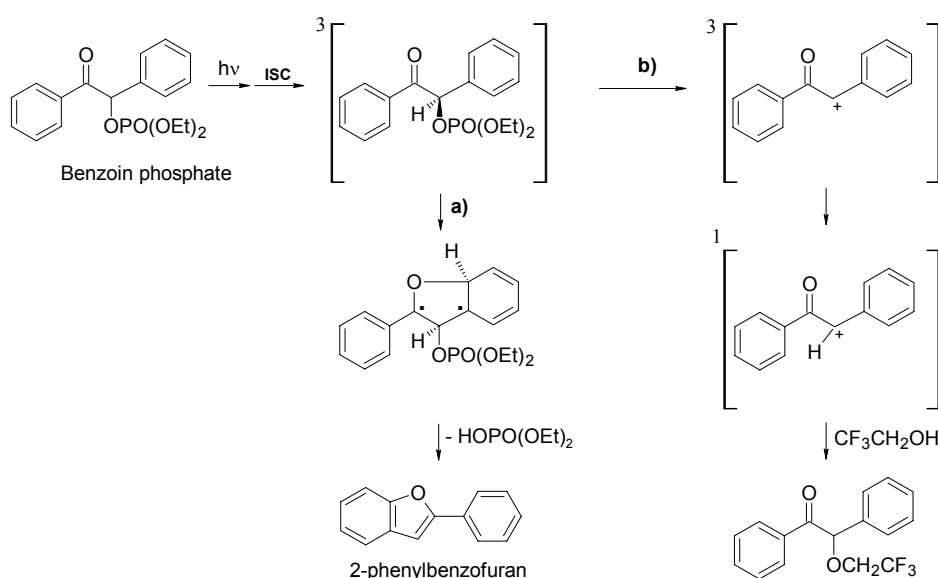
Scheme 6: Reaction mechanism of the unsubstituted benzoin group

They observed two transients upon direct LFP in aqueous acetonitrile solutions. After 30 ns a signal at 300 nm appeared which is attributed to the formation of the 2-phenylbenzofuran. In water another transient was observed at 570 nm, which decayed with a rate constant of 2.3×10^6 s^{-1}. This decay rate increased in the presence of oxygen, which suggests that the cation is in a triplet state. On the basis of picosecond pump-probe studies the 2-phenylbenzofuran is formed within 20 ns in most solvents. This fast transformation may be accomplished via a biradical intermediate, which has not been observed yet. It is assumed that it reacts faster than it is formed. Nucleophilic substitution can become a major pathway when trifluoroethanol is used as solvent. The transient observed at $\lambda_{max} = 570$ nm, $\tau = 660$ ns vide supra, was assigned to the triplet cation. DFT calculations and quenching studies confirmed the presence of the triplet cation. The decay of the triplet to the ground state

singlet cation takes place before the attack of the trifluoroethanol. The dispartment of the photoreaction was explained with the coexistence of two interconvertible conformers of the benzoin phosphate in the ground state. The gauche conformation is disfavoured by solvents which form strong hydrogen bonds to the carbonyl group and leads to the benzofuran. The anti conformation is instead favoured by protic solvents and heterolysis generates an extended benzyl cation which leads the reaction towards nucleophilic addition.

Even though the development of this PPG is fairly recent, only a few practical applications have been described. A major drawback of the benzoin group is the additional chiral centre introduced by the benzylic carbon which makes protection of optically active substrates problematic. A further disadvantage is that the by-product benzofuran absorbs light and acts as an internal light filter. The poor solubility of benzoin caged compounds which limits their biological applications has been sorted out by the recent development of a water soluble benzoin cage. An additional limitation is that the 3',5'-DMB group is very light sensitive and can photorelease under normal laboratory light which makes the following steps problematic. In order to solve this problem, Stowell et al.[27] developed a safety-catch benzoin PPG. They have used the Corey-Seebach dithiane addition method to synthesize benzoins via the dithiane protected adduct (Scheme 7). This allows complex protected molecules to be synthesized that can be kept photochemically inert until the dithiane moiety is converted to the parent ketone.
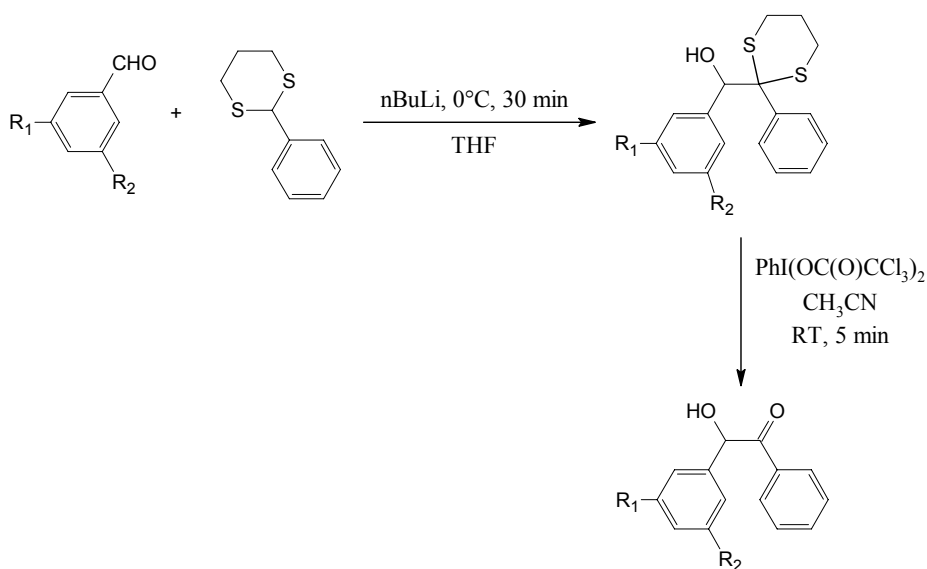
Scheme 7: Safety-catch benzoin protecting group

1.2.3. The Phenacyl Group

The phenacyl group was originally applied as a conventional protecting group. It was first observed as PPG by Sheehan and Umezawa[28] in 1973. They reported that irradiation of *p*-methoxyphenacyl benzoate in ethanol or dioxane gave benzoic acid in good yield (Scheme 8). Anderson and Reese[29] reported the photoreactions of *p*-methoxy and hydroxy phenacyl esters, which rearranged, partially, to methyl phenylacetates when irradiated in methanol. None of these earlier studies utilized the potential of these chromophores as PPG.
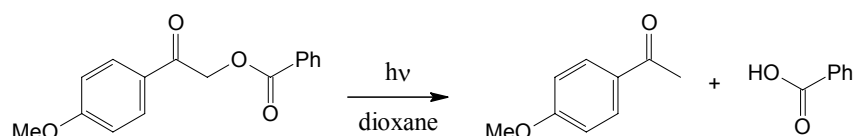
Scheme 8: Photorelease from phenacyl esters

The *p*-hydroxy substituted phenacyl group was introduced by Givens *et al.*[30] as efficient PPG. The *p*-hydroxyphenacyl (pHP) group has several features which makes it very attractive as a phototrigger. The pHP group is water soluble and has very fast rate of substrate release on the order of 1 ns, depending on the substrate. The quantum yields of photorelease are high. The main by-product *p*-hydroxyphenyl acetic acid is non-toxic and also has a hypsochromically shifted absorption spectrum with respect to the *p*-hydroxyphenacyl protected substrate. Therefore it does not have an impact on the light absorption in contrast to the by-product from the 2-nitrobenzyl derivatives. Moreover, the pHP group does not introduce a chiral centre. The pHP group is easy accessible by a simple synthetic route from commercially available *p*-hydroxyacetophenone.

A major disadvantage of the pHP protecting group is its low extinction coefficient at wavelengths above 320 nm. However, Conrad *et al.*[31] have managed to shift the absorption range of the *p*-hydroxyphenacyl chromophore to higher wavelengths by introducing methoxy substituents on the ring. They synthesized 3,5-dimethoxy-pHP esters of glutamate and γ-aminobutyric acid (GABA) and found that they absorb up to 400 nm. Regrettably, this modification led to significantly lower quantum yields of release.

Recent experimental and theoretical studies provide mechanistic information on the photorelease of substrates from the pHP group (Scheme 9). Nevertheless there are still question marks concerning the molecular changes implicated in the process and the identity of the intermediate.

Quenching studies investigated by Givens *et al.*[31] with naphthalene-2-sulfonate and potassium sorbate revealed that the reaction proceeds through the triplet excited state with a lifetime of 0.5 ns. At a later date Wirz and colleagues[32] explored the pHP diethyl phosphate and observed the triplet excited state by pump-probe spectroscopy (λ_{max} = 380 nm, τ = 0.4 ns in CH_3CN / H_2O = 1:1), quenchable by piperylene. The deprotection occurs either simultaneously or follows deprotonation of the para-hydroxyl group in the triplet excited state. The triplet pK_a of this chromophore was measured to be 3.6 versus 7.9 in the ground state. The acidity of the triplet should be considered, when new derivatives are designed. This is evident from the work of Conrad and Givens[33]. It is conjectured that the triplet phenoxide anion is the precursor to the release of the substrate and the hypothetical spirodienedione (SDD) intermediate.
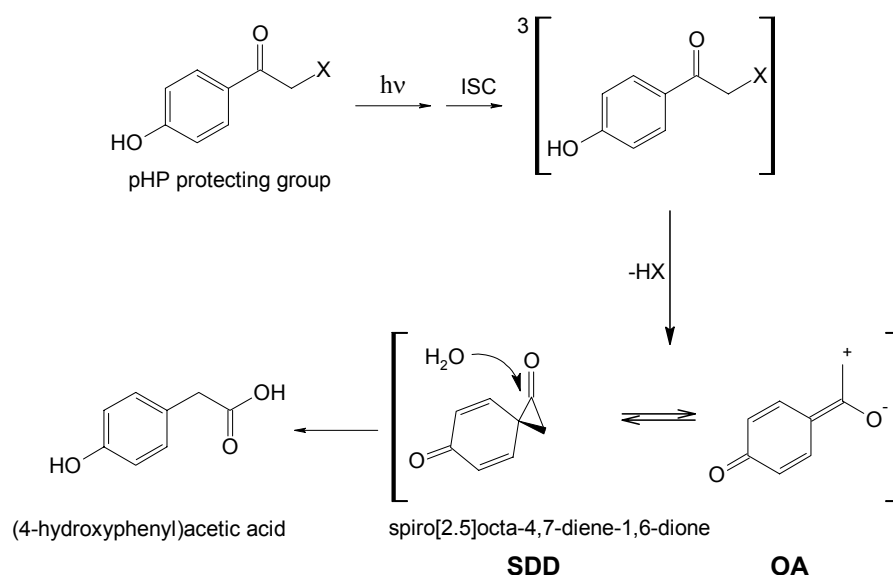
Scheme 9: Reaction mechanism of the *p*-hydroxyphenacyl protecting group

The SDD may also be in equilibrium with the oxyallyl valence isomer OA. DFT calculations support the formation of an open oxyallyl triplet, because the energy of the triplet SDD is slightly higher than the triplet diradical. It is assumed that the SDD is a highly reactive intermediate with a lifetime of less than 1 ns. The subsequent opening of the cyclopropane ring is not only driven by the decrease of ring strain but also by simultaneous rearomatization of the dienone. Up to now the SDD has eluded detection. Hydrolysis of the SDD leads to the final *p*-hydroxyphenylacetic acid, the only major photoproduct of the pHP group. Since the introduction of the pHP group there are only few biological studies where pHPs have been applied, but these investigations are very informative and show its excellent capability.

Klan *et al.*[33] introduced the 2,5-dimethylphenacyl (DMP) group as a PPG in the year 2000. They have made use of the highly efficient photoenolisation reaction of *o*-alkylaryl ketones to accomplish release of various functional groups. Photolysis of DMP esters **E** results in formation of the free acid in combination with 6-methylindan-1-one **F**, and in alcohol, an additional by-product, 1-(2,5-dimethylphenyl)ethanone **G** is noticed (Scheme 10).
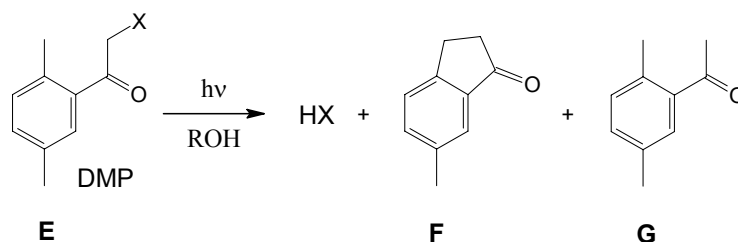
Scheme 10: Photorelease from 2,5-dimethylphenacyl esters

The proposed mechanism for photorelease[34] involves a photochemical enolization that occurs from the excited triplet state of the DMP chromophore (Scheme 11). The photoreaction is initiated via an intramolecular hydrogen abstraction to yield the triplet photoenol (^3E) **G** which subsequently decays to ground state *E*- and *Z*-photoenols. The *Z*-enol **H** undergoes fast reketonisation in hydrocarbon solvents. The release of substrate occurs from the longer-lived *E*-enol **H** with the formation of the cyclized 6-methylindan-1-one **F** by-product. In alcohol, addition of solvent rather than cyclization results in appearance of (2,5-dimethylphenyl)ethanone **G** as the by-product.
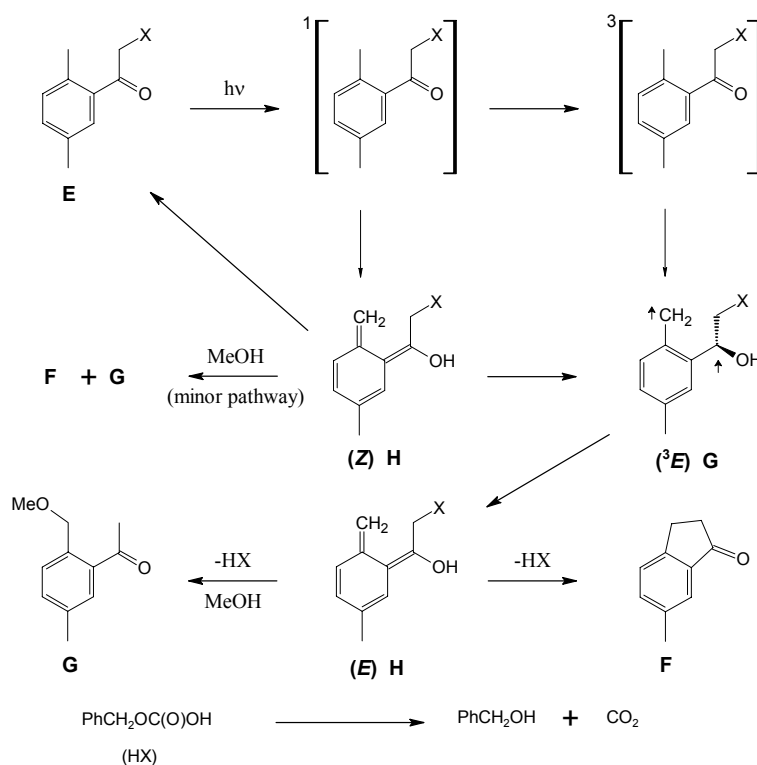
Scheme 11: Reaction mechanism of the 2,4-dimethylphenacyl protecting group

Analogous to the benzoin cages, safety-catch protecting groups have been developed based on the phenacyl group. Shaginian *et al.*[35] have developed and applied trimethoxyphenacyl-based orthogonal safety-catch protecting groups in light-directed radial combinatorial chemistry. They masked the carbonyl group of the phenacyl esters as dimethyl ketals and 1,3-dithianes which makes these cages photochemically inactive (Scheme 12). When needed, these molecules can be converted to the photolabile protecting group by reaction with aqueous acids and subsequently deprotected by irradiation.
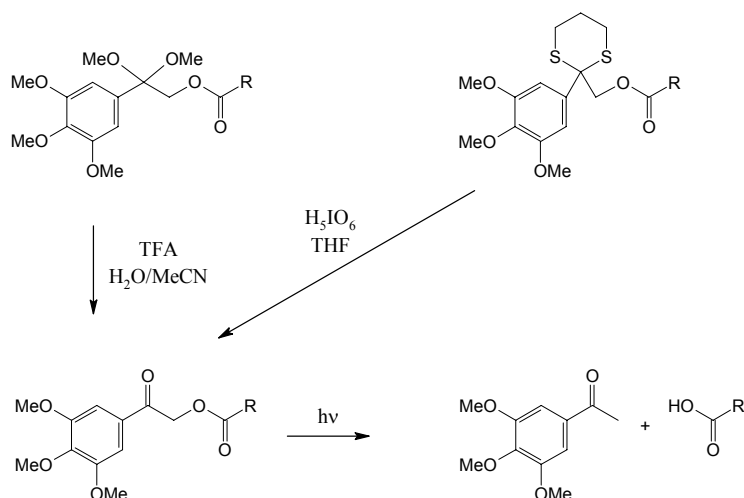
Scheme 12: Safety-catch protecting groups based on the trimethoxyphenacyl group

1.2.4. The Coumarinyl Group

Givens and Matuszewski[36] first reported on the photoactivity of 7-methoxycoumarin-4-ylmethyl (MCM) esters in 1984. They observed that this compound is readily converted to the free carboxylic acid and formation of the according hydroxymethylcoumarin (MCM-OH) by irradiation in aqueous media (Scheme 13).

MCM ester   **MCM**-OH
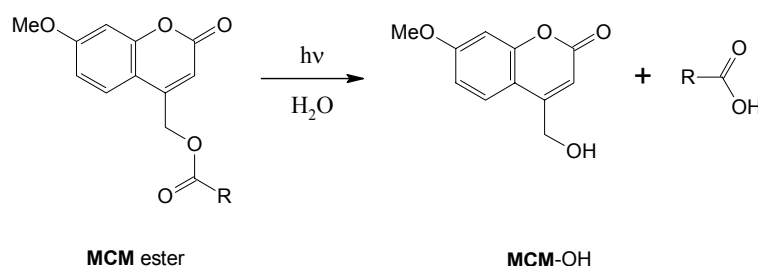
Scheme 13: Photorelease from MCM esters

Around 10 years later this reaction was reinvestigated to compare the photochemical properties of MCM-cAMP to those of the 1-(2-nitrophenyl)ethyl and desyl esters under a simulated physiological environment. The MCM-cAMP released the cAMP upon irradiation with light of 340 nm with almost quantitative yield. Since that time, the MCM group and their structural variants have been synthesized and employed to produce several caged compounds. The coumarins have the potential to replace the conventional PPGs because of quite a few reasons: Overall, coumarin type PPGs show large extinction coefficient, the spectral absorption extends to the visible region and can be shifted further by proper substituents. The coumarinyl groups show fast rate of photorelease and are practically useful for 2-photon excitation. Figure 3 shows a compilation of already available coumarin phototriggers.

7-alkoxy group
MCM (R = CH$_3$)
HCM (R = H)
ACM (R = CH$_3$CO)
PCM (R = CH$_3$CH$_2$CO)
CMCM (R = CH$_2$COOH)

6,7-dialkoxy group
DMCM (R = CH$_3$)
BCMCM (R = CH$_2$COOH)
BECMCM (R = CH$_2$COOEt)

6-bromo-7-alkoxy group
BHc (R = H)
BHc/Ac (R = CH$_3$CO)
BHc-diol (R = H) X=
R$_1$= H, Me, R$_2$= Ph

7-dialkylamino group
DEACM (R = CH$_3$CH$_2$)
DMACM (R = CH$_3$)
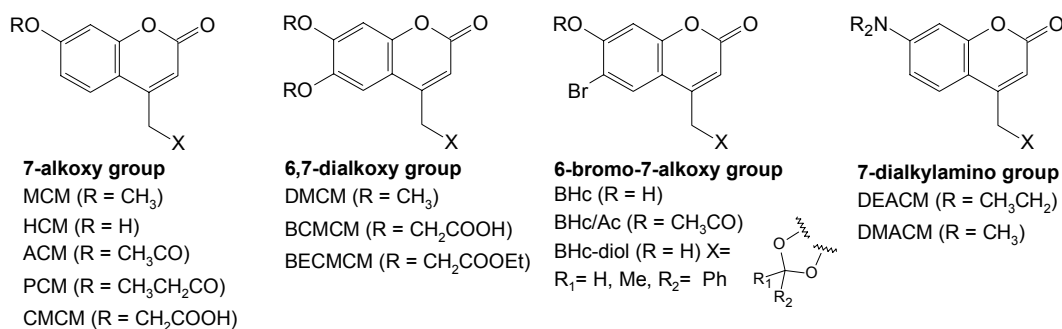
Figure 3: Acronyms and structures of coumarin-4-ylmethyl phototriggers

The coumarinyl group has been applied in several biological studies, including the photorelease of cyclic nucleotides[38-40], carboxylic acids[37] and phosphates[37]. The results are extremely promising. Very recently Hampp *et al.*[40-42] developed a novel photocleavable multifunctional linker system based on coumarin dimers, whose unique photochemical behaviour are well characterized[38]. They investigated the drug release from an acrylic polymer-drug conjugate with antimetabolites. The cleavage of the link between the drug and the polymer backbone can be triggered by both single- and two-photon absorption. They showed that it is possible to manufacture a polymeric drug delivery device with several drugs in different areas. Bendig and Schade[37] proposed a mechanistic scheme that outlines the photoreaction of the coumarinyl PPG (Scheme 14).

X = OPO(OEt)$_2$, OAc, OSO$_2$Me
R = OCH$_3$, OH, NEt$_2$, OCH$_2$COOH
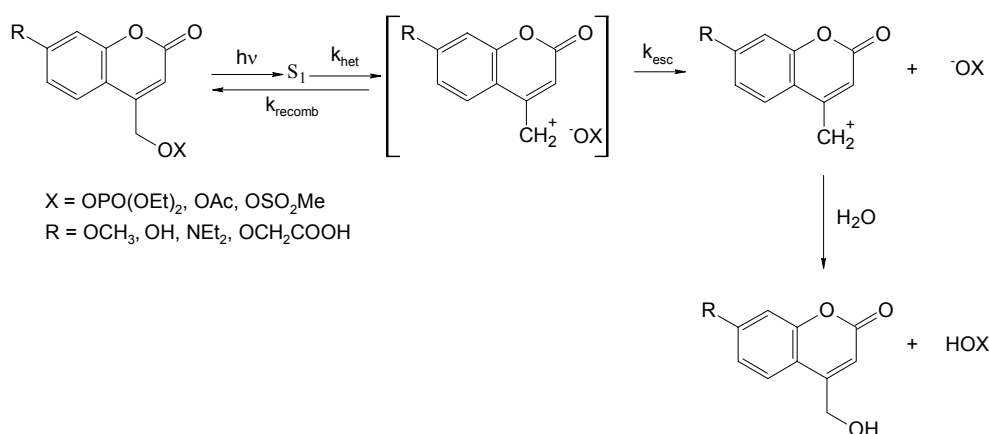
Scheme 14: Reaction mechanism of the coumarinyl protecting group

Upon photon absorption, the coumarinyl chromophore is promoted to its singlet excited state. Even though the coumarinyl group and its hydroxy analogue (HCM) are fluorescent, nearly all caged substrates from that series are only weakly fluorescent. The photolysis product hydroxymethylcoumarin shows a strong fluorescence. This strong fluorescence enhancement has been exploited to monitor the extent of reaction during photorelease. Heterolytic C-O fragmentation (k_{het}) follows the singlet excited state which is most likely the rate-determining step of release ($k_{het} \sim 10^9$ s^{-1}). The absence of evidence on the initial cleaving step prevents an unequivocal classification of heterolytic versus homolytic cleavage[37,39]. Schade has demonstrated that there is a correlation between the quantum efficiency and the polarity of the solvent. The more polar the solvent is, the better the solvation of the ion pair and this tends to result in higher quantum yields. Finally, the

resulting ion pair escapes from the solvent cage (k_{esc}) and the coumarin-4-ylmethyl cation gets trapped by the solvent.

The coumarinyl PPGs has only a few shortcomings. Some of the derivatives are not stable for long time in neutral aqueous media and none of the coumarin caged compounds are commercially available up to now. Nevertheless, the fast rate of photorelease and the applicability for 2-photon excitation preponderate and make the coumarinyl an extremely promising PPG.

1.2.5. Other Groups

The design of new photoremovable protecting groups is a challenging and rewarding undertaking. It is desirable to have a range of compounds with different characteristics to choose from. There is still the need for efficient and fast systems for poor leaving groups. Several laboratories established new versatile PPGs (Figure 4), however not all of them have been applied for biological studies so far.
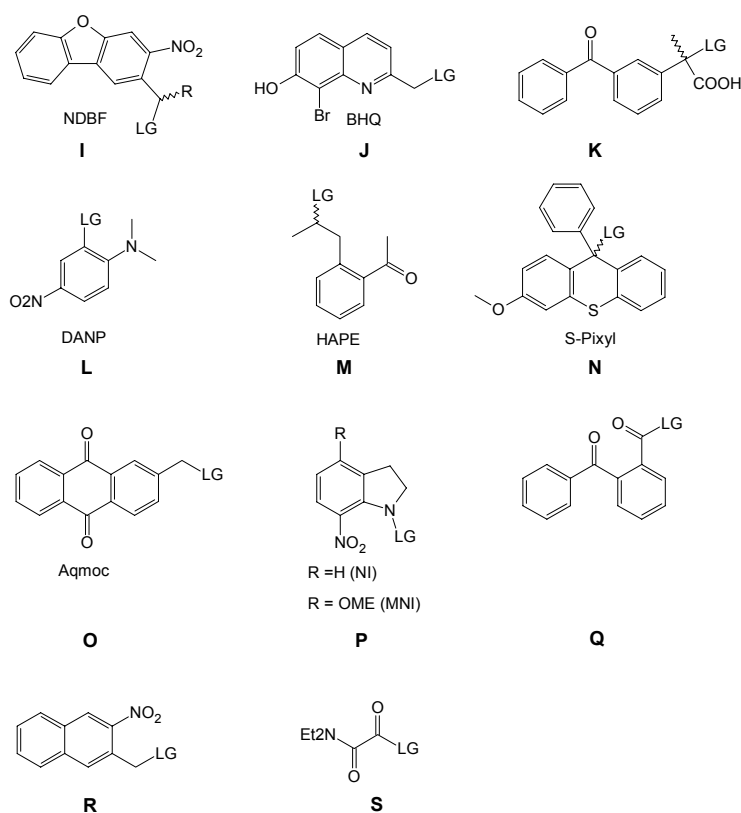
Figure 4: An incomprehensive overview of other PPGs
(LG = Leaving group, in some cases this includes a carbonate or carbamate linker)

Very recently Ellies-Davies *et al.*[47-49] introduced the nitrodibenzofurane (NDBF) chromophore **I** which has very promising properties: The NDBF protecting group is a very effective generic caging chromophore whose photochemistry is based upon the well-established 2-nitrobenzyl group. The extinction coefficient at λ_{max} = 330 nm is 18400 M^{-1} cm^{-1} and the quantum yield of photolysis is 0.7, moreover it is also suitable for two-photon activation. The NDBF-EGTA (caged calcium) is highly soluble in aqueous buffer at neutral pH and stable. A new PPG for carboxylic acids based on 8-bromo-7-hydroxyquinoline (BHQ) **J** which is a closely related analogue to the coumarinyl PPG has been described by Fedoryak and colleagues[40,41] in 2002. The major advantages of the BHQ are its high quantum efficiency, very low fluorescence and good solubility in aqueous buffers. The ketoprofen-derived caging group **K** was implemented by Scaiano and Lukeman[42] and could have great potential. This system shows high quantum yields ($\Phi \sim 0.7$), fast photorelease rates, excellent aqueous solubility due to the carboxylic function and gives an inert photoproduct. The authors reported efficient photorelease of carboxylic acids, halides and even alcohols (20%). Another caging group for carboxylic functionalities the 2-(dimethylamino)-5-nitrophenol (DANP) **L** was reported by Hess and co-workers[48]. This compound has a major absorption band near 400 nm and the substrate is released within 5 μs. Efficient photolysis takes place only at or below 360 nm with a quantum yield around 0.03 at 308 and 350 nm. One more carboxylic acid cage, the 1-[2-(2-hydroxyalkyl)phenyl]ethanone (HAPE) **M**, was introduced by Banerjee *et al.*[43] which releases the acid in 70-85 %. Boyd and Coleman[44] have shown that the 9-phenylthioxanthyl (S-pixyl) moiety **N** can be used as PPG in the synthesis of short oligonucleotides with conventional solid-phase protocols. Furuta *et al.*[45] established the anthrachinon-2-ylmethoxycarbonyl (Aqmoc) **O,** as a new PPG for alcohols that are connected through a carbonate linker. Caged galactose is released with a quantum yield of 0.1 and a rate constant of $\sim 10^6$ s^{-1}. 5′-Aqmoc-adenosine was also synthesized and photolysed to yield the adenosine in 91%. The 7-nitroindolines **P** have been used for more than two decades as PPGs. However only recently have they gained considerable attention[57,58]. Photocleavage involves the triplet excited state and proceeds in the submicrosecond range. The photoreaction is clean and depends strongly on the nature of the solvent. Gudmundsdottir[52] and co-workers reported the release of geraniol from 2-(2-isopropylbenzoyl)benzoate ester **Q** with a quantum yield of 0.62. They are interested in release of fragrances upon exposure to light, independent of the reaction media and thus

feasible in thin film-type applications. Singh *et al.*[46] introduced the 3-nitro-2-naphthalenemethanol **R** as new chromophore for PPGs. The photochemistry is based also on the 2-nitrobenzyl group and can be excited between the ranges of 300-400 nm and affords quantum yields ranging from 0.6 to 0.8. They released immunoglobulin (IgG) under physiological conditions efficiently. Steinmetz and colleagues[47] reported the photochemical release of carboxylate leaving groups from α-keto amides **S**. The caged substrates were unleashed upon exposure to $\lambda > 300$ nm in 70-90% yield with quantum yields of 0.3. The photorelease of GABA occurs on the sub-30 ms time scale.

1.3. Applications of Photoremovable Protecting Groups

Photoremovable protecting groups have found various applications in diverse fields, such as photolithography, multi-step organic synthesis, peptide synthesis, time-resolved x-ray crystallography etc. A couple of important applications will be discussed here. An introduction to the issue, plus a few fascinating investigations exemplifying the importance of PPGs, are provided in each section.

1.3.1. Photorelease of Neurotransmitters

The most active area in terms of the development and applications of caged compounds during the past several years has been in the area of caged neurotransmitters.

Neurotransmitters are chemicals that are used to relay, amplify and modulate electrical signals between a neuron and another cell.

Substances that act as neurotransmitters can be roughly categorized into three major groups:

- amino acids (primarily glutamic acid, GABA, aspartic acid and glycine)
- peptides (vasopressin, somatostatin, neurotensin, etc.)
- monoamines (norepinephrine NA, dopamine DA and serotonin 5-HT) and acetylcholine (ACh).

Neurotransmitters can be broadly classified into small-molecule transmitters and neuroactive peptides.

The Mechanism of Action:

Inside the cells, small-molecule neurotransmitter are generally packaged in vesicles. As soon as an action potential travels to the synapse, the rapid depolarization causes calcium ion channels to open. Calcium then stimulates the transport of vesicles to the synaptic membrane; the vesicle and cell membrane fuse, leading to the release of the packaged neurotransmitter, a mechanism called exocytosis.

Afterwards the neurotransmitters diffuse across the synaptic cleft to bind to receptors. The receptors are broadly classified into ionotropic and metabotropic receptors. Ionotropic receptors are ligand-gated ion channels that open or close through neurotransmitter binding. Metabotropic receptors, which can have a diverse range of effects on a cell, transduct the signal by secondary messenger systems or by G-proteins.

The Post-synaptic Effect:

The effect of a neurotransmitter is determined by its receptor. For instance, GABA can act on both, rapid or slow inhibitory receptors. Many other neurotransmitters, however, may have excitatory or inhibitory actions depending on which receptor they bind to. Neurotransmitters may trigger either excitatory or inhibitory post-synaptic potentials. That is, they may help the initiation of a nerve impulse in the receiving neuron, or they may discourage such an impulse by modifying the local membrane voltage potential. Glutamate is the most prominent of excitatory transmitters; GABA and glycine are inhibitory neurotransmitters. Many neurotransmitters are removed from the synaptic cleft by neurotransmitter transporters in a process called reuptake. Without reuptake, the molecules might continue to stimulate or inhibit the firing of the post-synaptic neuron. Digestion by an enzyme is a further mechanism for detachment of a neurotransmitter. Neuroactive peptides are often removed from the cleft by diffusion and are finally broken down by proteases. The actions of some drugs mimic those of naturally occurring neurotransmitters. The pain-regulating endorphins, for example, are similar in structure to heroin and codeine, which fill endorphin receptors to accomplish their effects. The wakefulness that follows caffeine consumption is the result of its blocking the effects of adenosine, a neurotransmitter that inhibits brain activity. Abnormalities in the production or functioning of certain neurotransmitters have been implicated in a number of diseases including

Parkinson's disease, amyotrophic lateral sclerosis (Motor Neuron Disease), and clinical depression. Caged neurotransmitters can provide unique and valuable information about fast synaptic responses in the central nervous system and the elucidation of the activation mechanism is important for the design of new therapeutic agents.

Thus, phototriggers enable the rapid photorelease of bioactive materials from inactive caged precursors. As ligand–protein interactions occur on a submillisecond timescale, the rapid and complete delivery of bioactive molecules is essential to study the fast kinetic events (either as a change in the concentration of chemical messengers and ions or as conformational changes) triggered by ligand binding. The advantages of caged neurotransmitters compared to traditional methods (e.g. cell flow technique) are that they can be preloaded into intra- or extracellular regions of the preparation, with an accurately determined amount of the inactive precursor. Afterwards it can be activated by light at a very precise time. In this manner, delays due to diffusion into the preparation and spatial and temporal inhomogenities are minimized. The variety of commercially available caged compounds (e.g. glutamates, γ-aminobutyric acid, carbachol, etc.) has been enlarged to a great extent and one can even create one's own particular caged molecule using commercially available caging kits[48].

The major "workhorse" neurotransmitters of the brain are glutamic acid and γ-aminobutyric acid (GABA). Glutamates have been used for mapping neuronal connectivity, probing neuronal integration and synaptic plasticity. Some examples of glutamate caged with different PPGs are shown below.
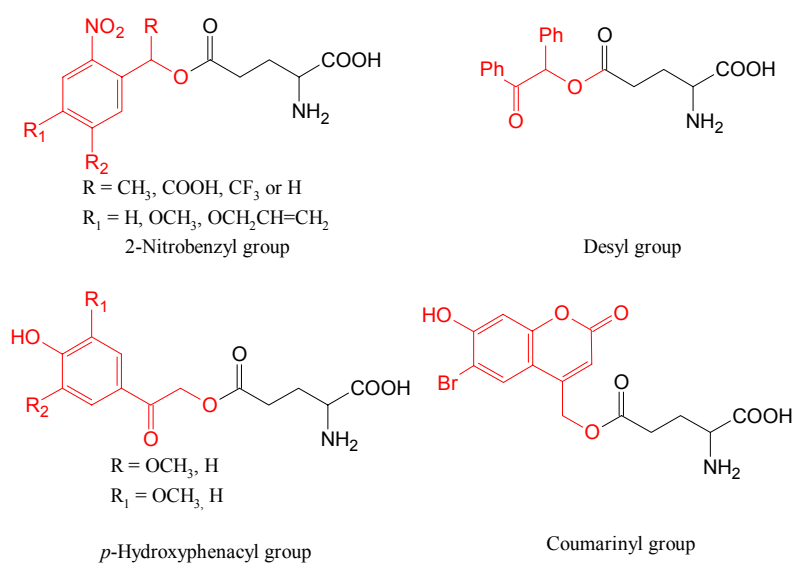
Figure 5: caged glutamate

Li *et al.*[49] reported the kinetics for the opening of the GluR1Q$_{flip}$ receptor channel. GluR1 is one of the four subunits of the α-amino-3-hydroxy-5-methyl-4-isoxazolepropionic acid (AMPA) receptor. As a subtype of ionotropic glutamate receptors, AMPA receptors mediate fast synaptic neurotransmission in the mammalian central nervous system. The GluR1 subunit plays a specific role in a wide range of biological functions such as the expression of synaptic plasticity, the formation of memory, the development of the dendritic architecture of motor neurons, the excitotoxic necrosis and the generation of sensitization by drugs of abuse. Photolysis of γ-*O*-(α-carboxy-2-nitrobenzyl)glutamate at 355 nm with pulsed light (pulse length = 8ns) from a Nd:YAG laser which was directed to the target by fibre optics liberated the glutamate with a time constant of ~30 μs. The reporters observed that, after the binding of glutamate, the channel opened with a rate constant of $(2.9 \pm 0.2) \times 10^4 \, s^{-1}$ and closed with a rate constant of $(2.1 \pm 0.1) \times 10^3 \, s^{-1}$. The fastest time by which the GluR1Q$_{flip}$ channel can open, was predicted to be 35 μs. This value is three times shorter than those previously reported. The minimal kinetic mechanism for channel opening consists of binding of two glutamate molecules, with the channel-opening probability being 0.93 ± 0.10. These findings identify GluR1Q$_{flip}$ as one of the temporally efficient receptors that transduces the binding of chemical signals into an electrical impulse.

Kandler *et al.*[50] used pHP caged glutamate to study the mechanisms of hippocampal synaptic plasticity. In the CA1 region of the hippocampus, several well-characterized forms of synaptic plasticity have been described, including long-term potentiation (LTP) and long-term depression (LTD). Long-lasting, activity-dependent changes in synaptic strength in the mammalian brain have been postulated to mediate a variety of important nervous system functions, including learning and memory. The approach was to block synaptic transmission and bathe hippocampal slices with caged glutamate, which, upon photolysis, transiently activates glutamate receptors. By using optical fibers, they activated focally independent sets of glutamate receptors on different regions of an individual cell's dendritic arbor. Paired post-synaptic depolarization with rapid repetitive light pulses (1 Hz) at one site, but not the other, caused a long-lasting depression of the light-induced glutamate currents at the test site, but not at the control site. Because the post-synaptic currents were directly activated by uncaged glutamate and not by synaptically released glutamate, this input-specific LTD must be due to some modification in the function and/or number of post-synaptic glutamate receptors. The results demonstrate unequivocally that post-synaptic glutamate receptors alone can express LTD.

1.3.2. Photorelease of Second Messengers

Second messengers are molecules that relay signals received at receptors on the cell surface such as the arrival of protein hormones, growth factors, etc. to target molecules in the cytosol and/or nucleus. But in addition to their job as relay molecules, second messengers serve to greatly amplify the strength of the signal. Binding of a ligand to a single receptor at the cell surface may end up causing massive changes in the biochemical activities within the cell. There are three major classes of second messengers:

- Cyclic nucleotide monophosphates
- Inositol trisphosphate and diacylglycerol
- Calcium ions

1.3.2.1. Cyclic Nucleotide Monophosphates (cNMP):

Cyclic Adenosine Monophosphate (cAMP)

Some of the hormones that achieve their effects through cAMP as a second messenger are adrenaline, glucagon and luteinizing hormone. cAMP is synthesized from ATP by the action of the enzyme adenylyl cyclase. Binding of the hormone to its receptor activates a G protein which, in turn, activates adenylyl cyclase. The resulting rise in cAMP turns on the appropriate response in the cell by either (or both) changing the molecular activities in the cytosol (often using Protein Kinase A) or turning on a new pattern of gene transcription.

Cyclic Guanosin Monophosphate (cGMP)

cGMP is synthesized from the nucleotide GTP using the enzyme guanylyl cyclase. cGMP serves as the second messenger for atrial natriuretic peptide, nitric oxide and the response of the rods of the retina to light. Some of the effects of cGMP are mediated through Protein Kinase G, a cGMP-dependent protein kinase that phosphorylates target proteins in the cell. Caged cAMP and cGMP are very useful in studying signalling pathways in cells, where spatial and temporal resolution is required. The cyclic nucleotides are rendered inactive by

esterification of the free phosphate moiety by several photoremovable protecting groups, with 2-nitrobenzyl and the coumarinyl derivatives being the most applied ones (Scheme 15 and 16).

DMNB-caged cAMPs R = H, R_1 = R_2 = OCH_3, Purine = adenin-9-yl
DMNB-caged cGMPs R = H, R_1 = R_2 = OCH_3, Purine = guanin-9-yl
BCMCNB-caged cAMPs R = R_2 = H, R_1 = $CON(CH_2COOH)_2$, Purine = adenin-9-yl
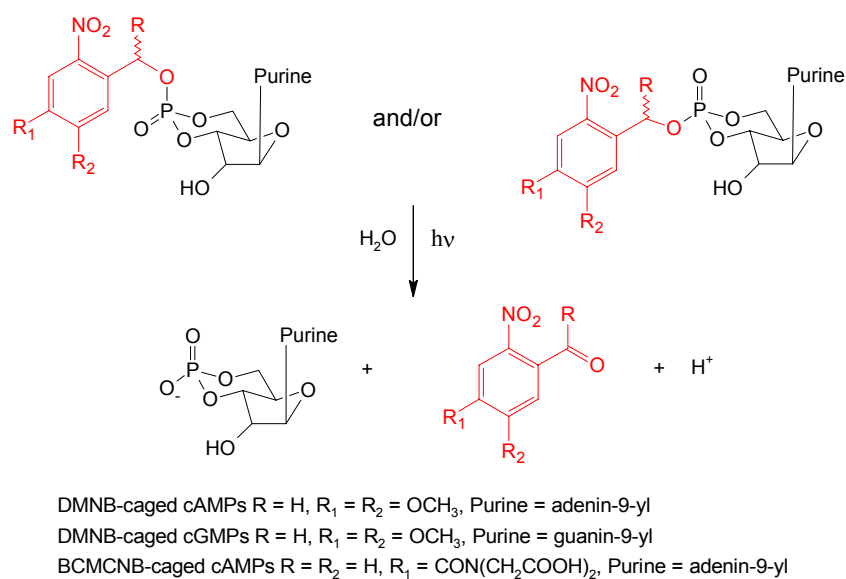
Scheme 15: Photolysis of the diastereomeres of nitrobenzyl-caged cNMPs

DMCM-caged cAMPs R_1 = R_2 = OCH_3, Purine = adenin-9-yl
BCMCM-caged cGMPs R_1 = R_2 = OCH_2COOH, Purine = guanin-9-yl
BECMCM-caged cAMPs R_1 = R_2 = OCH_2COOEt, Purine = adenin-9-yl
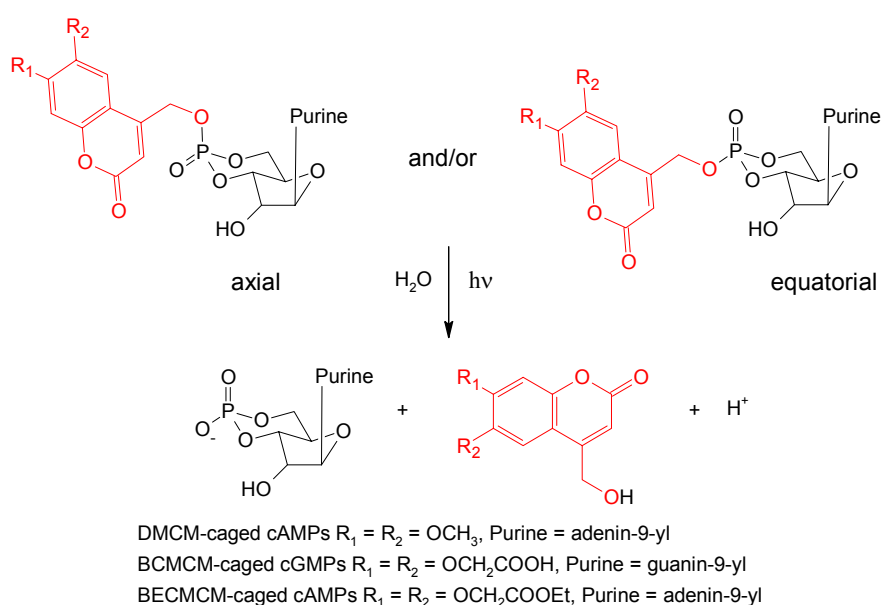
Scheme 16: Photolysis of the diastereomeres of coumarinylmethyl-caged cNMPs

Nache *et al.*[65] studied the activation and conformational changes of cyclic nucleotide-gated (CNG) ion channels by photolysis-induced jumps of the cGMP- or cAMP-concentration and by voltage steps. CNG ion channels play a key role in the sensory

transduction of vision and olfaction. The channels are opened by the binding of cyclic nucleotides. Native olfactory CNG channels are composed of three types of subunits: CNGA2, CNGA4, CNGB1b in the ratio 2:1:1. Upon heterologous expression, only CNGA2 subunits can form functional homotetrameric channels. For CNGA2 channels they showed that at equal degree of activation, the activation time course of homotetrameric channels was similar with cGMP and cAMP and it was also similar in homo- and heterotetrameric channels with the same cyclic nucleotide. Using chimeric channels constructed between retinal CNGA1 and olfactory CNGA2 channels, it was shown that both transmembrane and intracellular channel regions control the activation time course of the CNG channels. Nache *et al.* proposed a unique gating mechanism for homotetrameric and heterotetrameric channels that involves only three highly cooperative binding steps.

1.3.2.2. Inositol Trisphosphate (InsP$_3$) and Diacylglycerol (DAG)

Peptide and protein hormones as well as neurotransmitters like GABA bind to G-protein-coupled receptors that activate the intracellular enzyme phospholipase which hydrolyzes phospholipids, specifically phosphatidylinositol-4,5-bisphosphate (PIP$_2$). The hydrolysis of PIP$_2$ yields two products:

1) <u>Diacylglycerol </u>(DAG):

DAG remains in the inner layer of the plasma membrane. It recruits Protein Kinase C (PKC), a calcium-dependent kinase that phosphorylates many other proteins that bring about the changes in the cell. As its name suggests, activation of PKC requires calcium ions. These are made available by the action of the other second messenger InsP$_3$.

2) <u>Inositol-1,4,5-trisphosphate (InsP$_3$):</u>

This soluble molecule diffuses through the cytosol and binds to receptors on the endoplasmic reticulum causing the release of calcium ions into the cytosol. The rise in intracellular calcium triggers the response.

Walker *et al.*[58] investigated how the location of Protein Kinase C (PKC) by DAG determines whether cardiac function is stimulated or inhibited. Two-photon photolysis (780 nm, 20-25 mW) of Bhc-caged diC$_8$ (Figure 6) in different subdomains of rat cardiac

myocytes yielded different physiological responses, presumably because different subsets of PKC were activated. Remarkable in this study is that Bhc-diC$_8$ could be used at fourfold lower concentration than nitrobenzyl ether caged diC$_8$, due to greater sensitivity of Bhc to one-photon and two-photon excitation.
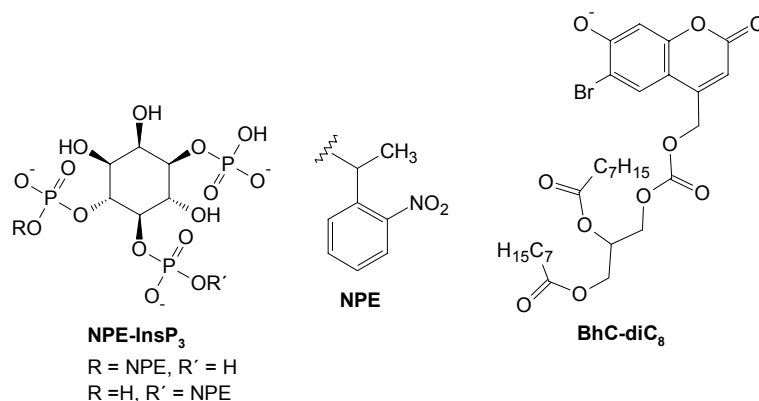
Figure 6: Caged InsP$_3$ and a Bhc-caged version of DAG, dioctanoylglycerol (diC$_8$)

A different approach to induce calcium concentration jumps in cells is the use of caged InsP$_3$. Li *et al.*[51] reported the synthesis of DMNB ether of an InsP$_3$ analogue and esterified the three phosphate groups to render the molecule membrane-permeable. It can therefore be loaded into intact, healthy cells, where the esters are cleaved by intracellular esterase. Subsequently they released the InsP$_3$ analogue with a quantum yield of 0.09, by rhythmic flashes of ultraviolet light (366 nm). Activation of the corresponding receptor in the endoplasmic reticulum leads to the release of Ca^{2+} from internal stores to the cytosol in an oscillating manner (Ca^{2+}-spikes) that stimulated gene expression by activating the nuclear factor of activated T cells (NF-AT). Li *et al.* found that oscillations in the concentration of intracellular Ca^{2+} were more effective than a single, prolonged increase, provided the period of each oscillation was roughly one minute - slower and faster frequencies were less efficient. In the case of the faster frequencies, this may have been due to desensitization of the InsP$_3$-receptor.

1.3.2.3. Calcium Ions

As the functions of InsP$_3$ and DAG indicate, calcium ions are also important intracellular messengers. In fact, calcium ions are probably the most widely used intracellular messengers. In response to many different signals, a rise in the concentration of Ca^{2+} in the

cytosol triggers many types of events such as muscle contraction, exocytosis (e.g., release of neurotransmitters at synapses; secretion of hormones like insulin), activation of T cells and B cells when they bind antigen with their antigen receptors, adhesion of cells to the extracellular matrix, apoptosis and a variety of biochemical changes mediated by Protein Kinase C. There are two main depots of Ca^{2+} for the cell: The extracellular fluid (ECF) and the endoplasmic reticulum. However, its level in the cell can rise dramatically when channels in the plasma membrane open to allow it in from the extracellular fluid or from depots within the cell such as the endoplasmic reticulum and mitochondria. There are three ways Ca^{2+} can get into and out of the cytosol:

1) The voltage-gated channels which open in response to a change in membrane potential.

2) The receptor-operated channels which are found in the post-synaptic membrane and open when they bind a neurotransmitter.

3) G-protein-coupled receptors (GPCRs). These are not channels but they trigger a release of Ca^{2+} from the endoplasmic reticulum as described above. They are activated by various hormones and neurotransmitters.

Ca^{2+} ions are returned to the ECF by active transport using an ATP-driven pump like the Ca^{2+}-ATPase of skeletal muscle and a Na^+/Ca^{2+} exchanger, or to the endoplasmic reticulum using a Ca^{2+}- ATPase.

As mentioned above, many physiological processes are triggered by influx of Ca^{2+} through the cellular membrane. Photolabile Ca^{2+}-chelators are used to define its role by rapid concentration jumps following a short laser pulse. Caged calcium reagents are unique among caged compounds, since release of Ca^{2+} depends on a change in the affinity of a photolabile chelator agent upon irradiation. In Figure 7 a few examples of commercially available Ca^{2+}-chelators are shown.
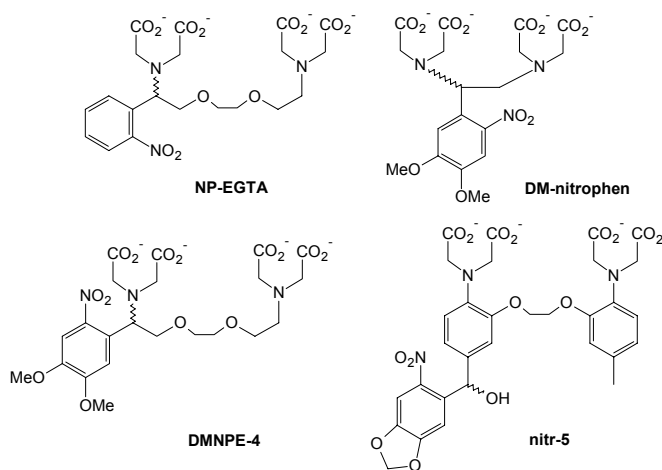
Figure 7: Commercially available Ca^{2+}-chelators

There are two different approaches to cage divalent cations (Scheme 17). The first, based on BAPTA ([1,2-bis(2-aminophenoxy)ethane-*N,N,N′,N′*-tetraacetic acid] consists of a series of compounds, the ´nitr´-series. Photocleavage of water from the alcohol junction leads to the formation of a carbonyl group which causes a decrease of the electron donating ability of the chelate and thereby lowers the ability to complex Ca^{2+}. The second approach is based upon the direct cleavage of the chelator (EDTA = ethylendiamine tetraacetic acid) and the title compound of this series has been called DM-nitrophen. The nitrophenyl-EGTA and DMNPE-4 (Figure 7) belong to the nitrobenzyl derived caging groups for Ca^{2+}, both work in the same way as DM-nitrophen but exhibit a higher affinity for Ca^{2+} over Mg^{2+}.
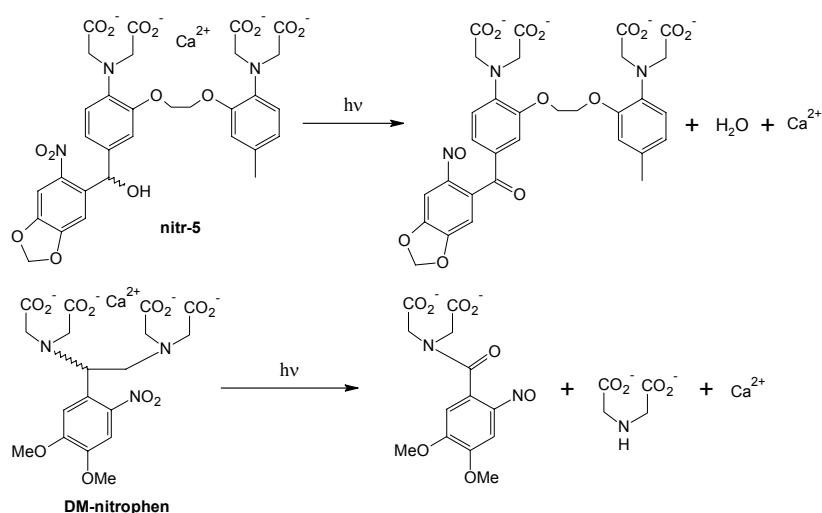
Scheme 17: Photolysis of caged Ca^{2+}

Soeller *et al.*[52] applied the DMNPE-4 (Figure 7) to study the Ca^{2+} movements within microscopic intracellular compartments like the nucleus. They probed nuclear Ca^{2+} diffusion by injection of the photolabile calcium chelator into mouse oocytes. Upon photolysis with 60 ms flashes of 700 nm light from a mode-locked Ti:S laser they observed the diffusion of Ca^{2+} with the fluorescent calcium indicators Fluo-3. Fluo-3 is essentially nonfluorescent without Ca^{2+} present, but the fluorescence increases at least 40 times on Ca^{2+} binding. Interestingly, the fluorescence from the indicator spread half as rapidly in the nucleus, indicating a slower rate of Ca^{2+} diffusion than in the cytoplasm.

1.3.3. Photoactivatable Fluorophores

The diffusional or active motion of molecules in biological systems under stationary conditions is traditionally measured by applying the fluorescence recovery after photobleaching (FRAP) technique. In this manner fluorescently labelled phospolipids or proteins are integrated into biological membranes or cells, allowed to equilibrate, photobleached in a spatially defined region of interest, and the movement of unbleached label into this area is then quantified. The complementary method to the FRAP is the photoactivation of fluorescence (PAF) attained by the photolysis of caged fluorophores (Fig. 8) attached to biomolecules and measurement of their dissipation. Caged fluorophores are fluorescent dyes which are covalently linked to PPGs whereby the fluorescence gets quenched. UV-Irradiation releases the fluorescent species and restores its absorption and emission properties in the visible region.
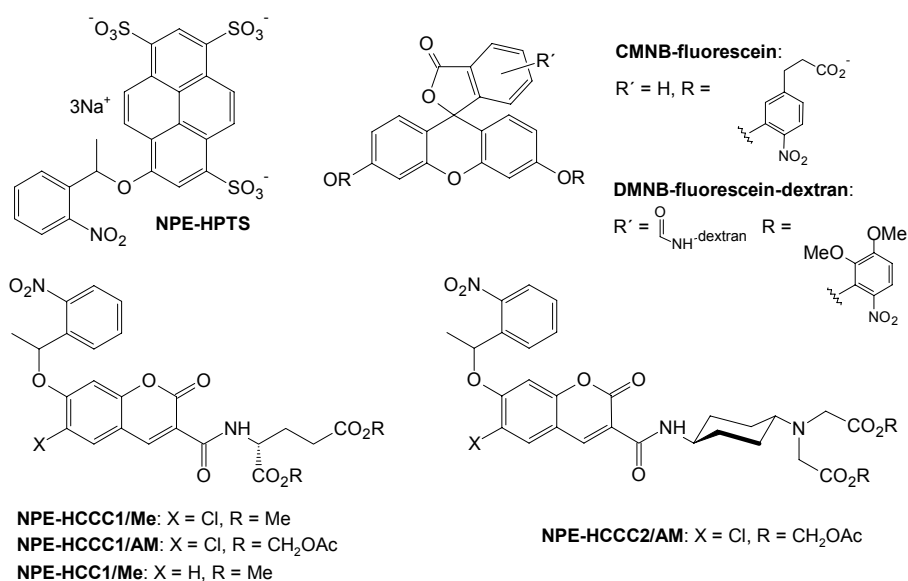
Figure 8: Caged fluorophores

In comparison to the FRAP, the PAF has several advantages. First, PAF generates a positive signal against a negative background and has a better signal to noise ratio. Second photolysis of the caged compounds is usually accomplished by irradiation with UV-light, and the unleashed fluorophore is then excited and monitored at longer wavelength. Third, PAF requires much less irradiation for photoactivation and consequently might reduce damage of the biological system through irradiation.

Svoboda *et al.*[53] investigated the diffusional coupling of dentric spines to shaft. Diffusional exchange of materials between the spine heads and dendritic shafts of neurons occurs through a narrow neck that connects the head to the shaft. Spines are neuronal protrusions, each of which receives input typically from one excitatory synapse. They contain neurotransmitter receptors, organelles, and signalling systems essential for synaptic function and plasticity. Numerous brain disorders are associated with abnormal dendritic spines. The authors used the photorelease of DMNB-fluorescein-dextran (Figure 8) to create a burst of fluorescence in a single spine head. Subsequently they monitored the diffusion of fluorescence inside the spine head to measure the timescale of diffusional equilibration. Their study produced consistent results, which demonstrate that diffusional exchange between spine head and dendrite is in the range of 20–100 ms, about a factor of 100 slower than expected for free diffusion over the small distances between spine and dendrite. Their measurements show that spine necks act as diffusion barriers, isolating spine heads from their parent dendrites for durations that are long on time scales of biochemical reactions. Diffusional compartmentalization of second messengers and activated enzymes could underlie synapse specificity in synaptic plasticity.

1.3.4. Solid Phase Synthesis, Caged Peptides and Proteins, DNA Microarray Fabrication and Photocleavable DNA Building Blocks

1.3.4.1. Solid Phase Synthesis (SPS)

Since Merrifield[54] pioneered solid phase synthesis back in 1963, the subject has changed radically. Merrifield's solid phase synthesis concept, first developed for a tetrapeptide, has spread in every field where organic synthesis is involved. Many laboratories and companies focused on the development of technologies and chemistry suitable to solid-phase synthesis.

In the basic method of solid phase synthesis, building blocks that have two functional groups are used. The two functional groups that are able to participate in the desired reaction between building blocks in the solution and on the bead can be controlled by the order of deprotection. One of the functional groups of the building block is usually

protected by a protective group. The starting material is a bead which binds to the building block. At first, this bead is added into the solution of the protected building block. After the reaction between the bead and the protected building block is completed, the solution is removed and the bead is washed. Afterwards the protecting group is removed and the above steps are repeated. After all steps are finished, the synthesized compound is cleaved from the bead.

This method is used for the synthesis of peptides, deoxyribonucleic acid (DNA), and other molecules that need to be synthesized in a certain alignment.

Solid phase synthesis is the most common method for synthesizing peptides. Usually, peptides are synthesized from the C- to the N-terminus of the amino acid chain in this method. The amino protecting groups mostly used in peptide synthesis are the 9-fluorenylmethyloxycarbonyl (Fmoc) and *t*-butyloxycarbonyl (Boc) group. Aside from them, PPGs have been recognized as being among the best protecting strategies. They offer the advantage of being essentially orthogonal to all traditional protecting groups, as they do not require any chemical reagents for deprotection. The 2-NB- and the pHP-group are commonly applied in the orthogonal protection of peptide synthesis. They have been used to protect carboxyl-, amino-, and hydroxy groups. Recently Bochet *et al.*[71-73] developed a PPG system consisting of the DMB- and the Nv-group that can be orthogonally deprotected using light of different wavelength (254 nm and 420 nm respectively). Wavelength orthogonality allows a set of photolabile protecting groups on the same molecule to be selectively removed by monochromatic light of different wavelengths. The ultimate goal would be a set of PPGs with wavelength orthogonality.

1.3.4.2. Caged Peptides and Proteins

PPGs are used not only in the synthetic methodologies in SPS but also in preparing caged peptides and proteins. Many proteins and peptides are known to regulate important biological processes. The most common way to prepare caged peptides and proteins is by the chemical modification of their amino acid residue. There are three methods corresponding to the type of side chains, amino-, thiol- and acid reactive. Amino groups can be modified with chloroformate- or chlorocarbamate-linked PPGs. Thiol groups can be transformed with the bromide derivate of the PPG to be caged and the carboxyl group with the diazo-derivative. This modification involves two disadvantages. One is that it is

difficult to control the position and the number of the modified site, as peptides and proteins contain multiple reactive functionalities. Second, there may not be an appropriate number of nucleophilic residues positioned at or near the desired site of modification, such as at the active site or at a protein-protein interaction site. Up to now there are only two methods which overcome the first problem, the nonsense codon suppression technique (NCST) and SPS. The NCST was introduced by Schultz *et al.*[74,75] in 1991. They used a nonsense codon and a corresponding t-RNA, loaded with the desired caged amino acid. A bit earlier an artificial four-base codon approach had been used by Endo *et al.*[55]. By both methods it is possible to introduce photolabile amino acids at a desired site in any peptide and protein. The groups of Tatsu[64,65] and Walker[66] have utilized SPS to synthesize caged peptides. They synthesized Fmoc amino acid derivatives of tyrosine and lysine containing photolabile protecting groups and have confirmed that these compounds are adapted for SPS of peptides without decomposition. The structure of the caged tyrosine residue is shown in Figure 9.
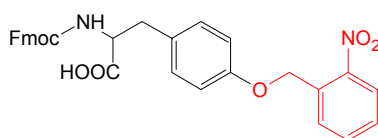
Figure 9: 2-Nitrobenzyl caged tyrosine residue

Tatsu and co-workers[64,65] incorporated caged tyrosine residue in the amino acid sequence of neuropeptide Y (NPY). NPY is a 36 amino acid polypeptide found in both peripheral and central nervous systems. NPY has been cast in a wide variety of potential roles, including regulation of blood pressure, anxiety, circadian rhythms and feeding behaviour. The authors showed that the binding affinity of caged NPY for the Y1 receptor was one or two orders of magnitude lower than that of intact NPY but increased to the value of the intact peptide within 7 µs upon irradiation with pulsed UV light.

Relatively few caged proteins have been described and fewer still have been evaluated in living cells. There are several formidable challenges associated with the preparation and study of these reagents, including covalent modification at the desired position on the target protein, introduction of the caged protein into the cell, and the subsequent photoactivation of the protein. The majority of studies reported to date have focused on methods used to prepare cage proteins (Figure 10).
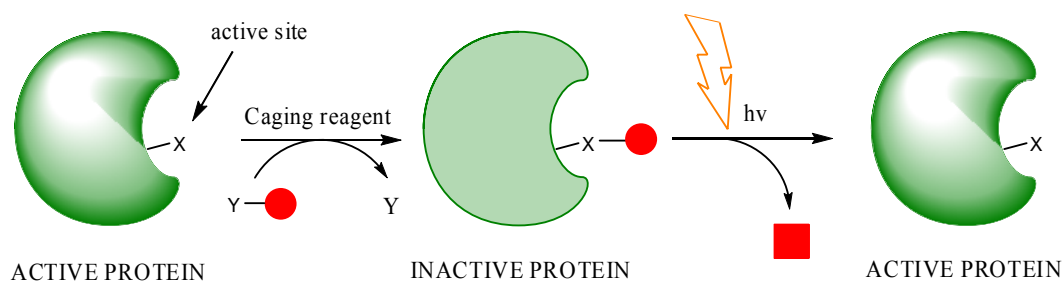
Figure 10: Typical procedure for caging and uncaging of a protein

In addition to the caging methods noted above, Hahn and Muir[56] prepared a caged protein via a semisynthesis using expressed protein ligation. In the latter instance, a recombinant protein was expressed as a C-terminal thioester, which was then ligated to a caged phosphopeptide that had been prepared via SPS. The synthetic strategy was used to create a cage construct of Smad2-MH2/SARA-SBD protein. Smad2 is a key element of the intracellular response to cytokines of the transforming growth factor β (TGF-β) superfamily, which are involved in a myriad of normal and disease processes, including development, tissue homeostasis and cancer. After irradiation, the caged protein releases the SARA-SBD moiety and thus the formation of a homotrimer is induced which then translocalizes into the nucleus. This approach opens an elegant way for the kinetic analysis of protein import and /or export processes of the nucleus.

Protein folding and especially the early events of it are poorly understood and very difficult to study. Kinetic studies of protein folding were so far largely limited to stopped-flow mixing, hydrogen-deuterium exchange and site-directed mutagenesis with time resolution of 100 μs at best. An interesting approach to study the complexity of protein folding processes was undertaken by Hansen *et al*.[57]. The authors used a photolabile linker to cyclise a hairpin and measured its refolding rate after photocleavage of the linker with a nanosecond laser pulse by using photoacoustic calorimetry. By monitoring and comparing the effects of two turn sequences on the refolding of a hairpin on the nanosecond time scale, the authors found that a one-residue difference in the turn region not only can change the stability and the equilibrium structure of the hairpin but can also affect the folding kinetics. The latter is usually not detected in traditional folding studies. Moreover, it is difficult to follow the fast folding kinetics of short peptides by spectroscopic methods. By measuring the heat released or absorbed during the refolding reaction, the introduction of a foreign chromophore is not required. The method is particularly useful for detecting local sequence effects on the early kinetic events of protein folding under ambient conditions

without resorting to temperature, pH, or pressure jumps and/or adding denaturants to the system.

1.3.4.3. DNA Microarray Fabrication and Photocleavable DNA Building Blocks

SPS, photolabile protecting groups and photolithography, have been combined to achieve light-directed, spatially addressable parallel chemical synthesis or simply microarray fabrication, to yield a highly diverse set of chemical products. Microarray technology includes protein-, antibody-, tissue- and chemical compound microarrays.

In this technique (developed by Fodor *et al.*[58] for peptides), the protected building blocks are affixed to a solid support. Irradiation occurs through a mask, and activates the selected areas by removal of the protecting group. After deprotection, the free functional group of the building block is exposed to reaction with another set of building block. Reaction only occurs on the activated sites. Repetition of the irradiation through masks with different patterns and varying the sequence of reactants leads to the desired set of products. For example, binary masking, one of many possible combinatorial synthesis strategies, yields 2^n compounds in n chemical steps. The generality of this approach is illustrated in Fig. 11.
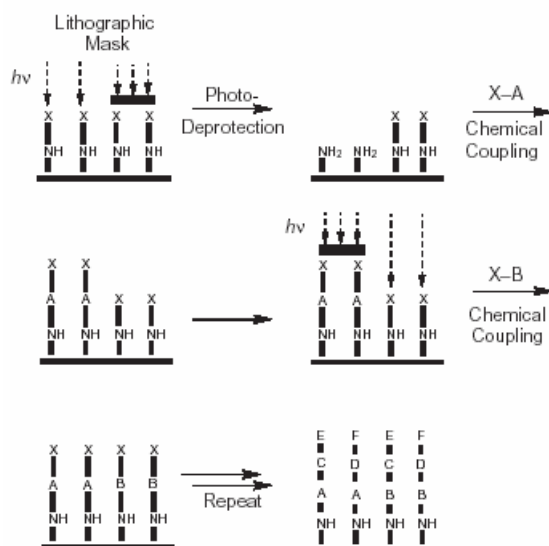
Figure 11: Light-directed, spatially addressable parallel chemical synthesis

The most common applied PPGs for light directed combinatorial synthesis are the

5-phenoxyphenyl-NPPoc-group

nitrobenzyl group, the dimethoxybenzoin group and the (nitrophenylpropyloxy)carbonyl group (NPPoc). The 5-phenoxyphenyl-NPPoc group shows superior performance with a half-time of deprotection of 16 s and a chemical yield of 98% that is superior to many other groups.
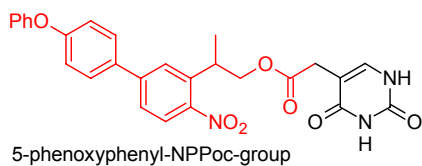
A DNA microarray (also commonly known as gene or genome chip or DNA chip) is a collection of microscopic DNA spots attached to a solid surface, forming an array for the purpose of expression profiling, monitoring expression levels for thousands of genes simultaneously. The anchored DNA segments are known as probes, thousands of which can be placed in known locations on a single DNA microarray. Microarray technology evolved from Southern blotting, whereby fragmented DNA is attached to a substrate and then probed with a known gene or fragment. Measuring gene expression using microarrays is relevant to many areas of biology and medicine, such as studying treatments, disease, and developmental stages.
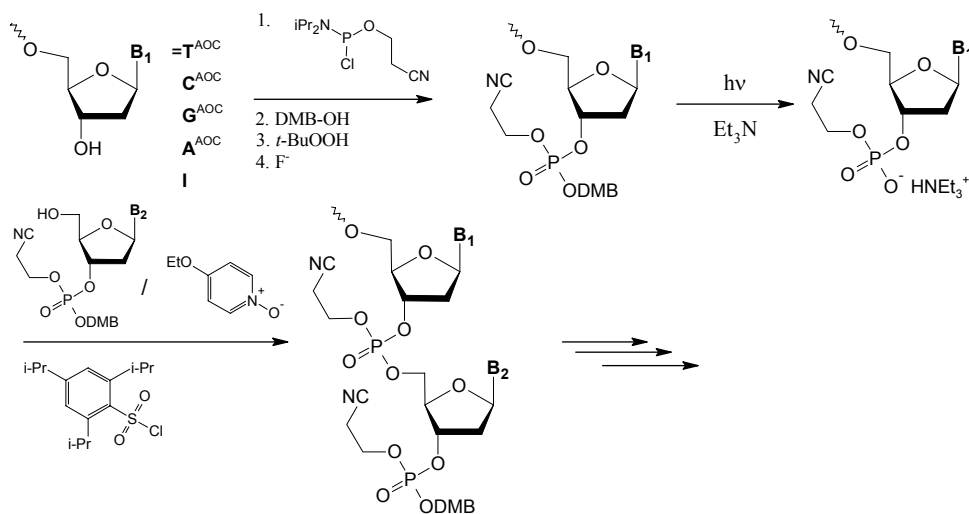
Scheme 18: Inverse DNA synthesis with 3´-DMB-phopshate

Pirrung *et al.*[63-65] developed a method to prepare short DNA sequences using light to deprotect a nucleoside 3'-phosphotriester, providing a phosphodiester useful for coupling with a free 5'-OH-nucleotide (Scheme 18). The dimethoxybenzoin group is used as the photoremovable protecting group for the 3'-phosphate. Cyanoethyl is most effective as the second protecting group on the phosphodiester and allyloxycarbonyl protecting groups (AOC) are used for the nitrogenous bases as they can be removed without cleaving the

DNA from the support. In this manner the authors prepared two simple trinucleotides in solution.

The literature in the microarray technology is plentiful and a good general review with many references is included in a recently published book[6].

1.3.5. Two-Photon Excitation

A relatively new approach in the photolysis of caged compounds is the two-photon excitation (2PE). 2PE refers to the nearly simultaneous absorption of two IR photons of identical frequency in order to excite a molecule from its ground state to a two-photon allowed excited state. The phenomenon was theoretically predicted by Maria Göppert-Mayer[59] in 1931 in her doctoral thesis. However, the first experimental verification was provided by Kaiser et $al.$[60] in 1961, since that is when lasers started to exist. They observed the first 2PE induced fluorescence of a $CaF_2:Eu^+$ crystal. In principal, every chromophore can be excited by this method, which essentially means that all of the presented PPGs can be successfully photolysed. The dark photochemistry or the reaction sequence that follows the excitation is, in most cases, the same as if the molecule was excited with UV radiation. One of the most distinguishing features of 2PE is that the probability of excitation is proportional to the square of the intensity of the excitation beam and to δ_μ, the two-photon absorption cross section measured in GM (1 Göppert-Mayer = $10^{-50} cm^3$ s photon^{-1}). This is different to one-photon excitation (1PE), where the probability depends linearly on the input intensity. In order to generate an appreciable amount of 2PE, high light intensities, such as those obtained from pulsed lasers are required. This technique employs short laser pulses of near-IR radiation in the range of 700-1100 nm. In addition, these lower-energy photons are less likely to cause damage outside of the focal volume. As a result, the photolysis occurs only in the focus of the laser beam, thus allowing for a greater spatial control. The focal volume can be as small as a femtoliter for a tightly focused laser. The development of ultra short tuneable lasers and confocal microscopes greatly accelerates the implementation of this method in many research areas. There are several caveats to using 2PE. Pulsed lasers are generally much more expensive, the microscope requires special optics to withstand the intense pulses. Many of the available PPGs suffer poor efficiency, when photolysed in this manner. The sensitivity of the PPG to 2PE induced photolysis is quantified by δ_μ and should exceed 0.1 GM to be useful[46].

A shortcoming of the 2PE is the fact that the laser power used in biological experiments should not exceed a certain limit (5-10 mW), above which a photodamage due to multiphoton absorption sets in. Multiphoton phototriggers with superior δ_μ will be needed and will play an increasing role in the exploration of cell physiology and other bio-relevant areas[6].

The selection of mentioned applications is highhanded and does not cover all existing applications. There are a number of other areas of research, e.g. time resolved x-ray[73], ultrafast pH jumps and photorelease of nitric oxide, where the PPGs are being used. New challenges are phototriggered drug delivery devices and photoactivatable prodrugs, where a pharmacologically active substance is caged and delivered with spatial and temporal control to specific regions of the human body. These are some of the future challenges, where PPGs will play important roles.

2. Objective

The main goal of the present work is to synthesize and study a novel photoremovable protecting group for acids and phosphates. Our idea is based on the photochemistry of 7-hydroxycoumarin-4-yl-methyl (HCM) acetate (Scheme 19), which is well established and described in the work of Furuta *et al.*[43].
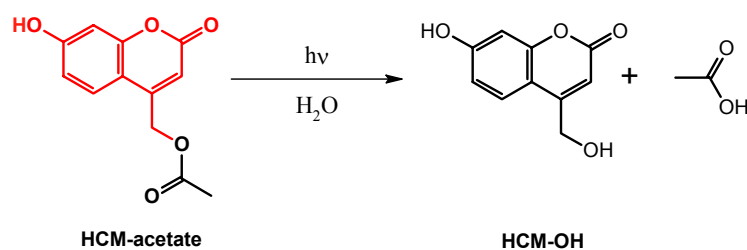
Scheme 19: Photolysis of HCM-acetate

They determined the HCM group as promising member of a newer generation of caging groups, because the unattached 7-hydroxycoumarin chromophore has an acceptable cross section for two-photon excitation of fluorescence. HCM-acetate shows high $\delta\mu$ values (1.07 and 0.13 GM at 740 and 800 nm) for hydrolysis to acetic acid and HCM-OH. The 6-bromo-7-hydroxycoumarin-4-yl-methyl group (Bhc) was designed to lower the pK_a of the C7 hydroxyl group, so that the O-H bond is deprotonated at pH 7, which would further increase the two-photon cross sections, and promote formation of the more strongly absorbing anion. The Bhc group is an efficient photolabile protecting group with a biologically useful cross section for two photon excitation.

We presumed that the same photochemistry would occur, if we extend the chromophoric system to the 3-hydroxy-6-fluorone chromophore. The structure relation between 7-hydroxycoumarin and the 6-hydroxyfluorone is shown in the following figure.
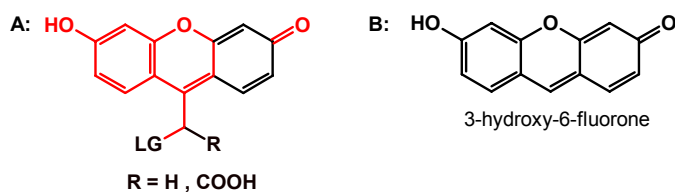
Figure 12: A: A new photoremovable protecting group for acids and phosphates (— Basic structure of the HCM group, LG = Leaving group) **B:** The 3-hydroxy-6-fluorone chromophore[68-70]

Upon excitation of the molecule with light, an electron is transferred from the highest occupied molecular orbital (HOMO) into the lowest unoccupied molecular orbital (LUMO). Hückel-computations (PM3) show a strong increase in the electronic densities in the para position to the oxygen atom in the six membered heterocycle for the coumarin anion as well as for the 3-hydroxy-6-fluorone anion (HFA) during HOMO → LUMO transition (Figure 13 and 14).
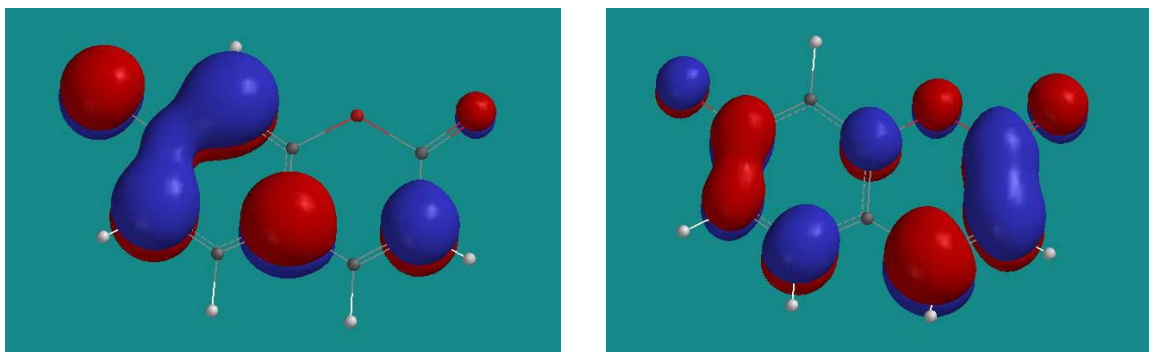
Figure 13: Orbital plots for the $S_0 \to S_1$ transition of the coumarin anion Left: HOMO; Right: LUMO
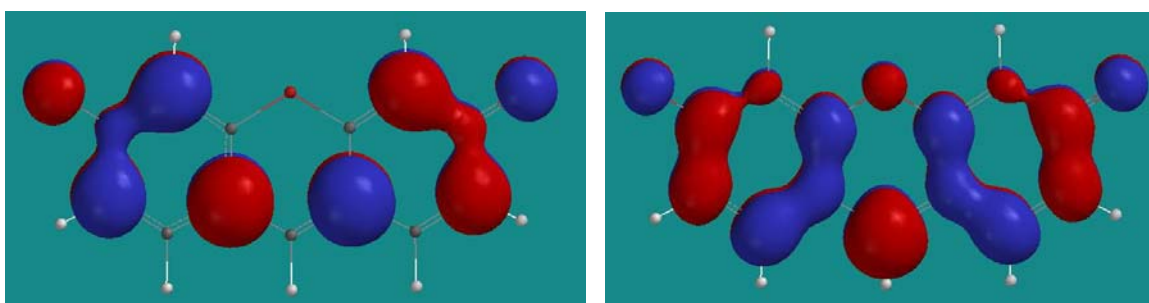
Figure 14: Orbital plots for the $S_0 \to S_1$ transition of the 3-hydroxy-6-fluorone anion
        Left: HOMO; Right: LUMO

The HFA has its absorption maximum in the visible region at 494 nm, which would be very promising for two-photon excitation[61], whereas the HCM lies around 325 nm.

Based on these facts we decided to synthesize at least one of the following two analogues of the 3-hydroxy-6-fluorone group (Figure 15).

LG = Br, OAc, OP=O(OEt)$_2$
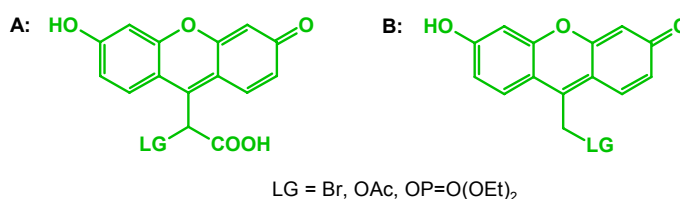
Figure 15: Desired analogues of 3-hydroxy-6-fluorone

Analogue A is based on the (6-hydroxy-3-oxo-3*H*-xanthen-9-yl)acetic acid and should have an enhanced solubility in comparison to B, the (6-hydroxy-3-oxo-3*H*-xanthen-9-yl)methyl group.

For the analogue itself, we want to synthesize three derivatives as model compounds, namely the bromide, the acetate and the diethyl phosphate. The bromide derivative is a good test compound to verify if our idea works, as the bromide is a good leaving group. The acetate and the diethyl phosphate derivative are milestones for future applications of the protecting group, including protection of phosphates and acid functions, as those functionalities are often targeted in biological applications.

Finally investigations concerning the pK_a of the hydroxy group of each model compound should be performed, for testing their applicability at physiological pH value, as well as determination of preliminary photochemical properties.

3. Results and Discussion

In this investigation, attempts were undertaken to synthesize a new photoremovable protecting group for a series of model compounds. The synthesis strategies and the results of these efforts are given in the following chapters.

3.1. Retrosynthetic Analysis, Literature Research and Starting Materials

The strategy was to implement first a retrosynthetic analysis[62] on the target molecule (TM) and afterwards to set about literature research on readily available starting materials (RASM). The TM was broken down into the following disconnections due to symmetry facts (Figure 16).
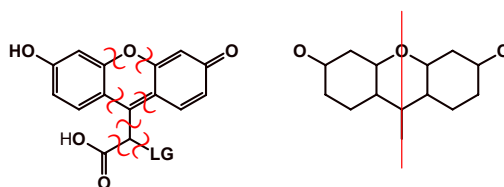
Figure 16: Chosen retrosynthetic analysis (left) due to the symmetry (right) of the target molecule

The skeleton of 3-hydroxy-6-fluorone (**4**) is the parent heterocyclic skeleton of the xanthene dye, fluorescein. The literature research gave the following result: Neckers *et al.* developed a series of 9-hydrogen and 9-cyano substituted fluorones, these compounds are useful as fluorescers and photoinitiators[63-66].
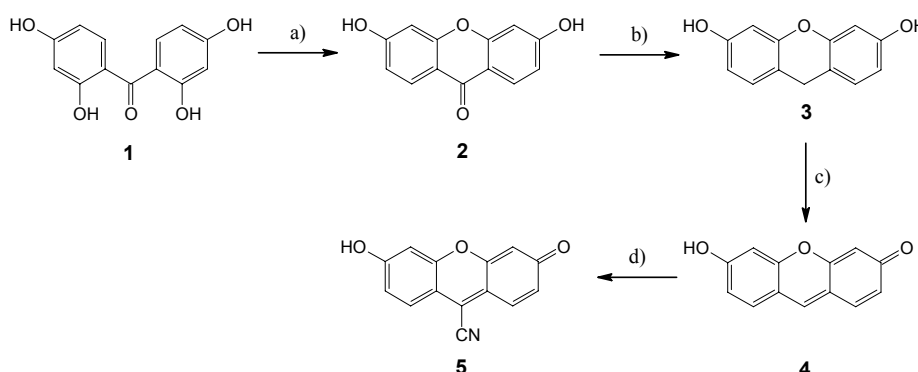
Scheme 20: Synthesis of 9-cyano-3-hydroxy-6-fluorone (**5**) according to Neckers *et al.* starting from 2,2′,4,4′-tetrahydroxybenzophenone (**1**). a)….H_2O/200°C; b)….BH_3/THF; c)….DDQ/EtOH; d)….KCN/DMF

This scheme offers beside the 9-cyano-3-hydroxy-6-fluorone the following precursors:

- 3,6-dihydroxy-9*H*-xanthen-9-one (**2**)
- 9*H*-xanthene-3,6-diol (**3**)
- 9-cyano-3-hydroxy-6-fluorone (**5**)

As xanthenes are some of the oldest known synthetic dyes such as fluorescein, rhodamine and ethyl eosin, as well as many others, there are plenty of reports. The first compound with a dibenzo[*b,e*]pyrylium structure (xanthylium), namely fluorescein, was developed by Baeyer in 1871[67], even though he proposed the constitution differently. Dibenzo[*b,e*]pyrylium ions are weak electrophiles and are stable only when associated with anions of a strong acid, such as chloride, perchlorate and hydrosulphate, etc. Condensations of aldehydes or anhydrides with resorcinols are usually accomplished in hot sulphuric acid[68-72].
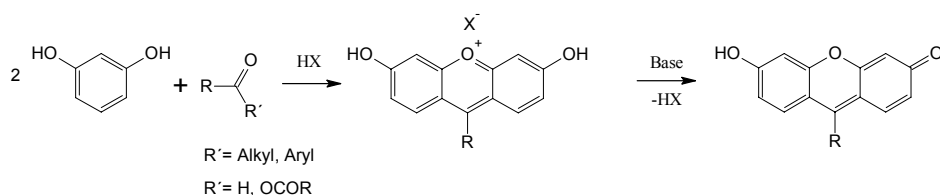
Scheme 21: Preparation of xanthene dyes according to Baeyer *et al*.

Reduction of dibenzo[*b,e*]pyrylium salt, typically with sodium borohydride in water gives the 10*H*-dibenzo[*b,e*]pyrans. Carbon nucleophiles such as methyl ketones and Grignard reagents attack at position C10 (Scheme 22).
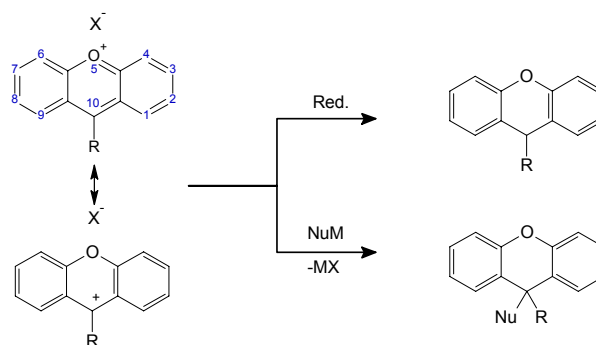
Scheme 22: Possible transformations of dibenzo[*b,e*]pyrylium salts

The result from the retrosynthetic analysis and from the literature led to the following chosen disconnection approach.
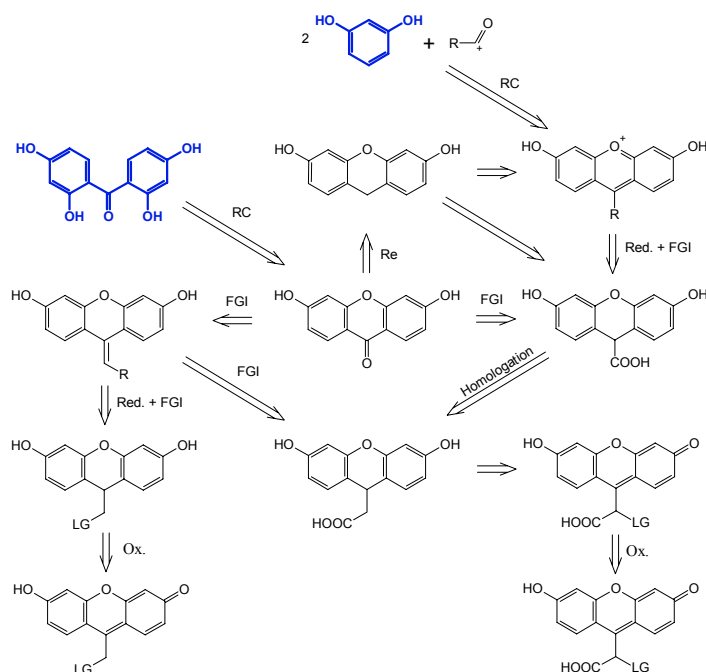
Scheme 23: A rough disconnection approach sketch: FGI...Functional group interconversion, RC...Ring closure, Red...Reduction, Ox...Oxidation. (— RASM)

Reactants, reaction conditions, and functionalities involved in the proposed synthetic scheme had to be considered in detail, for selecting a specific protective group. The methyl ether has been chosen for the protection of the phenols since there are efficient and easy methods for the preparation[1]. For the deprotection boron tribromide has been chosen, as it is the reagent of choice for the cleavage of ethers. It has been used widely to cleave ether protecting groups under mild conditions without affecting a large number of other functional groups[73,74]. Boron tribromide is compatible with the following functional groups: C=C, carbonyl, carboxyl, nitrile, nitro, methylenedioxy and ester.

3.2. Attempted Syntheses of Analogue A:
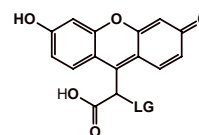
3.3. Attempted Synthesis of 6-Methoxy-3-oxo-3*H*-xanthene-9-carboxylic acid (7)

The synthesis of the 6-methoxy-3-oxo-3*H*-xanthene-9-carboxylic acid (**7**) should provide access to the desired analogue **A** (Scheme 24). The idea behind was that homologation of **7** via Arndt-Eistert or Kowalski and subsequent α-bromination would afford the methyl protected analogue **A** (Figure 17). The bromide should then give access to diethyl phosphate and acetate followed by deprotection to the desired analogue **A**.
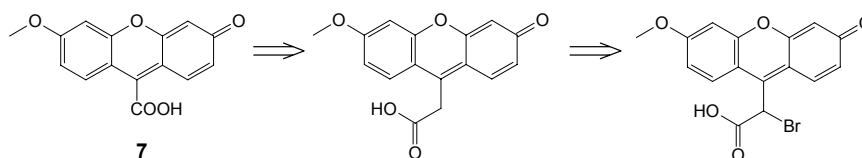
Scheme 24: Retrosynthesis which leads to analogue **A** starting from 6-methoxy-3-oxo-3*H*-xanthene-9-carboxylic acid **7**

The 9-cyano-3-hydroxy-6-fluorone (**5**) was synthesized according to Neckers *et al.* (Scheme 25). *O*-methylation of **5** was performed with dimethyl sulphate in the system K$_2$CO$_3$/acetone resulting in only 43% 6-methoxy-3-oxo-3*H*-xanthene-9-carbonitrile **6** after 6 h reflux. The subsequent hydrolysis with 50% H$_2$SO$_4$ failed, presumably due to assumed xanthylium salt formation and also very poor solubility of the nitrile.
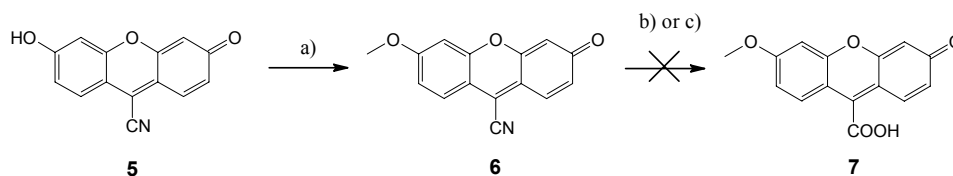
Scheme 25: Targeted sequence for the synthesis of 6-methoxy-3-oxo-3*H*-xanthene-9-carboxylic acid **7** starting from the 9-cyano-3-hydroxy-6-fluorone (**5**) via protection of the phenol and hydrolysis of the 6-methoxy-3-oxo-3*H*-xanthene-9-carbonitrile (**6**). The hydrolysis of **6** failed in this sequence. a)….dimethyl sulfate/K$_2$CO$_3$/acetone, b)….50% H$_2$SO$_4$, c)….KOH, H$_2$O, diethylene glycol.

Hydrolysis with potassium hydroxide in the system H₂O/diethylene glycol resulted surprisingly in the formation of 3-hydroxy-6-methoxy-9*H*-xanthen-9-one (**9**). The only reasonable explanation for this is a 1,6-conjugated substitution. Nucleophilic attack of the hydroxyl ion at position C9 leads to a 9-cyano-9-hydroxy-6-methoxy-9*H*-xanthen-3-olate intermediate (**7**) (Scheme 26). Subsequent regeneration of the quinone methide system via release of cyanide tends to result in the 9-hydroxy-6-methoxy-3*H*-xanthen-3-one (**8**), which is the minor tautomeric form of **9**. This also explains the moderate yield of **6**.
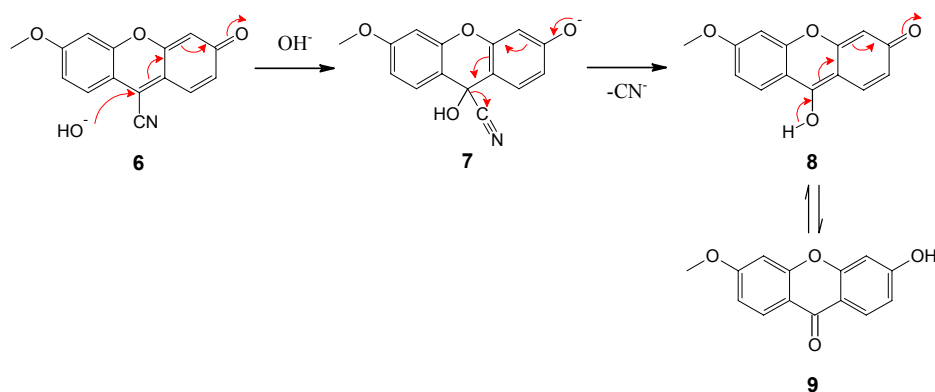
Scheme 26: Mechanism for the formation of 3-hydroxy-6-methoxy-9*H*-xanthen-9-one (**9**)
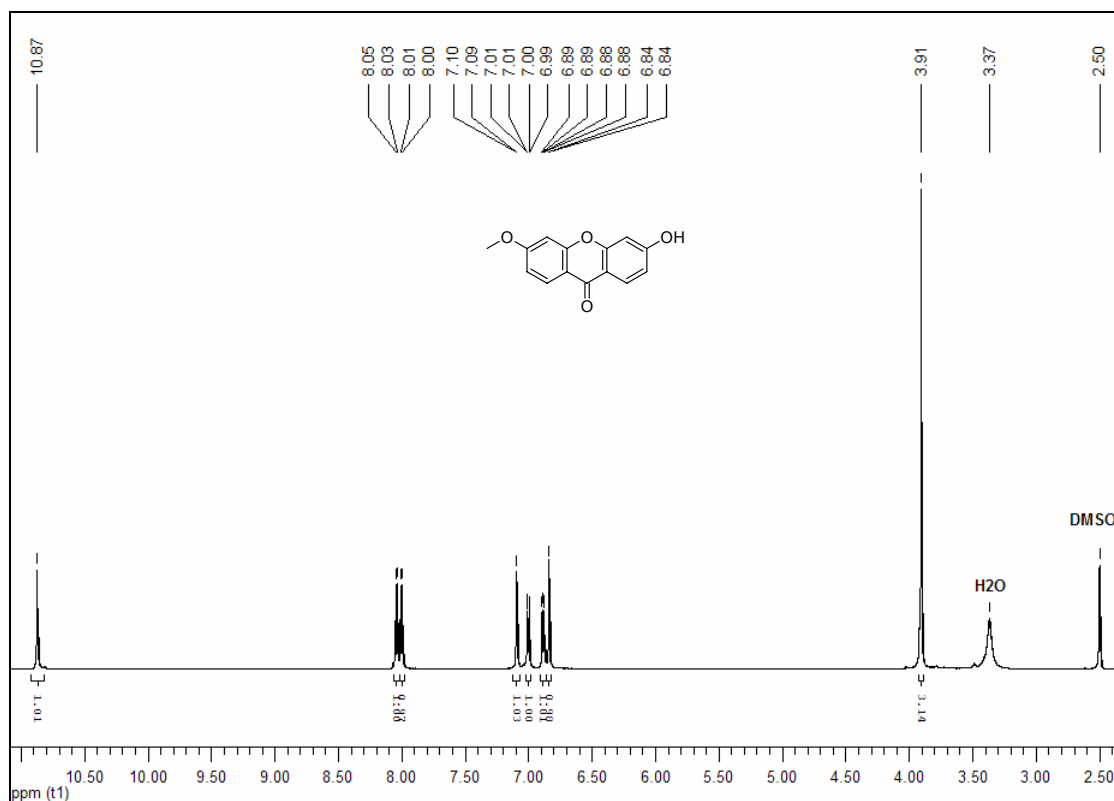
Figure 17: ¹H NMR spectrum (600 MHz, *δ*, *DMSO*-d₆, 25°C) of 3-hydroxy-6-methoxy-9*H*-xanthen-9-one (**9**).

3.4. Attempted Synthesis of 3,6-Dimethoxy-9*H*-xanthene-9-carboxylic acid (13)

The 3,6-dimethoxy-9*H*-xanthene-9-carboxylic acid (**13**) could be envisaged as further convenient precursor for both analogues, **A** and **B** (Scheme 27).
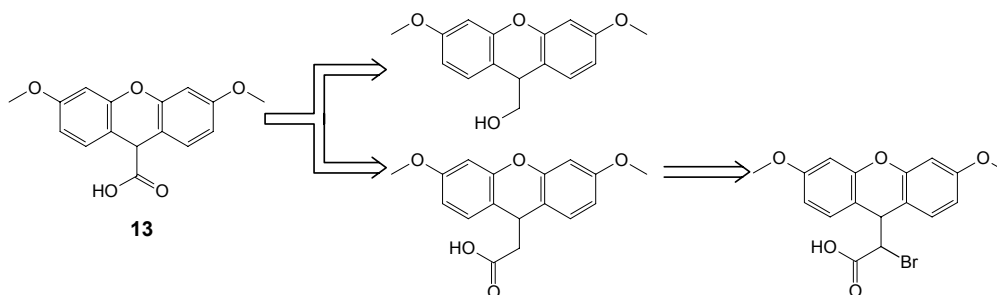
Scheme 27: Retrosynthesis starting from 3,6-dimethoxy-9*H*-xanthene-9-carboxylic acid (**13**) which leads to precursors for analogue **A** and **B**

Therefore efforts were undertaken to achieve the synthesis of compound **13** by carbon skeleton extension. The following two routes were considered (Scheme 28). On route A, addition of trimethylsilyl cyanide (TMSCN) to the *O*-methyl protected 3,6-dihydroxy-9*H*-xanthen-9-one (**10a**) should give the corresponding trimethylsilylated cyanohydrin **11**, followed by hydrolysis in the presence of tin (II) chloride to achieve the carboxylic acid **13**. On route B, reduction of the *O*-methyl protected ketone with sodium borohydride to 3,6-dimethoxy-9*H*-xanthene (**12**) and subsequent metalation at the position C9 using butyl- or phenyllithium, followed by treatment with carbon dioxide should afford carboxylic acid **13**.
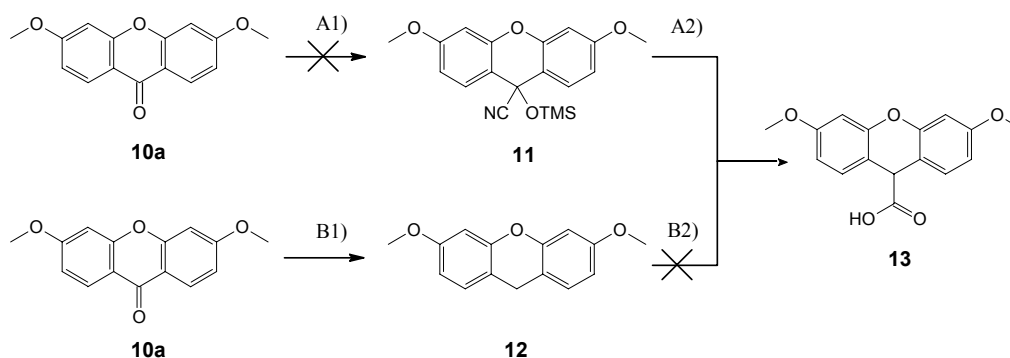
Scheme 28: Targeted sequences for the synthesis of 3,6-dimethoxy-9*H*-xanthene-9-carboxylic acid (**13**) starting from 3,6-dimethoxy-9*H*-xanthen-9-one (**10a**) via Route A or B: A1)….TMSCN/ZnI$_2$/CH$_2$Cl$_2$, A2)….SnCl$_2$·(H$_2$O)$_2$/AcOH/HCl conc., B1)….NaBH$_4$/EtOH, B2)…..RLi/CO$_2$.

3.4.1. Attempted Synthesis of 3,6-Dimethoxy-9*H*-xanthene-9-carboxylic acid (13) via Route A

Complete *O*-methylation of 3,6-dihydroxy-9*H*-xanthen-9-one (**2**) was performed with dimethyl sulphate in the system K_2CO_3/acetone resulting in 93% 3,6-dimethoxy-9*H*-xanthen-9-one (**10a**) after 20 h reflux (Scheme 29).
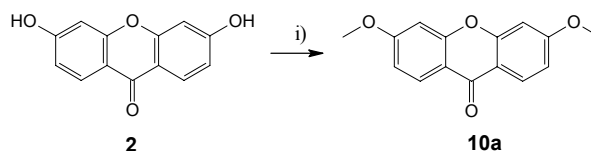
Scheme 29: Synthesis of 3,6-dimethoxy-9*H*-xanthen-9-one (**10a**). i)…. dimethylsulphate/K_2CO_3/acetone

The trimethylsilyl cyanide (TMSCN) addition to 3,6-dimethoxy-9*H*-xanthen-9-one (**10a**) according to Schoepp *et al.*[75] did not provide the desired trimethylsilylated cyanohydrin **11** and thereby route A failed. One possible reason is that the addition of cyanides to aldehydes or ketones is usually an equilibrium reaction that may lie too far to the left for diaryl ketones.

3.4.2. Attempted Synthesis of 3,6-Dimethoxy-9*H*-xanthene-9-carboxylic acid (13) via Route B

The reduction of 3,6-dimethoxy-9*H*-xanthen-9-one (**10a**) to the 3,6-dimethoxy-9*H*-xanthene (**12**) was carried out with sodium borohydride in
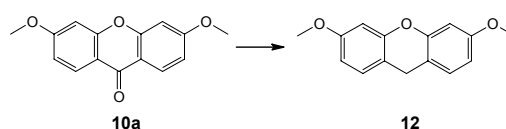
ethanol as per Kulkarni *et al.*[76]. After 8 h refluxing, removal of ethanol, acidic hydrolysis and purification via preparative TLC led to the xanthene **12** in 67.3 % yield. Subsequent metalation with butyllithium in dry Et_2O under argon at room temperature, followed by bubbling a stream of dry carbon dioxide through the solution at -78°C, acidifying and extraction leads to an unsatisfying mixture of diverse xanthene derivatives, and thus route B failed. This procedure failed assumedly due to Snieckus ortho lithiation[77]. Directed ortho metalation is an adaptation of electrophilic aromatic substitution in which electrophiles attach themselves exclusively to the ortho-position of a direct metalation

group (DMG) through the intermediary of an aryllithium compound. The DMG interacts with lithium through a hetero atom. Examples of DMGs are the methoxy group, a tertiary amine group and an amide group.
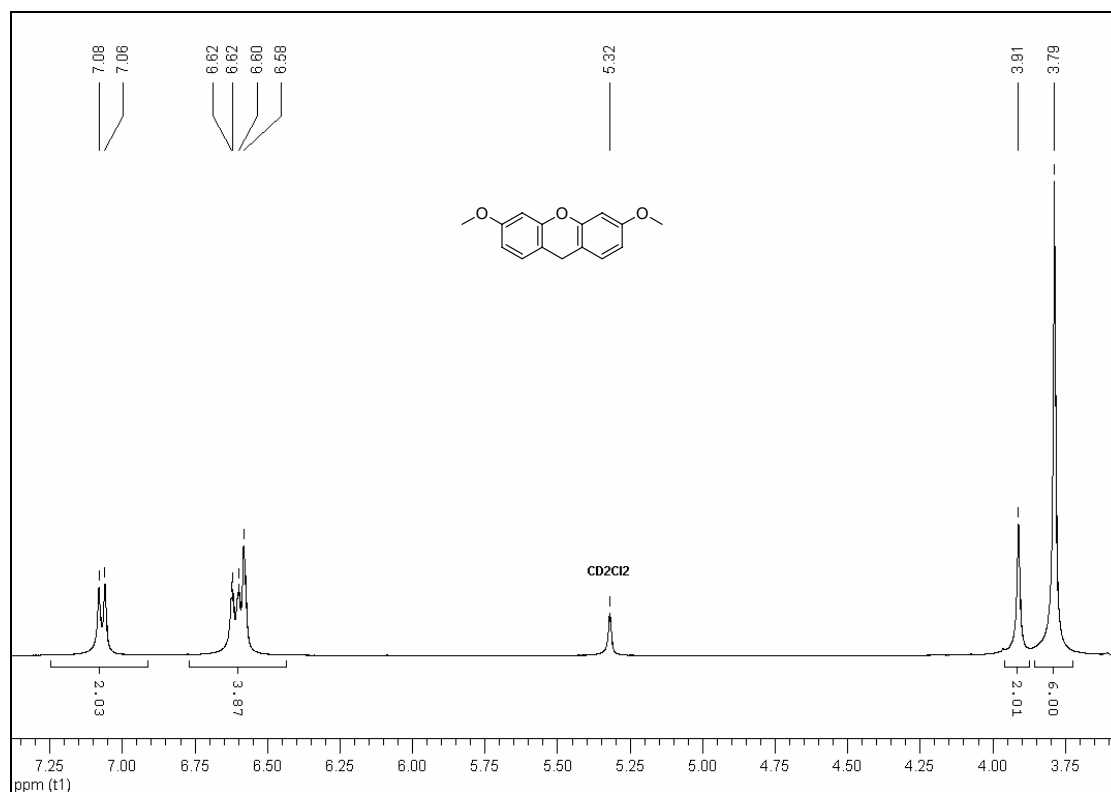
Figure 18: ^{1}H NMR spectrum (400 MHz, δ, CD_2Cl_2, 25°C) of 3,6-dimethoxy-9H-xanthene (**12**).

3.5. Attempted Synthesis of Dimethyl bromo(3,6-dimethoxy-9*H*-xanthen-9-yl)malonate (15)

Manganese (III) acetate has been used for the carbon-carbon bond formation between dimethyl bromomalonate (**14**) and 3,6-dimethoxy-9*H*-xanthene (**13**). Manganese (III) acetate is known as a one-electron oxidant. The synthesis of dimethyl bromo(3,6-dimethoxy-9*H*-xanthen-9-yl)malonate (**15**) was prepared according to the procedure of Nishino *et al.*[78] in refluxing glacial acetic acid (Scheme 30).
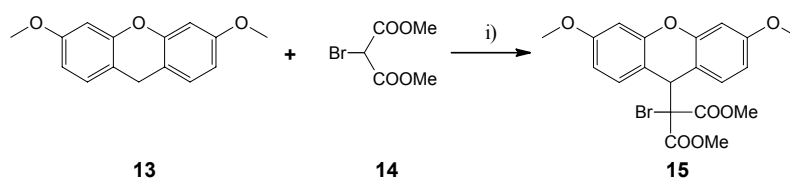
Scheme 30: Synthesis of dimethyl bromo(3,6-dimethoxy-9*H*-xanthen-9-yl)malonate (**15**) according to the procedure of Nishino *et al.* i)….Mn(OAc)$_3$·3H$_2$O/AcOH/reflux.

However, its purification turned out to be very difficult due to the similarity of R$_f$-values and the solubility of the contaminating by-products. Even after two preparative TLCs with different eluents, the main product **15** could not been obtained in a form pure enough for further reaction, maybe due to instability of **15**. By using NMR spectroscopy it could be confirmed, that dimethyl bromo(3,6-dimethoxy-9*H*-xanthen-9-yl)malonate (**15**) was formed.
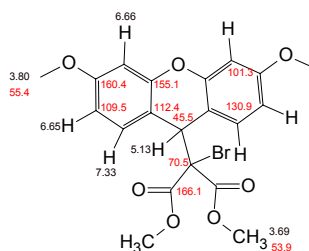
Figure 19: Structural assignment of dimethyl bromo(3,6-dimethoxy-9*H*-xanthen-9-yl)malonate **15**

3.6. Attempted Synthesis of Ethyl (3,6-dimethoxy-9*H*-xanthen-9-yl)acetate (17)

Another possibility to obtain analogue **A** is via carbon-carbon bond formation through Wittig-Horner type condensation (Scheme 31).
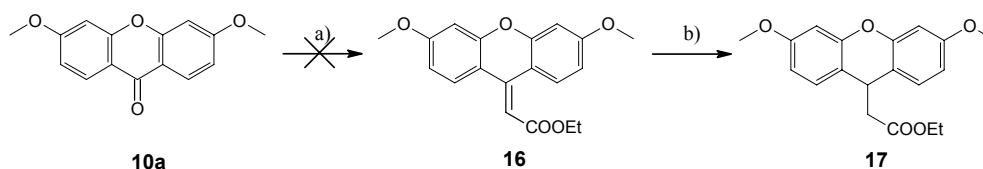
Scheme 31: Targeted sequence for the synthesis of ethyl (3,6-dimethoxy-9H-xanthen-9-yl)acetate (**17**) starting from 3,6-dimethoxy-9*H*-xanthen-9-one (**10a**) via Horner-Wadsworth-Emmons reaction (HWE), followed by catalytic hydrogenation of ethyl (3,6-dimethoxy-9H-xanthen-9-ylidene)acetate (**16**). The HWE was unsuccessful in this sequence. a)….(EtO)$_2$P(O)CH$_2$COOEt/Base, b)….Pd-C (10%)/EtOH.

Ethyl (3,6-dimethoxy-9*H*-xanthen-9-ylidene)acetate (**16**) seems to be an ideal precursor for the synthesis of compound **17**. For this purpose, the Horner-Wadsworth-Emmons reaction was chosen. Condensation of triethyl phosphonoacetate in the presence of a strong base (NaH or KHMDS) should gain **16**. The stereochemical outcome is not deemed relevant, since the next step involves hydrogenation. Thus catalytic hydrogenation of the unsaturated ester **16** in the presence of Pd-C should result in the reduction of the double bond to afford **17**.

No conditions were found to effect the HWE-reaction. Interestingly the reaction was sluggish or did not proceed at all. One possible reason for the failure of this reaction could be the sterical hindrance of the formation of the 1,2-oxaphosphetane intermediate, due to the fact that xanthones are sterically hindered ketones.

In conclusion, all the attempts to access the targeted analogue **A** failed due the reasons mentioned above, therefore the focus was set on the synthesis of analogue **B**.

3.7. Attempted Synthesis of Analogue B:
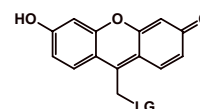
The synthesis of the (3,6-dimethoxy-9*H*-xanthen-9-yl)methanol (**24a**) should provide access to the desired analogue **B** (Scheme 32). The idea behind was that functional group interconversion of **24a** and subsequent deprotection, followed by oxidation, would afford the analogue **B**. Two possible routes to obtain precursor **24a** (Scheme 32) were considered. Route A follows the Wittig strategy by carbon skeleton extension through coupling with (methoxymethyl)triphenylphosphonium chloride, followed by hydrolysis and reduction to afford **24a**.
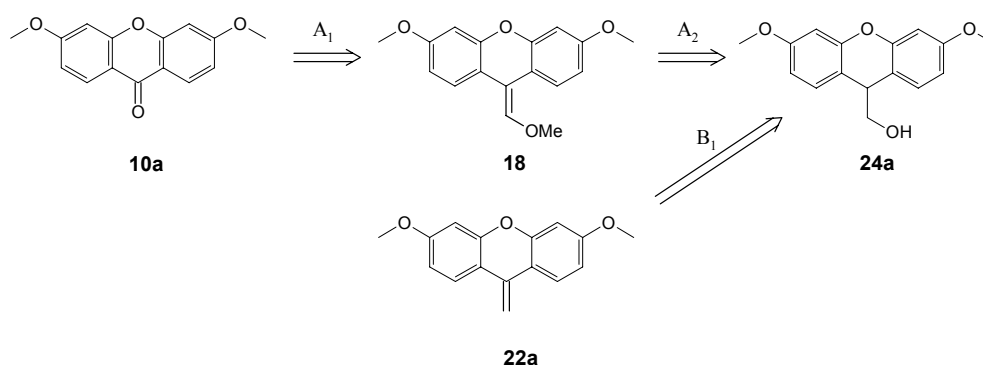
Scheme 32: Retrosynthesis starting from **10a** or from 3,6-dimethoxy-9-methylene-9*H*-xanthene (**22a**) which leads to the precursor (3,6-dimethoxy-9*H*-xanthen-9-yl)methanol (**24a**) for analogue **B**.

As the HWE-reaction on 3,6-dimethoxy-9H-xanthen-9-one (**10a**) failed, the Wittig reaction was ruled out for the synthesis of precursor **24a** via route A, focusing on the route for analogue **B**. An promising precursor for the synthesis of 3,6-dimethoxy-9H-xanthen-9-yl)methanol (**24a**) constitutes the (3,6-dimethoxy-9-methylene-9H-xanthene (**22a**). Hydroboration of the terminal olefin **22a** followed by treatment with hydroperoxide should afford the alcohol **24a**. A literature search based on olefination of ketones to obtain the terminal olefin **22a** gave the following results: 1) Evans *et al.*[86,87] prepared 3,6-diethoxy-9-methylene-9H-xanthene (**22b**) via exhaustive C-methylation of the appropriate ketone **10b** with trimethyl aluminium (Scheme 33).
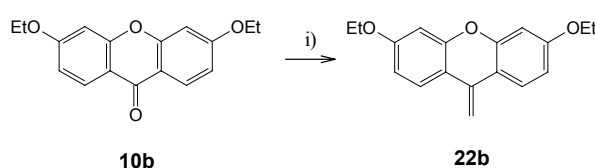
Scheme 33: Synthesis of 3,6-diethoxy-9-methylene-9H-xanthene (**22b**) according to Evans *et al.*
i)….Me$_3$Al/Benzene/Nitrogen

2) Poronik *et al.*[79] synthesized **22a** through condensation of resorcinol with acetic anhydride followed by neutralization and methylation (Scheme 34).
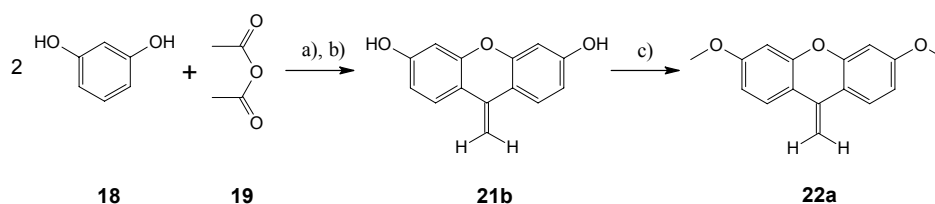
Scheme 34: Synthesis of 3,6-dimethoxy-9-methylene-9H-xanthene (**22a**) according to Poronik *et al.*
a)….HBr, b)….Pyridine, c)….CH$_3$OTs/K$_2$CO$_3$.

3.7.1. Synthesis of 3,6-Dimethoxy-9-methylene-9*H*-xanthene (22a)

By preparing 3,6-dimethoxy-9-methylene-9H-xanthene (**22a**) as described by Poronik *et al*.[79] we discovered discrepancies. They claim having obtained **21b** by treatment of the 3,6-dihydroxy-9-methylxanthenium bromide (**20**) with pyridine and subsequent removal of pyridinium bromide with water, which is incorrect. In fact they obtained mainly 6-hydroxy-9-methyl-3*H*-xanthen-3-one (**21a**) (Scheme 35) that is the tautomeric form of **21b** as we will show by the following facts. First, the absorption spectrum is similar to that of 3-hydroxy-6-fluorone (**4**) (Figure 20). Second, they recorded the ^{1}H NMR of the product obtained in d_6-DMSO because of poor solubility and that was the origin for their misinterpretation. The enol form **21b** is stabilized by hydrogen bonding between its OH and the d_6-DMSO, which serves as a hydrogen bond acceptor and that is the reason why they observed **21b**. Reports of Rappoport *et al*.[80] and Amat-Guerri *et al*.[70,72] on similar compounds support this finding.
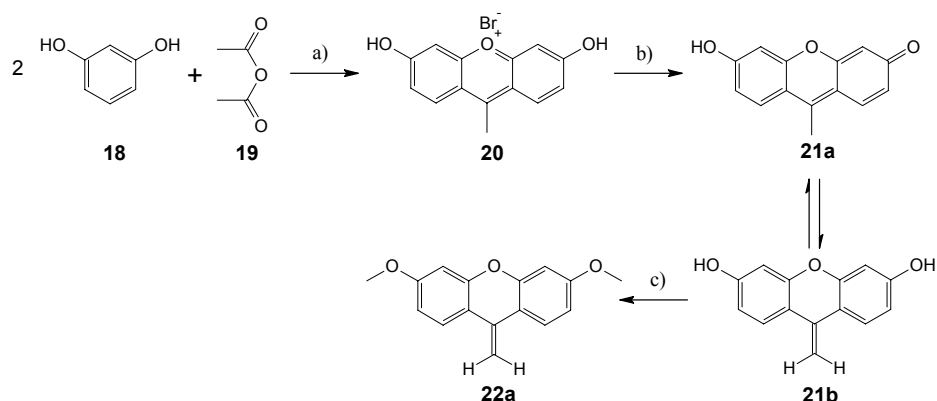
Scheme 35: Synthesis 3,6-dimethoxy-9-methylene-9*H*-xanthene (**22a**) starting from resorcinol and acetic anhydride. (a)……HBr 46%, 90 °C; (b)……Pyridine/water; (c)……Dimethyl sulphate/K$_2$CO$_3$/acetone
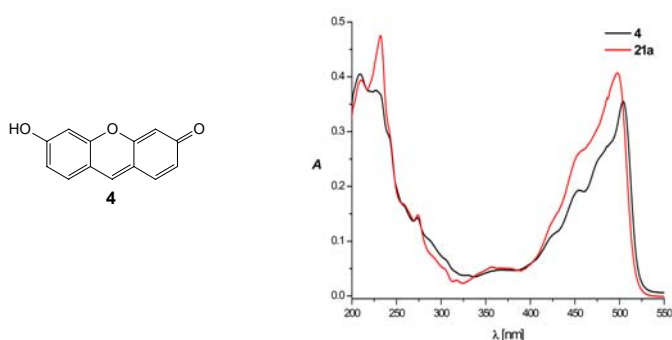
Figure 20: Absorption spectra of **4** (—, λ_{max} = 504 nm) and **21a** (—, λ_{max} = 498 nm) in EtOH

Third, attempts to obtain the 9-(hydroxymethyl)-9*H*-xanthene-3,6-diol (**24b**) (Scheme 36) via hydroboration of the assumed olefin **21b** in THF, followed by oxidation resulted only in the formation of 9-methyl-9*H*-xanthene-3,6-diol (**23**).
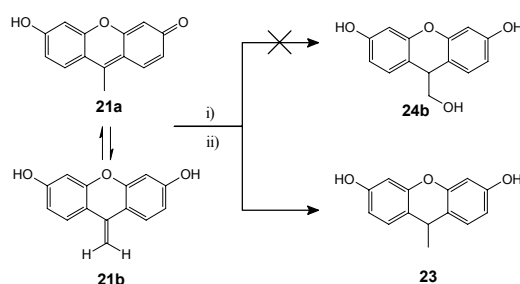
Scheme 36: Attempt for the Synthesis of 9-(hydroxymethyl)-9*H*-xanthene-3,6-diol (**24b**). The synthesis failed due to fact that **21** mainly exists in the tautomeric form **21a**. i)….BH$_3$/THF, ii)….NaOH/H$_2$O$_2$.

The condensation of resorcinol with acetic anhydride in hydrobromic acid at 90°C for 5 h gave the 3,6-dihydroxy-9-methylxanthenium bromide **20** in 32 % yield (based on **18**). Poronik *et al*. did not investigate the analysis and structural assignment of **20**. Here compound **20** was fully characterized on the basis of combustion analysis, IR, UV/Vis, MS and NMR spectra[81], particularly by 2D NMR measurements including HMQC, HMBC, COSY and N*O*ESY experiments. The ^{1}H NMR spectrum of the cation in CF$_3$COOD is shown in Figure 21.
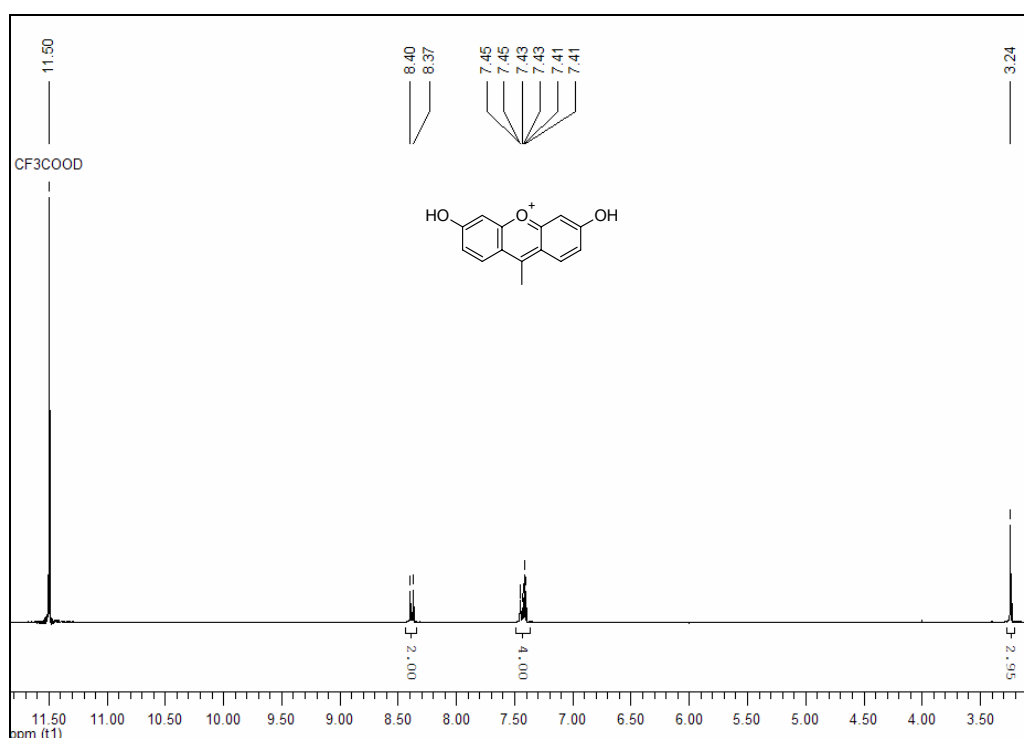
Figure 21: ^{1}H NMR spectrum (400 MHz, δ, *CF$_3$COOD*, 25°C) of the 3,6-dihydroxy-9-methylxanthenium-cation (**20**).

Treatment of **20** with pyridine and subsequent removal of the formed pyridinium bromide by adding water gives **21a** in 93 % yield through precipitation. The ^{1}H NMR spectrum of **21b** (**21a** in DMSO) is shown in Figure 22.
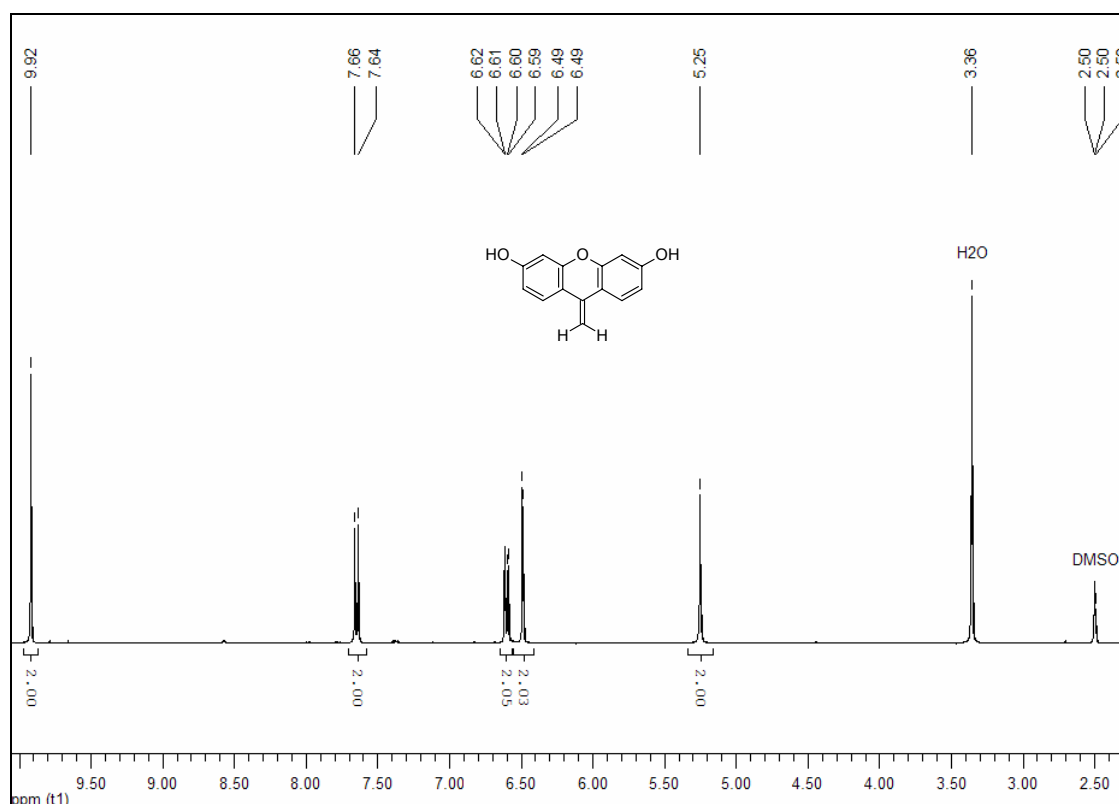
Figure 22: ^{1}H NMR spectrum (400 MHz, δ, DMSO-d$_6$, 25°C) of 9-methylene-9H-xanthene-3,6-diol (**21b**).

Poronik *et al*. applied the system methyl tosylate/K$_2$CO$_3$/18-crown ether-5 for the conversion of **21a** to **22a**, but they did not mention any solvent in their report. The *O*-methylation of **21a** was performed with dimethyl sulphate in the system K$_2$CO$_3$/acetone, which resulted in 86 % 3,6-dimethoxy-9-methylene-9H-xanthene **22a** after 22 h reflux. The methylation is possible, because of the conditions of the reaction. Acetone is a polar aprotic solvent which also forms intermolecular hydrogen bonds and therefore forces the formation of the 9-methylene-9H-xanthene-3,6-diol intermediate.

The synthesis of 3,6-dimethoxy-9-methylene-9H-xanthene (**22a**) was also carried out according to Evans *et al*. [86,87] by adding one third of a 2M trimethyl aluminum solution to the suspension of the ketone in benzene at room temperature, followed by warming up to 50°C until it became homogeneous. After cooling down to 25 − 30°C, the remaining two thirds of Me$_3$Al were added. The reaction was completed by heating at 60°C for 40

minutes followed by hydrolysis and work up led to **22a** in a comparable 70% yield (73%[82]). By a slightly modified procedure, **22a** was obtained in an almost quantitative yield (98 %). The reaction was carried out in a mixture of benzene and toluene in the ratio of 3:2 instead of benzene, and the reaction was completed at 65°C for 90 minutes. The ^{1}H-NMR spectrum of **22a** is shown below in Figure 23
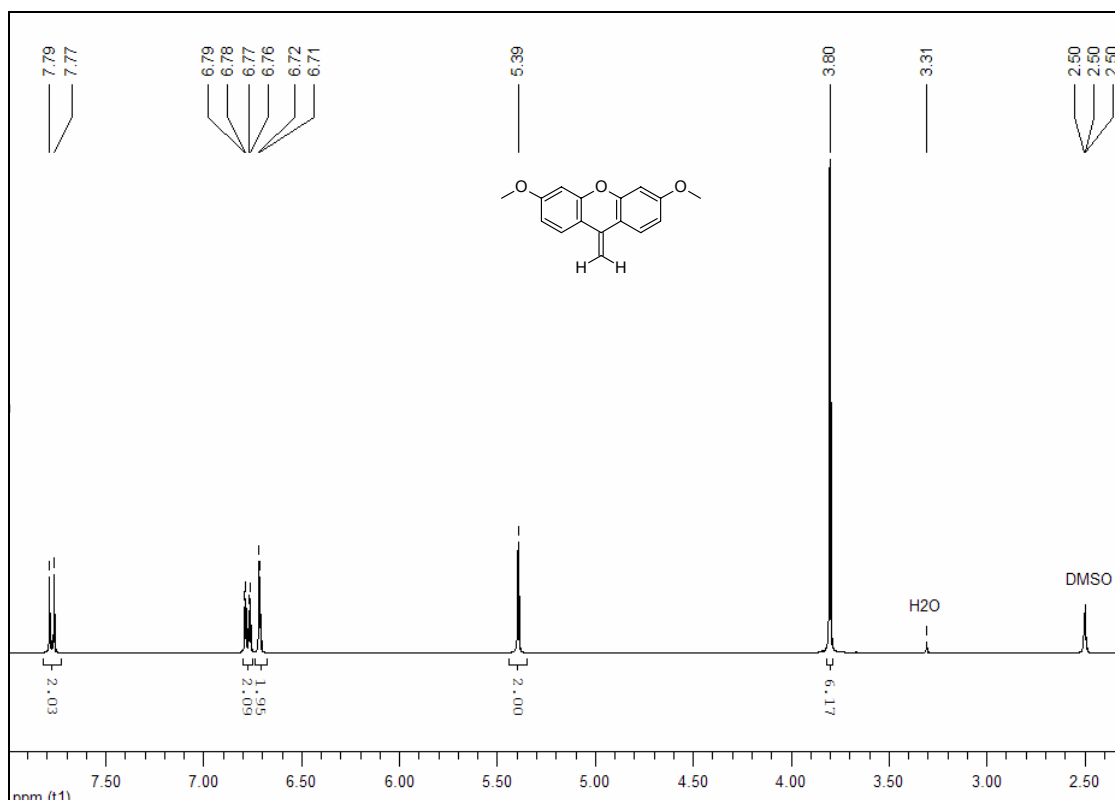
Figure 23: ^{1}H NMR spectrum (400 MHz, δ, *DMSO*-d$_6$, 25°C) of 3,6-dimethoxy-9-methylene-9*H*-xanthene (**22a**).

The synthesis according to Poronik *et al*. (Route A) starting from resorcinol yielded **22a** in 25% overall yield, whereas the synthesis according to Mole *et al*. (Route B) proceeded in 83% overall yield (Scheme 37).

Compound **22a** has to be stored under argon atmosphere because it is oxidized to 3,6-dimethoxy-9*H*-xanthen-9-one (**10**) (apparently photochemically) or it can be purified before use by extraction with hot hexane.
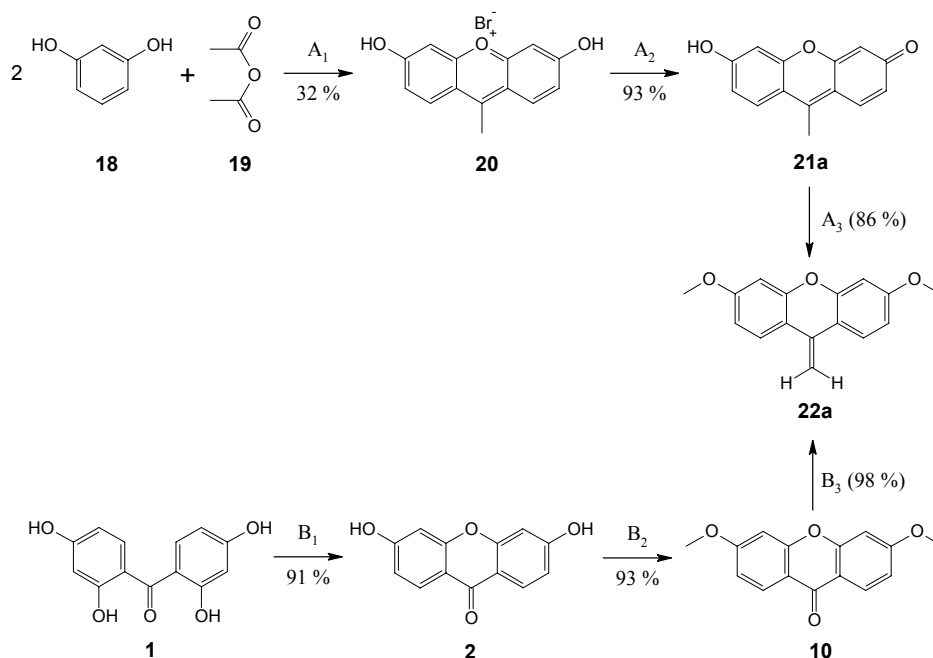
Scheme 37: Comparative overview of route A (overall yield 25 %) and B (overall yield 83 %) to obtain 3,6-dimethoxy-9-methylene-9H-xanthene (**22a**)

3.7.2. Synthesis of (3,6-Dimethoxy-9H-xanthen-9-yl)methanol (24a) as a Key Compound for (3,6-Dimethoxy-9H-xanthen-9-yl)methyl Group Appended Caged Molecules

The synthesis of the key compound (3,6-dimethoxy-9H-xanthen-9-yl)methanol (**24a**) can be achieved by conversion of 3,6-dimethoxy-9-methylene-9H-xanthene (**22a**) by hydroboration and oxidation reaction. This two-step reaction converts an alkene into an alcohol by the net addition of water across the double bond. Hydroboration-oxidation is an anti-Markovnikov reaction, with the hydroxyl group attaching to the lesser substituted carbon. Tetrahydrofuran is the standard solvent used for this reaction.

Thus, the 3,6-dimethoxy-9H-xanthen-9-yl)methanol (**24a**) was synthesized according to conventional procedures[83,84] by adding a 1M BH_3-THF complex solution to 3,6-dimethoxy-9-methylene-9H-xanthene (**22a**) in THF, followed by addition of a 3 M solution of aqueous sodium hydroxide and subsequent treatment with a 30% hydroperoxide solution. Work up and purification by column chromatography (SiO_2, $CHCl_3$/MeOH =20/1) afforded **24a** in 89 % yield (Scheme 38).
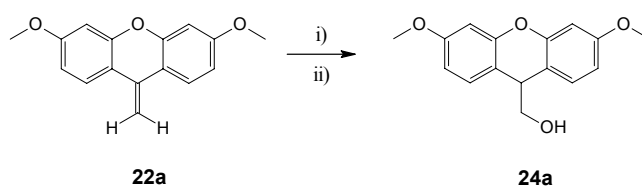
Scheme 38: Synthesis of (3,6-dimethoxy-9*H*-xanthen-9-yl)methanol (**24a**) starting from 3,6-dimethoxy-9-methylene-9*H*-xanthene (**22a**) via hydroboration and subsequent oxidation. i).... BH₃/THF, ii)....NaOH/H₂O₂.

Compound **24a** was fully characterized on the basis of combustion analysis, IR, UV/Vis, MS and NMR spectra, particularly by 2D NMR measurements including HMQC and COSY. The ¹H NMR spectrum of **24a** is shown below.
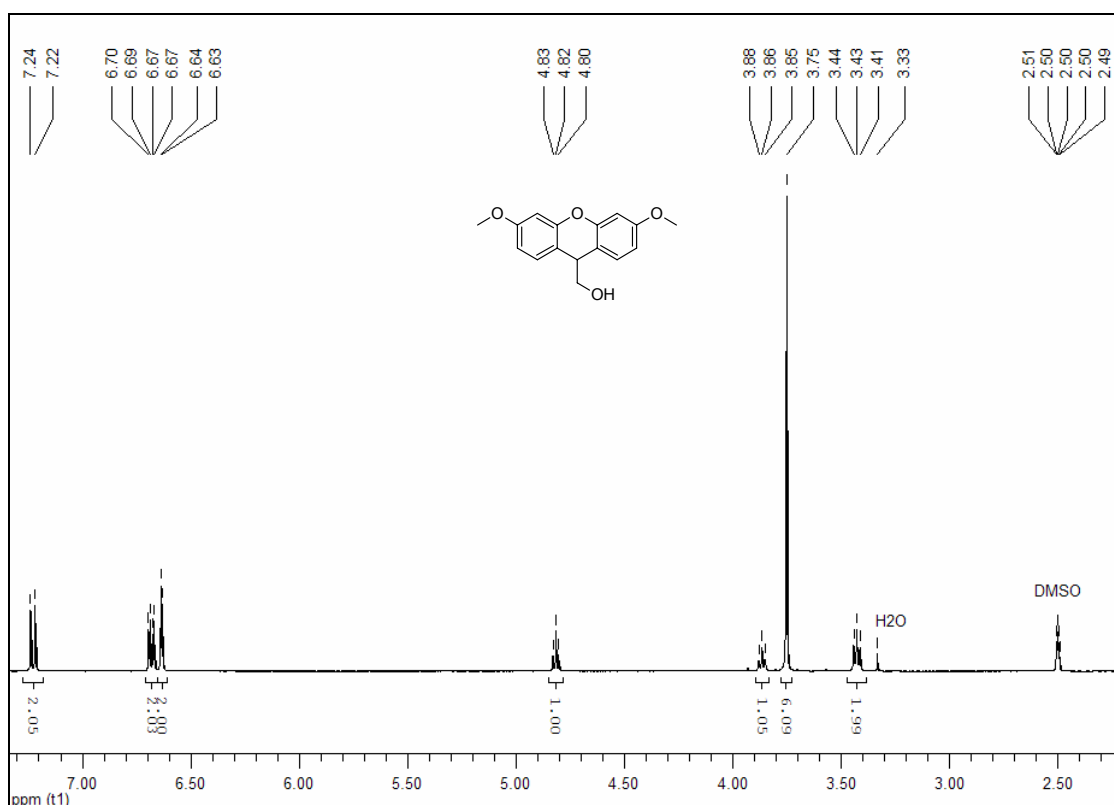
Figure 24: ¹H NMR spectrum (400 MHz, δ, *DMSO*-d₆, 25°C) of (3,6-dimethoxy-9*H*-xanthen-9-yl)methanol (**24a**).

An important key compound for the synthesis of (3,6-dimethoxy-9*H*-xanthen-9-yl)methyl caged molecules constitutes the (3,6-dimethoxy-9*H*-xanthen-9-yl)methanol (**24a**), due to the fact that **24a** can be transformed into them via nucleophilic substitution (Scheme 39).
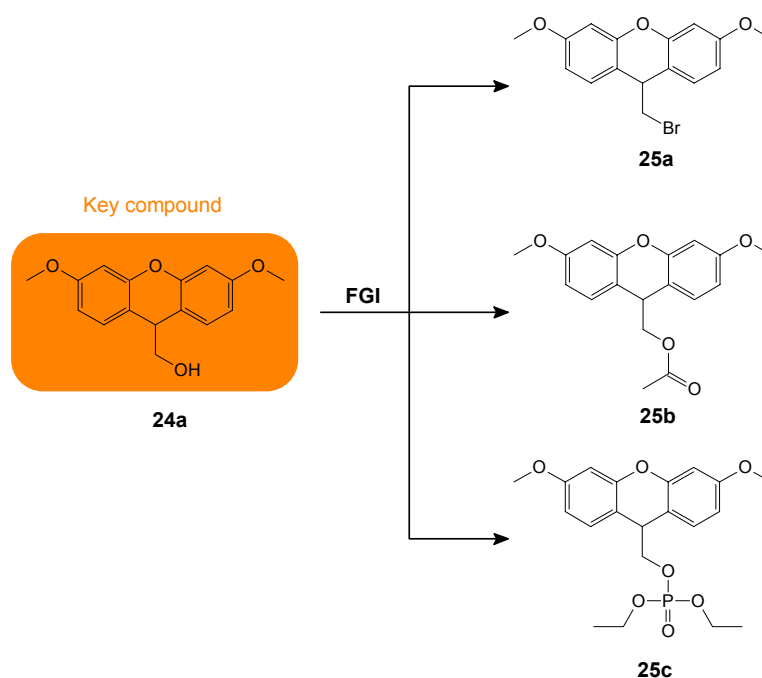
Scheme 39: Synthesis of the (3,6-dimethoxy-9*H*-xanthen-9-yl)methyl group appended caged molecules via functional group interconversion of the key compound **24a**

3.7.2.1. Synthesis of 9-(Bromomethyl)-3,6-dimethoxy-9*H*-xanthene (25a)

A variety of procedures have been developed for the transformation of the corresponding alcohols into alkyl halides. The choice of a suitable reagent is usually dictated by the sensitivity of the alcohol and other functional group in the molecule. A general method for converting alcohols to bromides involves reactions with thionyl bromide or phosphorus tribromide. These reagents are useful for alcohols that are neither acid-sensitive nor tending to structural rearrangements. Because of the very acidic solutions involved, these methods may be prone to deprotect the methyl ether and therefore a milder reagent was sought. A very important method for activating alcohols toward nucleophilic substitution is by transforming them to alkoxyphosphonium ions. One of the most convenient methods for converting alcohols to bromides is based on *in situ* generation of a bromophosphonium ion by reaction of triphenyl phosphine (Ph_3P) with carbon tetrabromide (CBr_4)[85].

Consequently, the conversion of **24a** was performed with 1.2 molar equivalents Ph$_3$P and 2.6 molar equivalents CBr$_4$ in dichloromethane, followed by purification via column chromatography to give the bromide **25a** in 97% yield (Scheme 40).
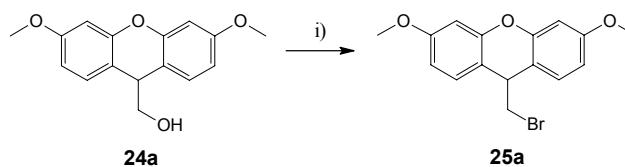
Scheme 40: Synthesis of 9-(bromomethyl)-3,6-dimethoxy-9*H*-xanthene **25a** starting from (3,6-dimethoxy-9*H*-xanthen-9-yl)methanol (**24a**) via hydroboration and subsequent oxidation. i)….Ph$_3$P/CBr$_4$/CH$_2$Cl$_2$/Argon.

Compound **25a** was fully characterized on the basis of combustion analysis, IR, UV/Vis, MS and NMR spectra, particularly by 2D NMR measurements including COSY experiment. The ^{1}H NMR spectrum of **25a** is shown in Figure 25.
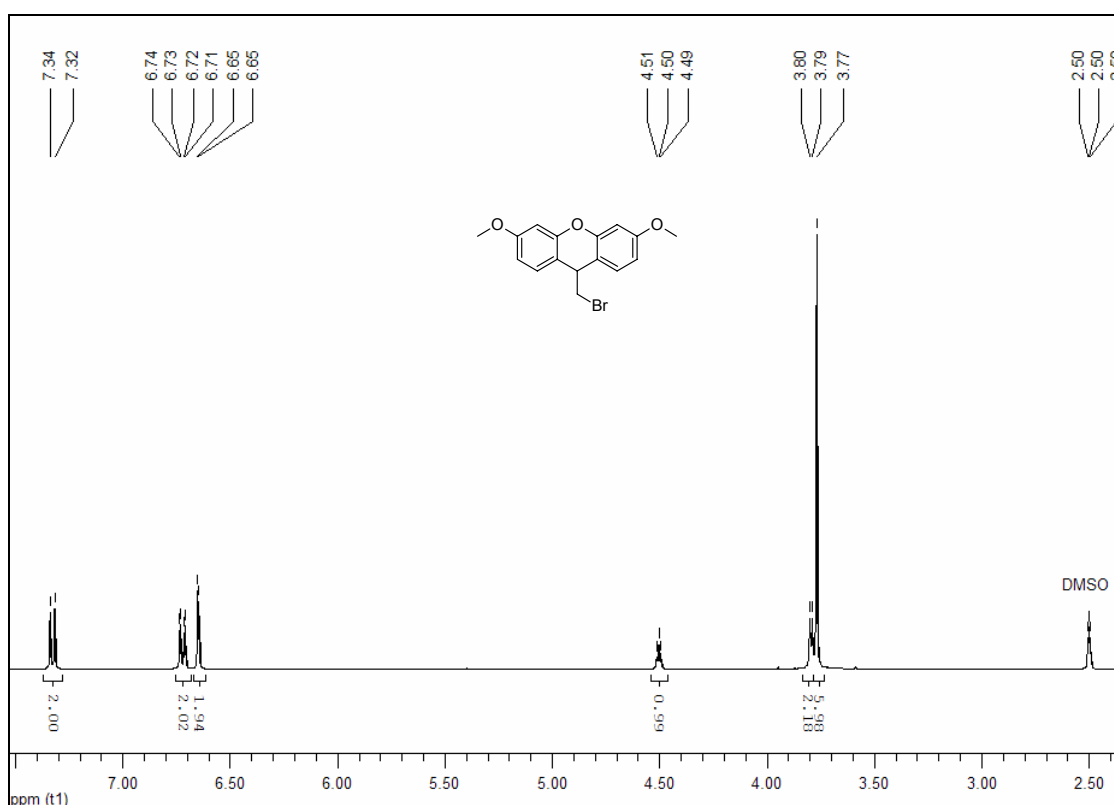
Figure 25: ^{1}H NMR spectrum (400 MHz, δ, *DMSO*-d$_6$, 25°C) of 9-(bromomethyl)-3,6-dimethoxy-9*H*-xanthene (**25a**).

3.7.2.2. Synthesis of (3,6-Dimethoxy-9*H*-xanthen-9-yl)methyl acetate (25b)

The best general method for the preparation of carboxylic esters is the reaction between acyl halides or anhydrides with alcohols or phenols. Most often pyridine or 4-(*N,N*-dimethylamino) pyridine (DMAP) is used as a catalyst. Either the catalyst is used in excess or triethylamine (Et$_3$N) is added to combine with the acid formed. Thus, the alcohol **24a** was converted according to conventional procedures[86,87] by adding Et$_3$N and DMAP to a solution of **24a** in acetic anhydride into the acetate **25b** in 98 % yield (Scheme 41).
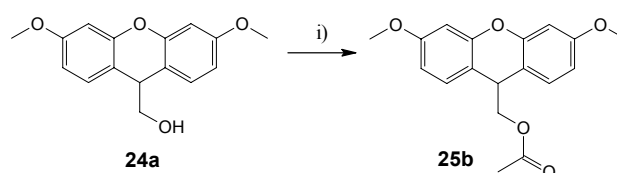
Scheme 41: Synthesis of (3,6-dimethoxy-9*H*-xanthen-9-yl)methyl acetate (**25b**) starting from (3,6-dimethoxy-9*H*-xanthen-9-yl)methanol (**24a**) via acetylation. i)….Ac$_2$O/DMAP/Et$_3$N.

Compound **25b** was fully characterized on the basis of combustion analysis, IR, UV/Vis, MS and NMR spectra, particularly by 2D NMR measurements including COSY experiment. The ^{1}H NMR spectrum of **25a** is shown in Figure 26.
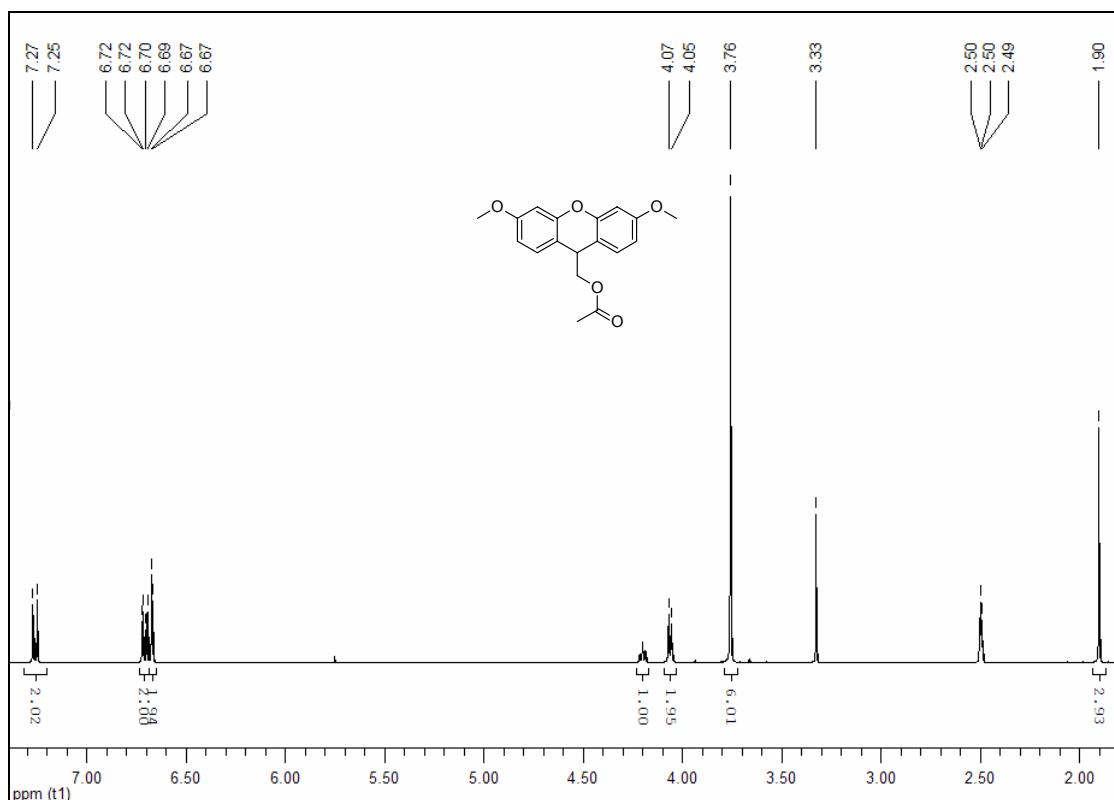
Figure 26: ^{1}H NMR spectrum (400 MHz, *δ, DMSO*-d$_6$, 25°C) of (3,6-dimethoxy-9*H*-xanthen-9-yl)methyl acetate (**25b**).

3.7.2.3. Synthesis of (3,6-Dimethoxy-9*H*-xanthen-9-yl)methyl diethyl phosphate (25c)

The synthesis of (3,6-dimethoxy-9H-xanthen-9-yl)methyl diethyl phosphate **(25c)** can be achieved either by phosphorylation of the bromide **25b** or of the alcohol **24a**. Bendig *et al*. [38] prepared caged cAMP by substitution of the 4-(bromomethyl)coumarin by using the tetra-*n*-butylammonium salt of cAMP (prepared from cAMP via ion exchange with tetra-*n*-butylammonium hydroxide). Due to the fact that diethyl chlorophosphate is readily available, the phosphorylation of the alcohol **24a** was accomplished in a similar manner to the acetylation above. Thus, compound **25c** was synthesized by adding diethyl chlorophosphate to a solution containing **24a** and DMAP in dichloromethane. Work up and purification by preparative TLC (SiO$_2$, Hexane/EtOAc = 3/2) afforded **25c** in 55 % yield (Scheme 42).
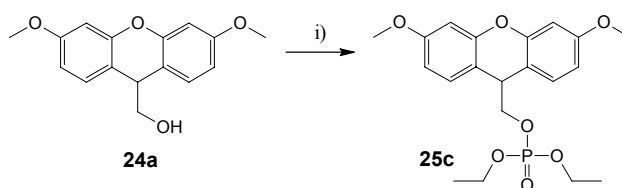
Scheme 42: Synthesis of (3,6-dimethoxy-9*H*-xanthen-9-yl)methyl diethyl phosphate (**25c**) starting from (3,6-dimethoxy-9*H*-xanthen-9-yl)methanol (**24a**) via phosphorylation. i)….(EtO)$_2$POCl/DMAP/CH$_2$Cl$_2$/Argon.

Compound **25c** was fully characterized on the basis of combustion analysis, IR, UV/Vis, MS and NMR spectra, particularly by 2D NMR measurements including HMQC, HMBC, COSY and N*O*ESY experiments. The ^{1}H NMR spectrum of **25c** is shown in Figure 27.
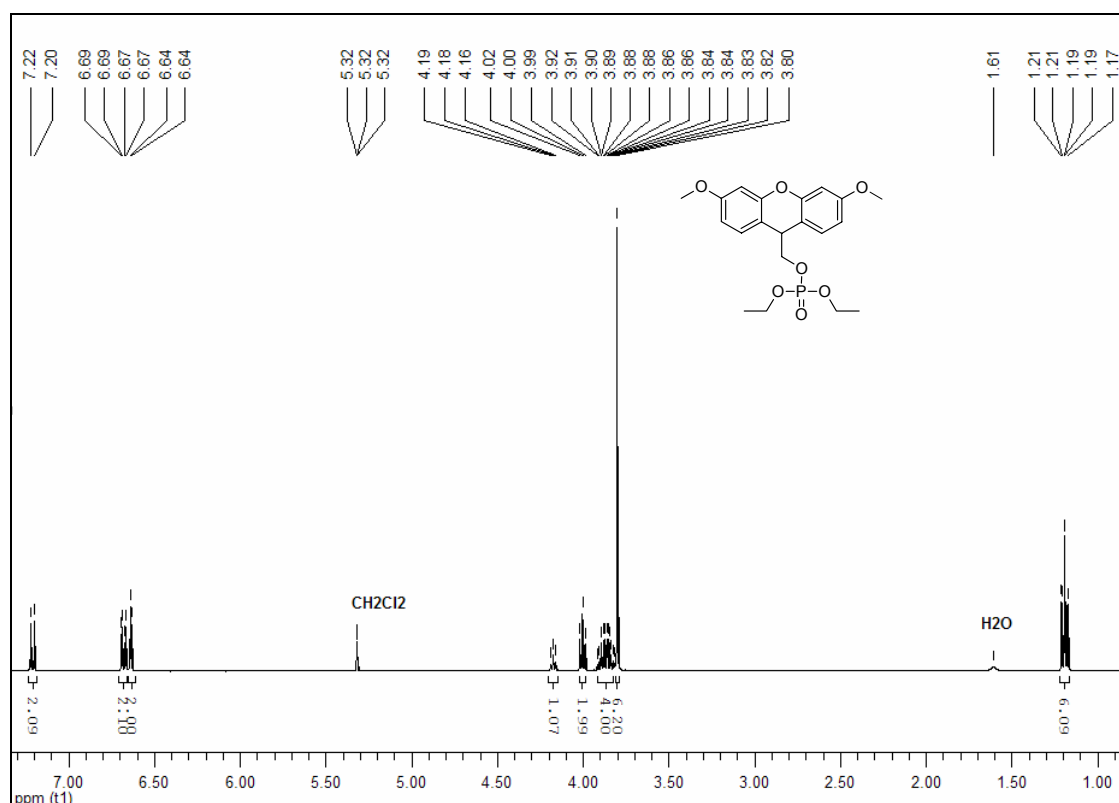
Figure 27: ^{1}H NMR spectrum (400 MHz, δ, CD_2Cl_2, 25°C) of (3,6-dimethoxy-9H-xanthen-9-yl)methyl diethyl phosphate (**25c**).

The methylene moiety of -O-CH_2-CH_3 in **25c** shows a complex spin-spin coupling pattern due to geminal diastereotopic [88,89] non-equivalence, $^3J_{P-H}$- and vicinal coupling. The signal of the methylene moiety of -CH-CH_2-O- results in a triplet because of $^3J_{P-H}$- and vicinal coupling.
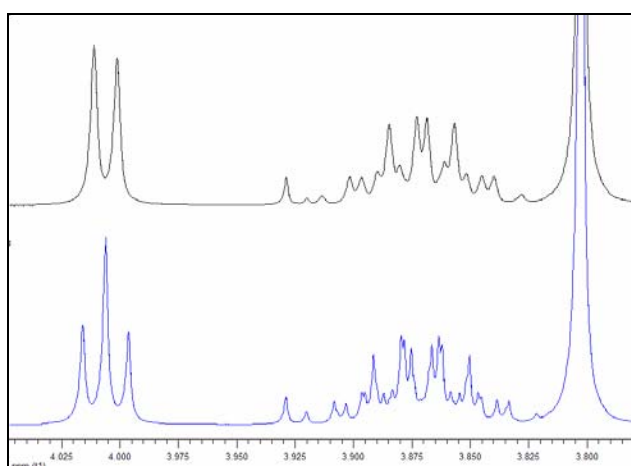
Figure 28: ^{1}H NMR (600 MHz) spectrum (—) and ^{31}P decoupled spectrum (—) of the CH_2- moieties of (3,6-dimethoxy-9H-xanthen-9-yl)methyl diethyl phosphate (**25c**) in CD_2Cl_2 at 25°C.

(-CH-**CH₂**-O-….left; O-**CH₂**-CH₃….middle; CH₃O-….right)
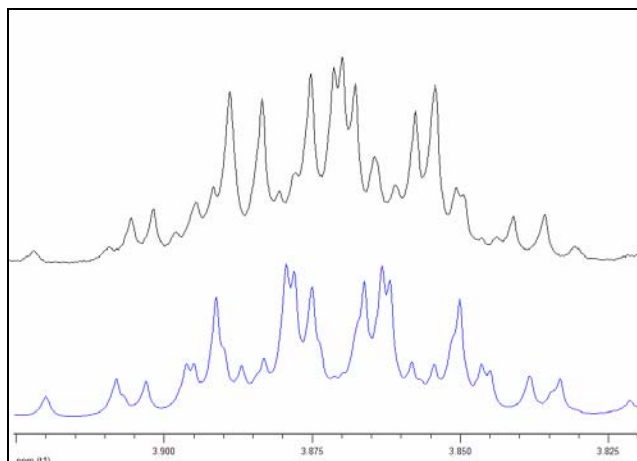
Figure 29: 600 MHz ^{1}H NMR spectrum (—) and **CH_3** decoupled spectrum (—) of the O-CH$_2$-moiety of (3,6-dimethoxy-9H-xanthen-9-yl)methyl diethyl phosphate (**25c**) in *CD$_2$Cl$_2$* at 25°C.

3.7.2.4. Deprotection of the (3,6-Dimethoxy-9H-xanthen-9-yl)methyl Group Appended Caged Molecules

The cleavage of ethers is a versatile reaction in organic synthesis. The conversion of alcohols or phenols to ethers and their subsequent cleavage constitutes an important method for the protection of hydroxy groups. Boron tribromide is regarded as one of the reagents of choice for the dealkylation of ethers[73]. Despite its efficiency, the primary advantage claimed in favour of BBr$_3$ is that the cleavage is affected under mild conditions and thus the need for the use of strongly acidic or basic reaction conditions can be avoided. The reaction is conveniently carried out in dichloromethane, benzene or hexane at room temperature. If milder conditions are needed, the reactants are mixed at -78°C and allowed to warm to room temperature.

Consequently, the deprotection was carried out by adding in each case a 1M solution of BBr$_3$ to a solution of the compounds **25a**, **25b** or **25c** in dichloromethane at -78°C. The resulting mixtures were warmed up to -10°C, followed by hydrolysis and extraction with ethyl acetate (Scheme 43). It is recommended to use at least one equivalent of boron tribromide for each methoxy group and one equivalent for each equivalent of a Lewis base which may complex with boron tribromide[90]. Removal of the *O*-methyl groups on **25c** was achieved with 8 equivalents of BBr$_3$ providing diol **26c** in 66%, and the 6-methoxy derivative **26d** was isolated in 21% yield. As a result of this, it was necessary to increase

the amount of BBr₃ to 13 equivalents, to obtain full deprotection of **25c**. The deprotection afforded the compounds **26a**, **26b** and **26c** in 97 – 99% yield.

R₁			R₁	R₂	
Br		**25a**	Br	H	**26a**
OAc		**25b**	OAc	H	**26b**
OPO(OEt)₂		**25c**	OPO(OEt)₂	H	**26c**
			OPO(OEt)₂	CH₃	**26d**
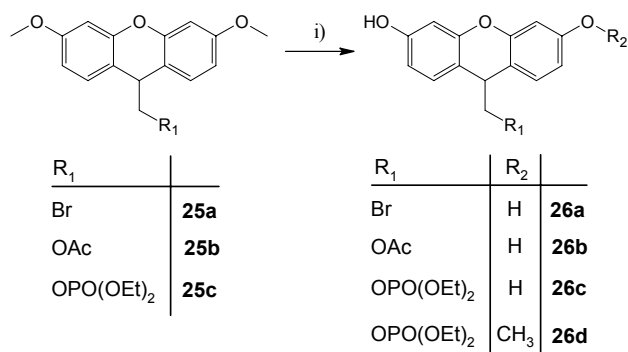
Scheme 43: Synthesis of the (3,6-dihydroxy-9*H*-xanthen-9-yl)methyl group appended caged molecules **26a**, **26b**, **26c** and **26d** starting from the (3,6-dimethoxy-9*H*-xanthen-9-yl)methyl group appended caged molecules **25a**, **25b** and **25c** via deprotection. i)….BBr₃/CH₂Cl₂/Argon/-78°C → -10°C.

Compound **26a**, **26b** and **26c** were fully characterized on the basis of combustion analysis, IR, UV/Vis, MS and NMR spectra, particularly by 2D NMR measurements including HMQC, HMBC, COSY and N*O*ESY experiments. The ¹H NMR spectra of **26a**, **26b** and **26c** are shown in Figure 30 – 32.
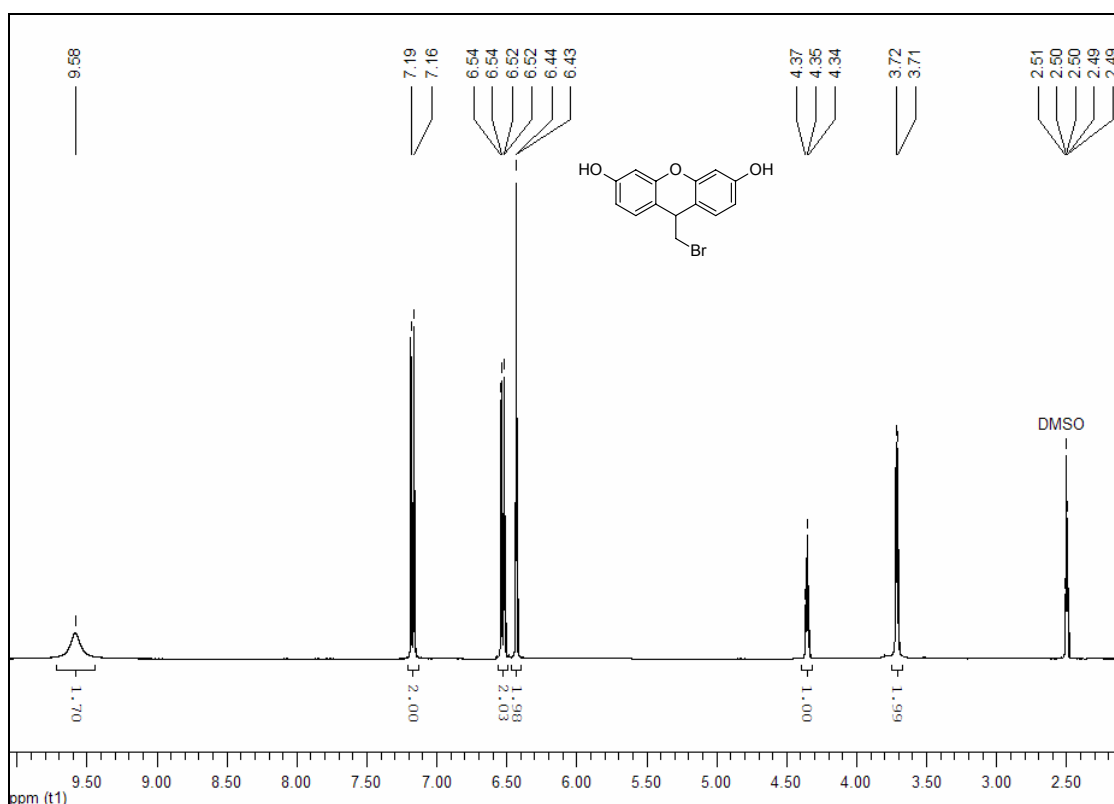
Figure 30: ¹H NMR spectrum (400 MHz, *δ*, *DMSO*-d₆, 25°C) of 9-(bromomethyl)-9*H*-xanthene-3,6-diol (**26a**).
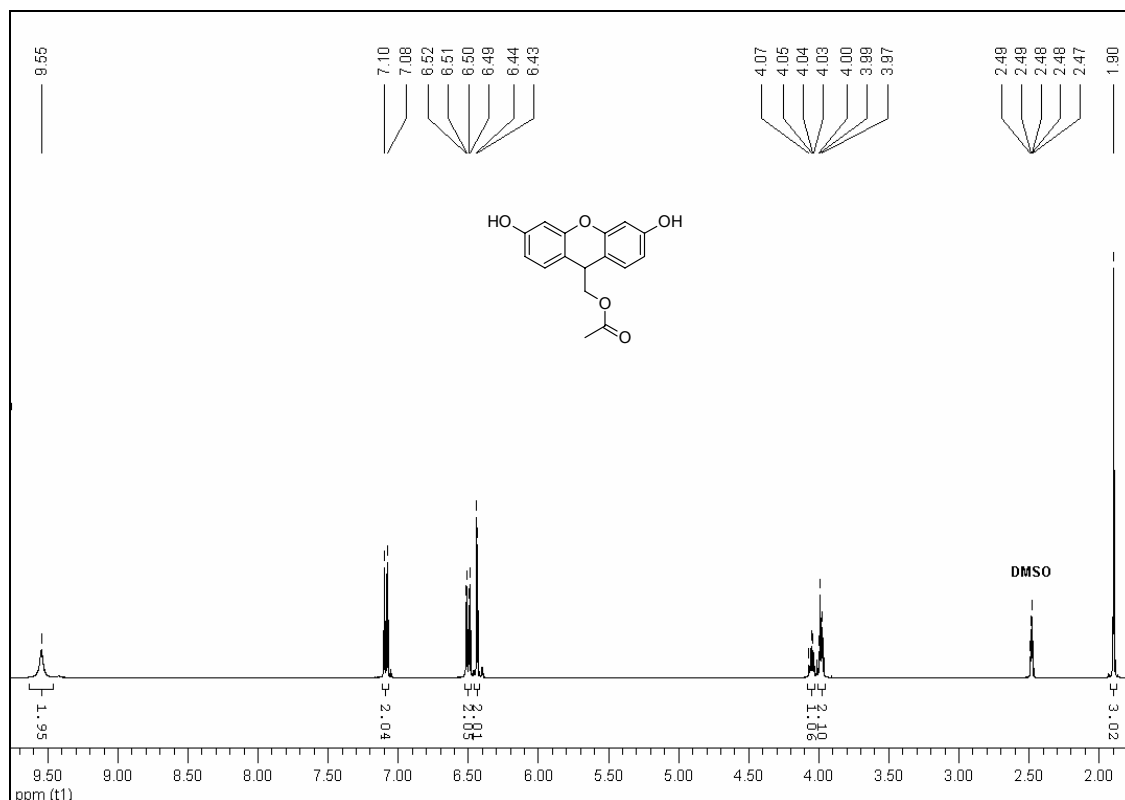
Figure 31: ^{1}H NMR spectrum (400 MHz, δ, *DMSO*-d$_6$, 25°C) of (3,6-dihydroxy-9*H*-xanthen-9-yl)methyl acetate (**26b**).
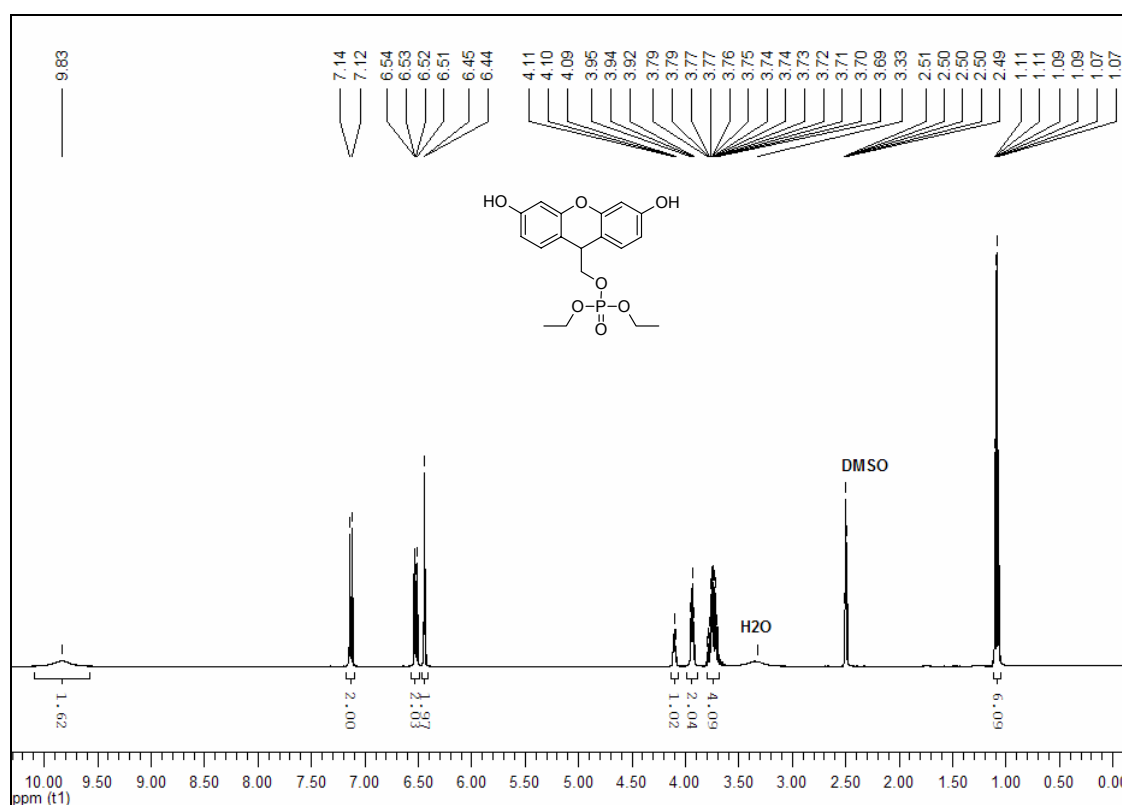
Figure 32: ^{1}H NMR spectrum (400 MHz, δ, *DMSO*-d$_6$, 25°C) of (3,6-dihydroxy-9*H*-xanthen-9-yl)methyl diethyl phosphate (**26c**).

Compound **26d** was fully characterized on the basis of IR, MS and NMR spectra, particularly by 2D NMR measurements including HMQC, HMBC, COSY and N*O*ESY experiments. The ^{1}H NMR spectrum of **26d** is shown in Figure 33.
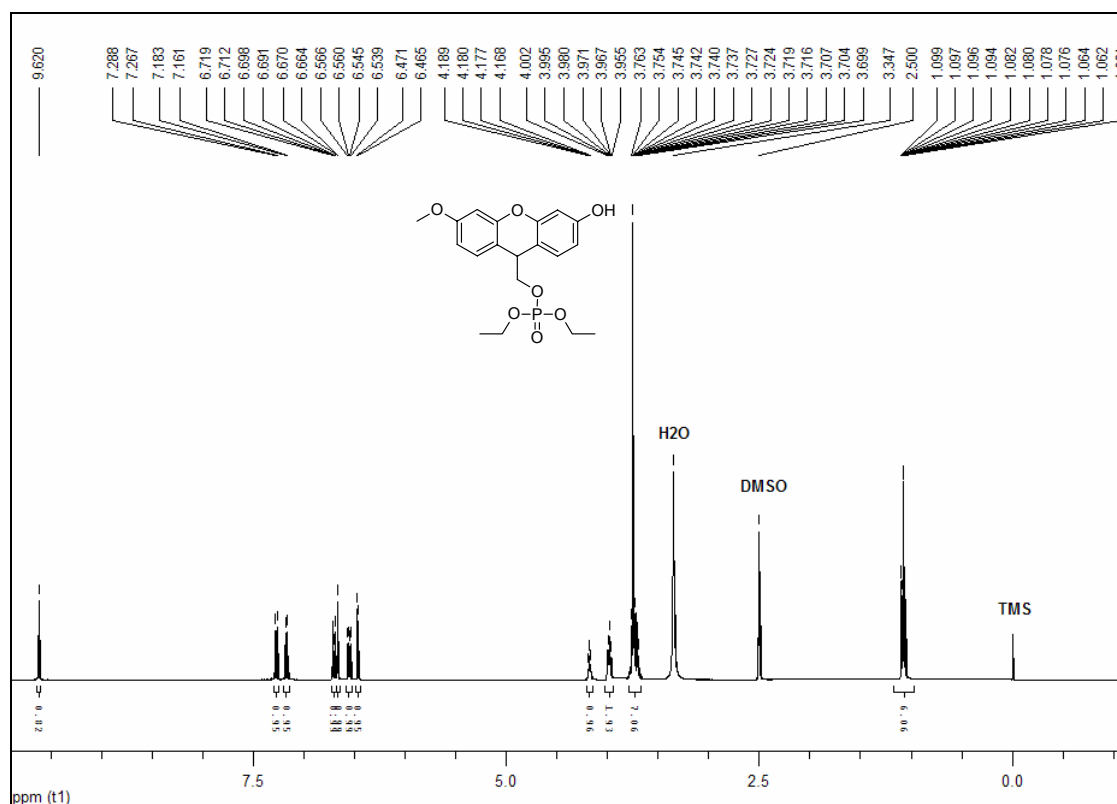
Figure 33: ^{1}H NMR spectrum (400 MHz, *δ*, *DMSO*-d$_6$, 25°C) of diethyl (3-hydroxy-6-methoxy-9*H*-xanthen-9-yl) methyl phosphate (**26d**).

3.7.2.5. Oxidation of the (3,6-Dihydroxy-9*H*-xanthen-9-yl)methyl- to the (6-Hydroxy-3-oxo-3*H*-xanthen-9-yl)methyl Group Appended Caged Molecules

The oxidations were carried out according to Neckers *et al.*[91] with 2,3-dichloro-5,6-dicyano-1,4-benzoquinone (DDQ), which is a powerful oxidant that performs a large number of useful reactions under relatively mild conditions. Reactions with DDQ are usually carried out in an inert solvent such as benzene, THF, dioxane or AcOH, but dioxane or hydrocarbon solvents are often favoured because of the low solubility of the hydroquinone by-product.

At first, the conversion of the diol **26a** to the quinine methide **27a** was effected by adding DDQ to a solution of **26a** in dry ethanol at room temperature. After 1h, the formed precipitate was filtered off, subsequent washing and drying resulted in only 48% **27a**.

Neckers *et al*. had obtained the 3-hydroxy-6-fluorone **4** in 90% yield. Therefore it was necessary to find another solvent for the reaction. After solubility tests of **4** and of the hydroquinone by-product in different solvents, the decision was made to use acetonitrile as solvent.

The oxidations of the diols were then carried out in dry acetonitrile with DDQ to afford the compounds **27a**, **27b** and **27c** in 95, 80 and 81% yield, respectively (Scheme 44).

R			LG	
Br	**26a**		Br	**27a**
OAc	**26b**		OAc	**27b**
OPO(OEt)$_2$	**26c**		OPO(OEt)$_2$	**27c**
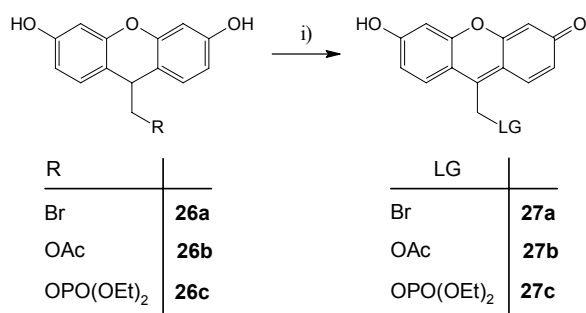
Scheme 44: Synthesis of the (6-Hydroxy-3-oxo-3*H*-xanthen-9-yl)methyl group appended caged molecules **27a**, **27b** and **27c** starting from the (3,6-dimethoxy-9*H*-xanthen-9-yl)methyl group appended caged molecules **26a**, **26b** and **26c** via oxidation (LG…Leaving group). i)….DDQ/CH$_3$CN/Argon.

Scheme 45 shows the overall yield of the three-step synthesis of the (6-hydroxy-3-oxo-3*H*-xanthen-9-yl)methyl group appended caged molecules.

R			R			LG	overall yield	
Br	**25a**		Br	**26a**		Br	91%	**27a**
OAc	**25b**		OAc	**26b**		OAc	76%	**27b**
OPO(OEt)$_2$	**25c**		OPO(OEt)$_2$	**26c**		OPO(OEt)$_2$	44%	**27c**
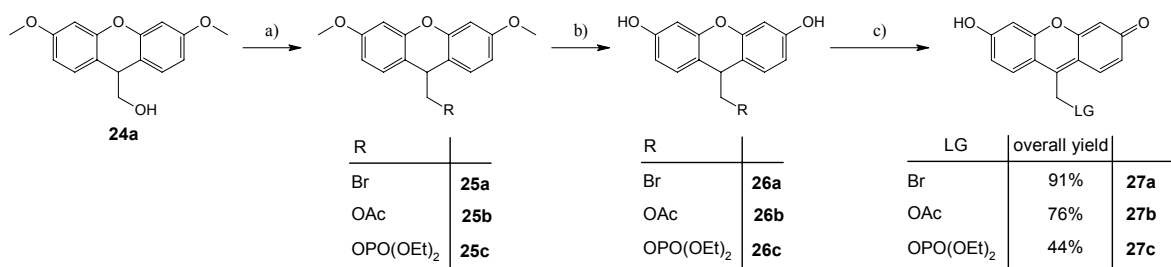
Scheme 45: Overview of the three-step synthesis of the (6-Hydroxy-3-oxo-3*H*-xanthen-9-yl)methyl group appended caged molecules starting from **24a** via functional group interconversion (FGI), deprotection and oxidation. a)….FGI, b)….BBr$_3$/CH$_2$Cl$_2$/Argon, c)….DDQ/CH$_3$CN/Argon.

Compounds **27a**, **27b** and **27c** were fully characterized on the basis of IR, UV/Vis, MS and NMR spectra, particularly by 2D NMR measurements including HMQC, HMBC, COSY and N*O*ESY experiments. The ^{1}H NMR spectra of the enolic forms of **27a**, **27b** and **27c** are shown in Figure 34 – 36, due to fact that DMSO-d_6 was used as solvent for recording the NMR spectra.
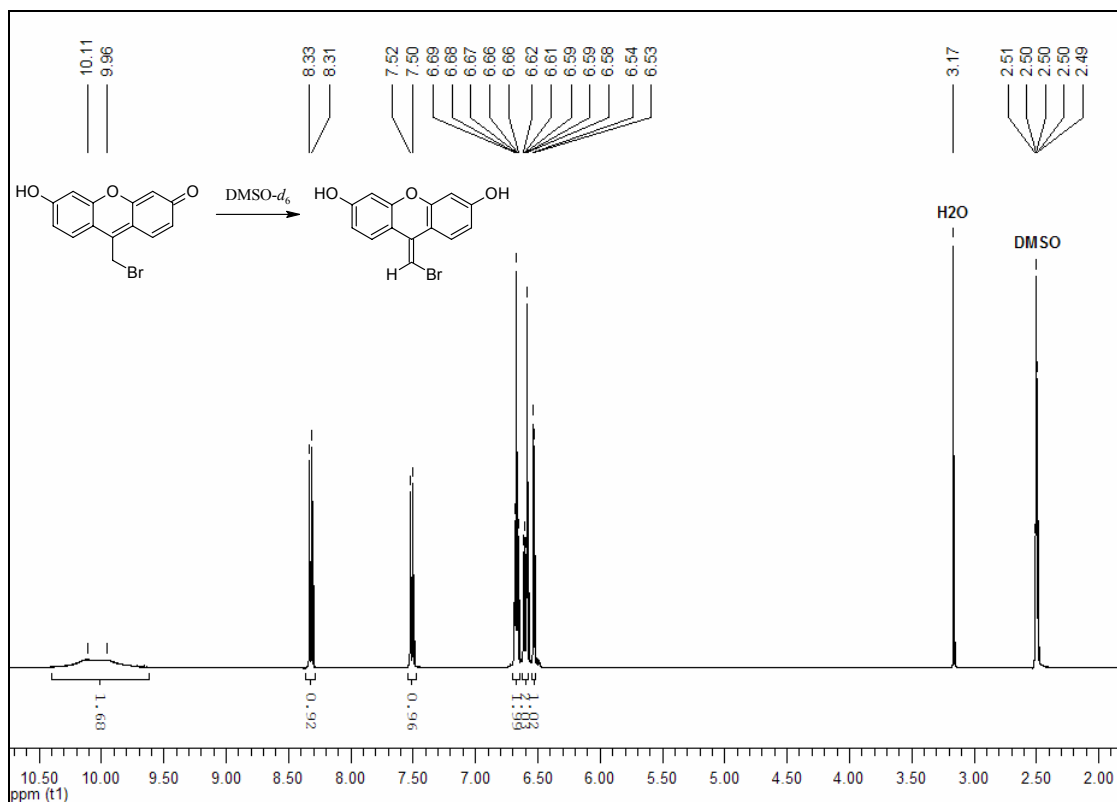
Figure 34: ^{1}H NMR spectrum (600 MHz, δ, DMSO-d$_6$, 25°C) of 9-(bromomethyl)-6-hydroxy-3H-xanthen-3-one (**27a**).
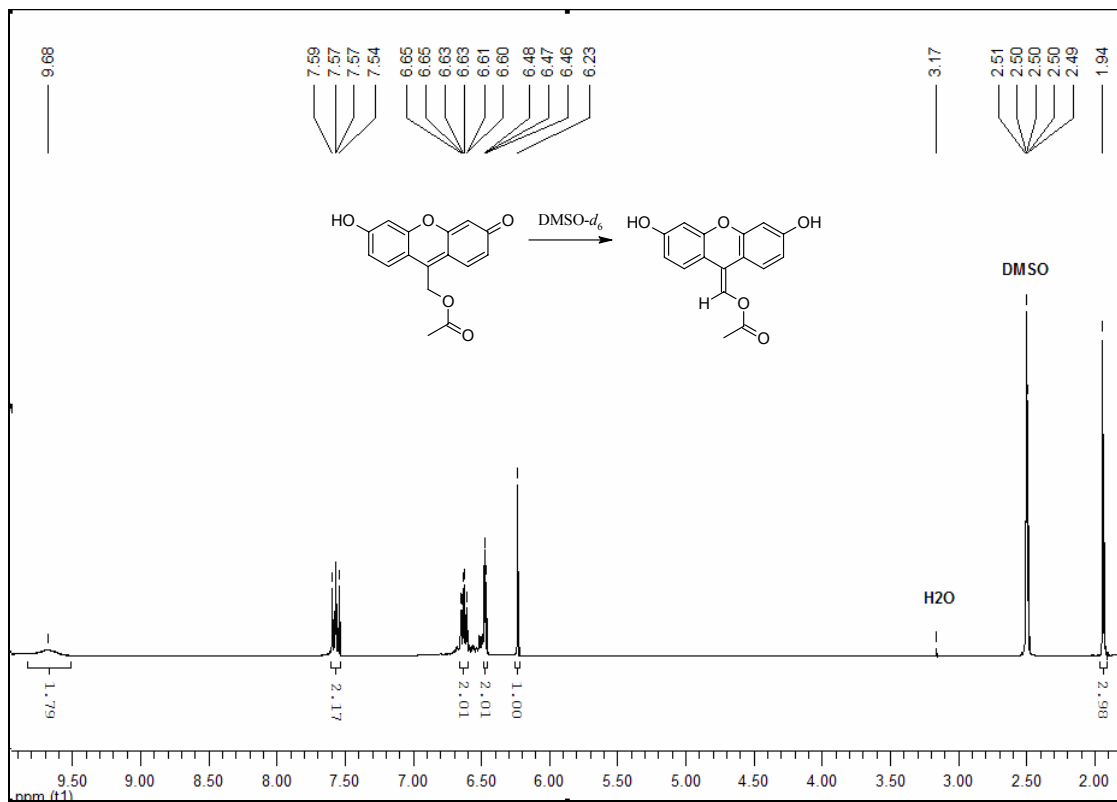
Figure 35: ^{1}H NMR spectrum (400 MHz, δ, DMSO-d$_6$, 25°C) of (6-hydroxy-3-oxo-3H-xanthen-9-yl)methyl acetate (**27b**).
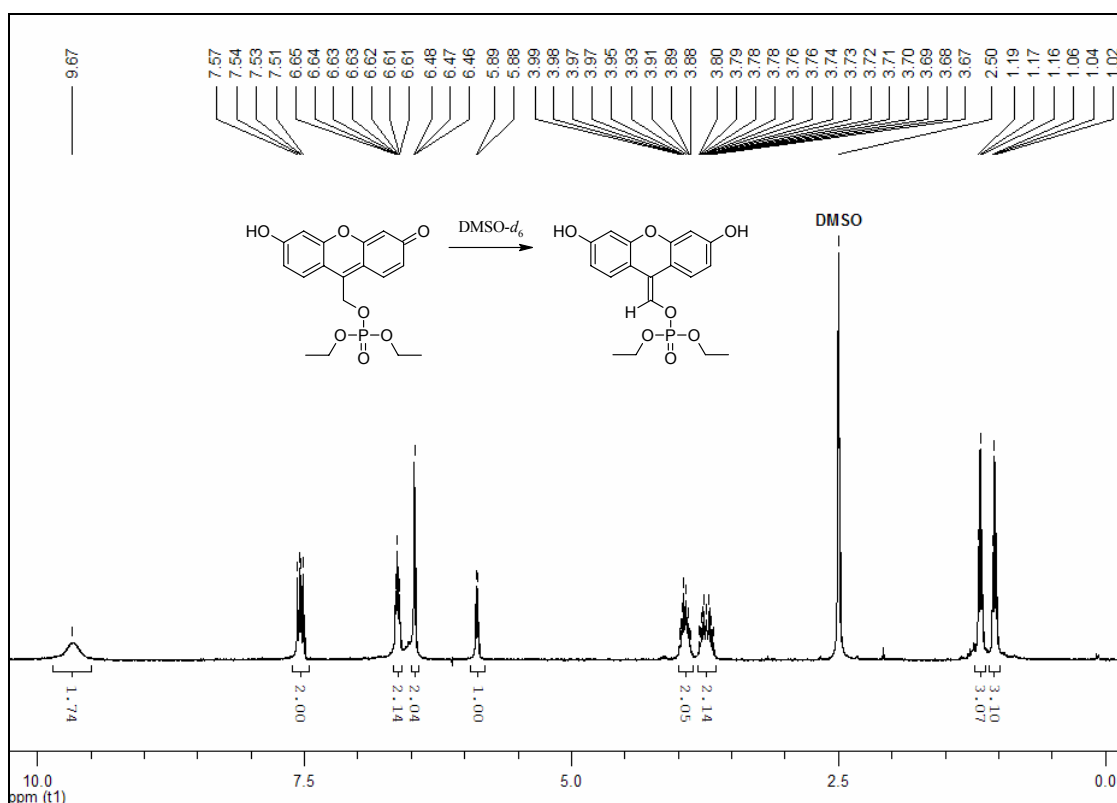
Figure 36: ^{1}H NMR spectrum (400 MHz, δ, *DMSO*-d[6], 25°C) of diethyl (6-hydroxy-3-oxo-3*H*-xanthen-9-yl)methyl phosphate (**27c**).

The diethyl phosphate derivative **27c** shows a unique anisochrony of the two ethyl groups. The two ethyl groups display separate signals, indicative for their diastereotopic environment. Interestingly, one -O-CH[2]- moiety splits into two separate signals (Figure 37). Chemical shift nonequivalence of geminal groups is commonly observed in tetracoordinate phosphorus compounds which possess a prochiral group directly bonded to an asymmetric phosphorus atom or bonded through oxygen to phosphorus[89,92].
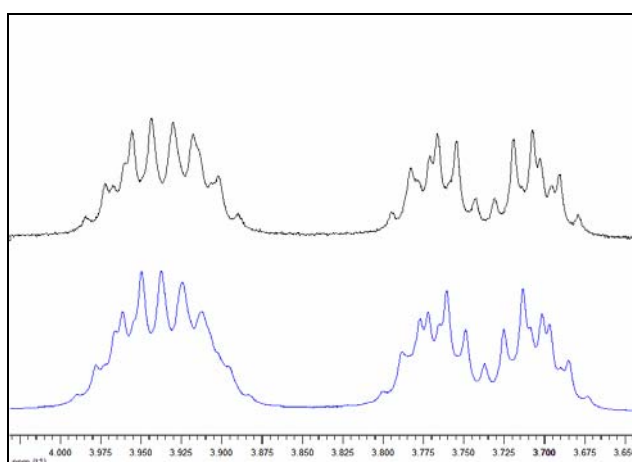
Figure 37: 600 MHz ^{1}H NMR spectrum (—) and ^{31}P decoupled spectrum (—) of the two -O-CH[2]- moieties of diethyl (6-hydroxy-3-oxo-3*H*-xanthen-9-yl)methyl phosphate (**27c**) in *CD[2]Cl[2]* at 25°C.

3.8. Spectral Properties of the Prototropic Forms of the PPG Model Compounds in Aqueous Solution

It became necessary to determine the pK_a values for the PPG, in order to know if they are deprotonated at physiological conditions (pH = 7.0), because the deprotonated form is expected to be more reactive.

Two model compounds were prepared. The titrations were conducted at constant ionic strength, I = 0.1 M, and 25°C. The resulting acidity constants are, therefore, dissociation quotients $K_{a,c}$ at I = 0.1 M. A detailed description of the experimental procedure and analysis is given in the experimental part (Page 126). The acidity constants of the compounds were determined by three independent runs and the results as well as the error limits are shown in the Table 1 (Page 75).

The first model compound, 3-hydroxy-6-fluorone (**4**), was found to have a $pK_{a,1}$ of 2.93 $\pm$ 0.06 and a $pK_{a,2}$ of 6.17 $\pm$ 0.02 (Scheme 46, Figure 38).
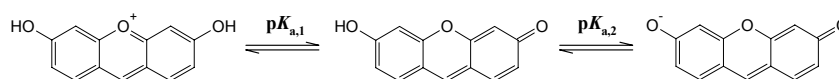
Scheme 46: Protolytic equilibria of 3-hydroxy-6-fluorone **4**

The spectra of the anionic, neutral and cationic species are shown in Figure 38C. The anionic species has its absorption maximum at 489 nm, for the neutral species $\lambda_{1,max}$= 447 nm and $\lambda_{2,max}$ = 471 nm and the cationic species absorbs at 435 nm. Thus, at pH = 7.0, 87 % of the monodeprotonated form is present.

A: 3D course of the spectrophotometric titration

B: 2D course of the spectrophotometric titration

C: Electronic spectra of the prototropic forms of **4** in aqueous solution. A…Cation, B….Neutral species, C….Anion

D: Species distribution of **4**. The total concentration is arbitrarily set to 1M. A…Cation, B….Neutral species, C….Anion
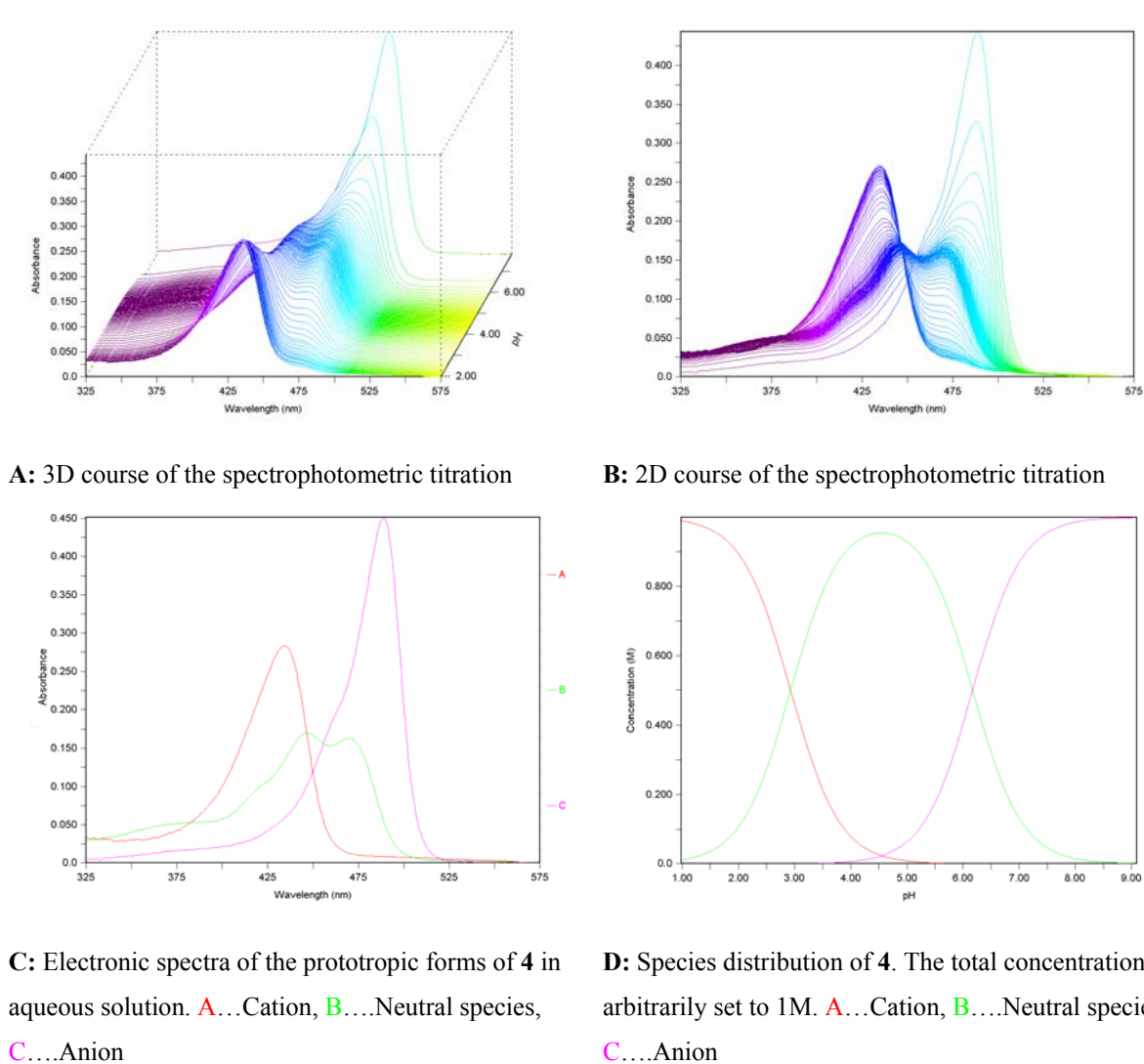
Figure 38: Spectrophotometric determination of the pK_a values of **4** in aqueous solution at pH= 1.9 –7.4;

Investigation of the protonation equilibria of **21**, **27a**, **27b** and **27c** in aqueous solutions presented more of a problem, because two tautomeric forms may participate in the protonation. Moreover, at high pH a dianionic species exists. (Scheme 47).
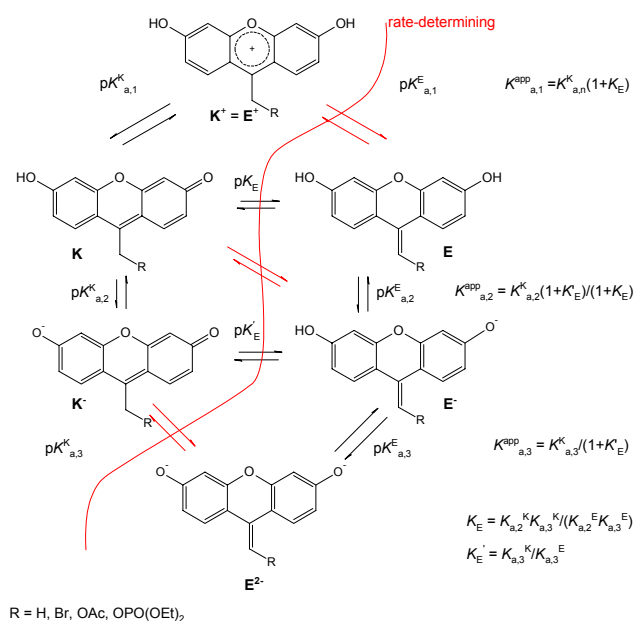
Scheme 47: Protolytic equilibria of **21, 27a, 27b** and **27c**

In such a case, the experimental dissociation constants, $pK_{a,1}$ and $pK_{a,2}$, are composites of the keto and the enol forms. The ratio of concentrations K/E and K^-/E^- is constant, regardless of the pH, provided that the equilibria are established rapidly on the time scale of the measurements. Consequently, the neutral and monodeprotonated forms behave spectrally as though they were a single species.

Only the region below pH = 8 was considered, because in the basic region, hydrolysis of the compounds **27a**, **27b** and **27c** is expected to occur and therefore $pK_{a,3}$ was not determined.

The spectra obtained with the second model compound, 6-hydroxy-9-methyl-3*H*-xanthen-3-one (**21a**), obeyed the model (Figure 39) i. e. assumption of rapid K/E and K⁻/E⁻ equilibria appeared to hold. Compound **21a** was found to have a p$K_{a,1}$ of 3.44 ± 0.11 and a p$K_{a,2}$ of 6.31 ± 0.03. The spectra of the anionic, neutral and cationic species are shown in Figure 39C. The anionic species has its absorption maximum at 481 nm, r the neutral species $\lambda_{1,max}$= 445 nm and $\lambda_{2,max}$= 465 nm, and the cationic species absorbs at 426 nm. At pH= 7.0, 83 % of the monodeprotonated form is present.
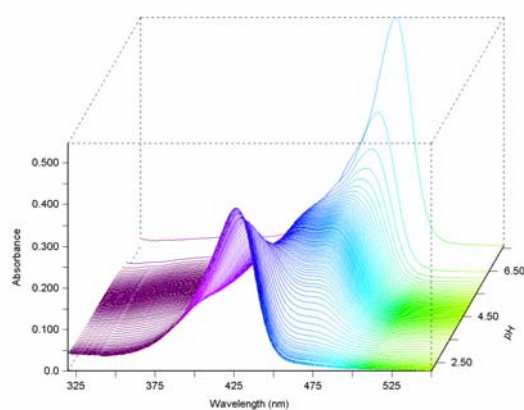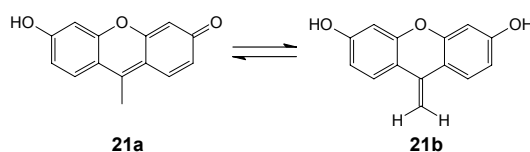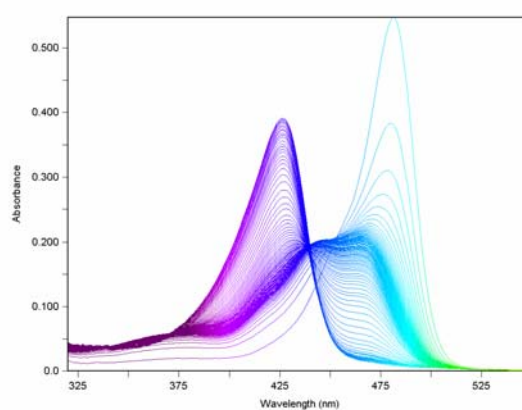
21a   **21b**

A: 3D course of the spectrophotometric titration

B: 2D course of the spectrophotometric titration
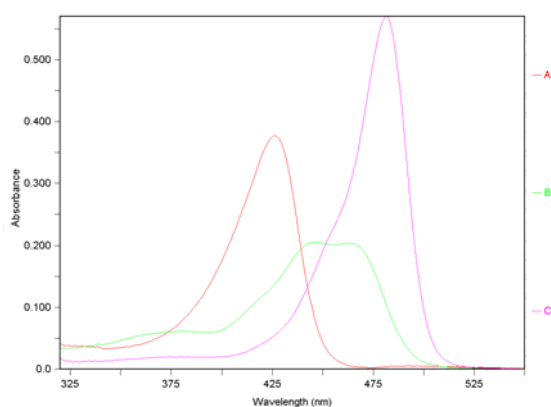
C: Electronic spectra of the prototropic forms of **21** in aqueous solution. A…Cation, B….Neutral species, C….Monoanion
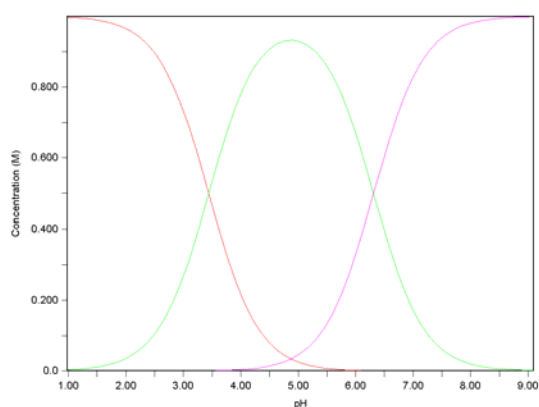
D: Species distribution of **21**. The total concentration is arbitrarily set to 1M. A…Cation, B….Neutral species, C….Monoanion

Figure 39: Spectrophotometric determination of the pK_a values of **21** in aqueous solution at pH = 1.9 –7.4.

The 9-(bromomethyl)-6-hydroxy-3*H*-xanthen-3-one (**27a**) also adequately fitted the used diprotic acid model and was found to have a p$K_{a,1}$ of 2.86 $\pm$ 0.06 and a p$K_{a,2}$ of 6.08 $\pm$ 0.06. The spectra of the anionic, neutral and cationic species are shown in Figure 40C. The anionic species has its absorption maximum at 519 nm, for the neutral species λ_{max} = 473 nm and the cationic species absorbs at 453 nm. At pH = 7.0, 89 % of the monodeprotonated form is present.
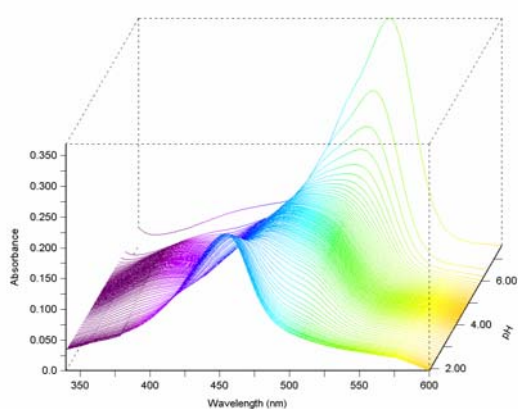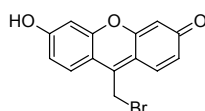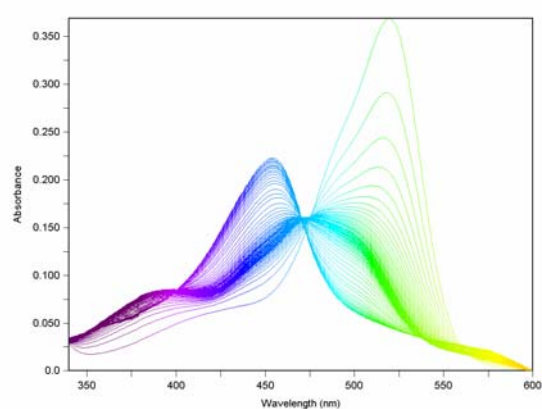
A: 3D course of the spectrophotometric titration

B: 2D course of the spectrophotometric titration
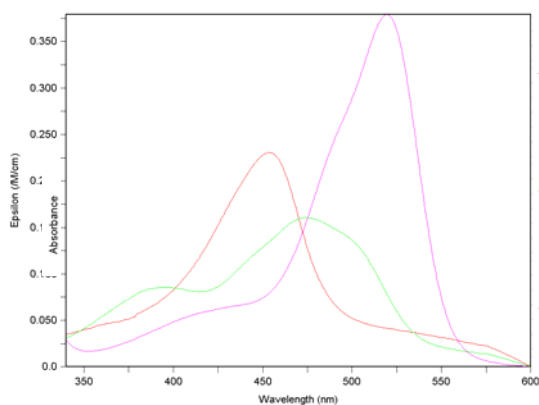
C: Electronic spectra of the prototropic forms of **27a** in aqueous solution. A…Cation, B….Neutral species, C….Monoanion
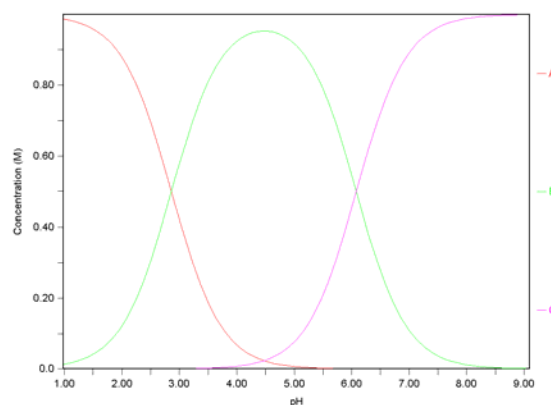
D: Species distribution of **27a**. The total concentration is arbitrarily set to 1M. A…Cation, B….Neutral species, C….Monoanion

Figure 40: Spectrophotometric determination of the pK_a values of **27a** in aqueous solution at pH = 1.9 –7.4.

The pK_a determination of compounds **27b** and **27c** failed because the spectral matrix in Figure 41 and 42 do not obey the model (2 pK_a) which is used for the calculation of the acidity constants. This indicates that the rate for adjusting of the involved keto-enol equilibria is too slow. Another point which should be considered is that the compound may be decompose at acidic pH, because at pH ~ 2 mainly the cationic species should exist, and therefore the extinction coefficient should be much higher. In order to determine only p$K_{a,2}$ the titration was conducted with a solution of the compound in 2-(*N*-morpholino)ethanesulfonic acid (MES) buffer, but this attempt failed also due to the reasons mentioned above (Scheme 41B).
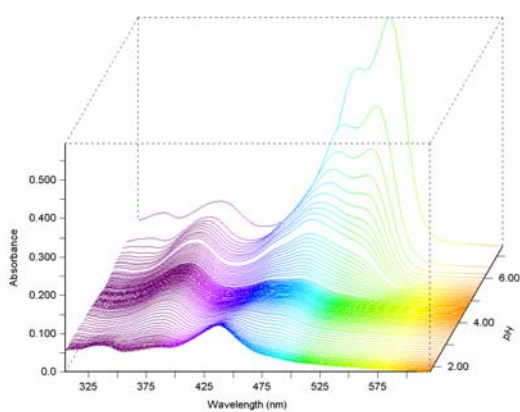
A1: 3D course of the spectrophotometric titration of **27b** in 0.1M NaOAc pH = 1.9 − 7.4
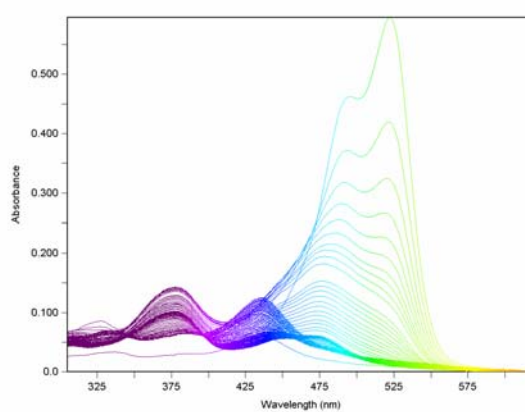
A2: 2D course of the spectrophotometric titration of **27b** in 0.1M NaOAc pH = 1.9 − 7.4

MES
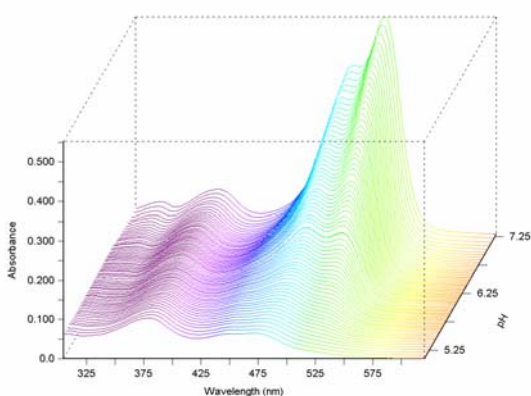
B1: 3D course of the spectrophotometric titration of **27b** in MES buffer (pK_a = 6.21)
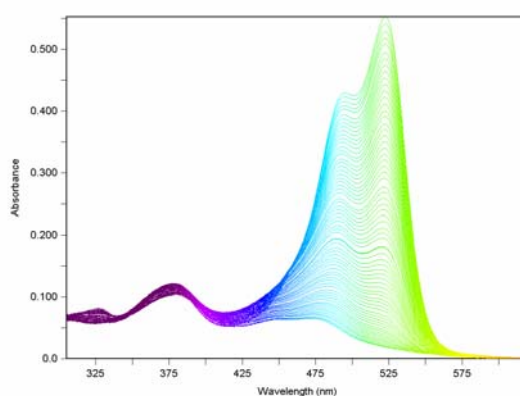
MES

B2: 2D course of the spectrophotometric titration of **27b** in MES buffer (pK_a = 6.21)

Figure 41: Attempted determination of the pK_a values of **27 b**
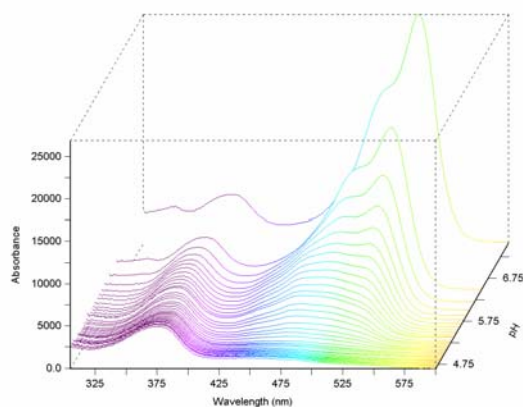
A1: 3D course of the spectrophotometric titration of **27c** in 0.1M NaOAc pH = 4.7 − 7.4
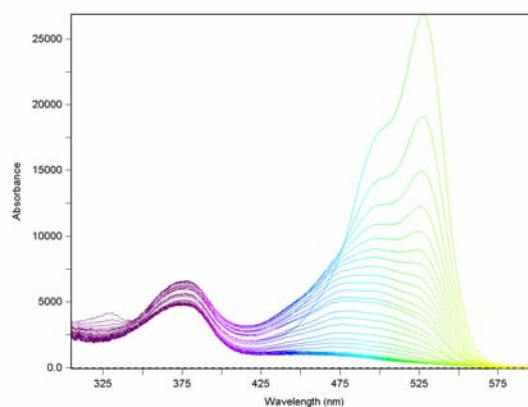
A2: 2D course of the spectrophotometric titration of **27c** in 0.1M NaOAc pH = 4.7 − 7.4

Figure 42: Attempted determination of the pK_a values **of 27 b**
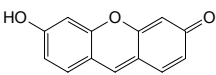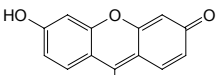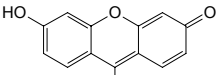
Compound	p$K_{a,1}$	p$K_{a,2}$
4	6.192	2.990
	6.155	2.867
	6.176	2.930
	Mean = 6.174 SD = 0.019	**Mean = 2.929 SD = 0.062**
21a	6.303	3.518
	6.341	3.480
	6.293	3.317
	Mean = 6.312 SD = 0.025	**Mean = 3.438 SD = 0.107**
27a	6.140	2.795
	6.013	2.913
	6.094	2.877
	Mean = 6.082 SD = 0.064	**Mean = 2.862 SD = 0.061**

Table 1: Determination of the pK_a values of **4**, **21a** and **27a**

Assuming that the compounds **27b** and **27c** have p$K_{a,1}$ and p$K_{a,2}$ values similar to those of **27a**, we presume that at pH = 7.0, approximately 80 % of the monodeprotonated forms are present.

The molar extinction coefficients of the compounds **27a**, **27b** and **27c** at pH = 7.0 were determined by linear fitting of the absorption against the concentration from at least 5 solutions and the results are shown in Table 1.
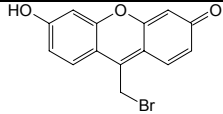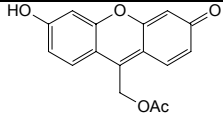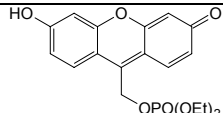
Model compound	λ_{max} [nm]	$\varepsilon \, / \, dm^3 \cdot mol^{-1} \cdot cm^{-1}$
27a	519	25752
27b	522	22723
27c	528	24463

Table 2: Molar extinction coefficients of the compounds **27a**, **27b** and **27c**

3.9. Irradiation Experiments

All compounds were photolysed in water at pH = 7.0 (phosphate buffer, I = 0.1 M) with a medium-pressure mercury lamp. A band-pass filter was used to isolate the desired atomic emission line (λ = 546 nm). A detailed description of the experimental conditions is given in the experimental part.

All attempts to identify the photoproduct failed up to now. The photoproduct was isolated by the following two approaches. First, the reaction mixture after preparative irradiation (20 - 30 mg) in buffered aqueous solution (pH = 7.0) was acidified to pH = 4, followed by extraction with ethyl acetate. Purification by RP-HPLC failed. Several species were isolated which, when resubmitted to HPLC (to test if they are stable), partially merged into each other. The second approach was accomplished by preparative irradiation in doubly distilled water, followed by evaporation of water and recording of an NMR spectrum directly from the reaction mixture in DMSO-d_6. This attempt failed by reason of appearance of at least two similar species and as well decomposition. The conclusion is that the photoproduct also undergoes a tautomeric equilibrium. Another possibility to isolate and identify the photoproduct is by "freezing" the tautomeric equilibrium through derivatisation, e.g. acetylation of the hydroxy functionalities, but this is still under examination.

The pK_a is a useful guide to leaving group ability. The ability of an anion to behave as leaving group depends necessarily on its stability, how willing it is to accept a negative charge. A low pK_a-value indicates stable conjugate base. Table 3 shows the pK_a of the conjugate acids of the leaving groups which have to be examined.

Conjugate acid of the leaving group	HBr	HOPO(OEt)$_2$	AcOH
pK_a	-9.00	0.71	4.76

Table 3: pK_a-values of acids released during photolysis

Thus, the bromide and the diethyl phosphate are good leaving groups, whereas the acetate is a poor leaving group.

3.9.1. Photorelease of Bromide from 9-(Bromomethyl)-6-hydroxy-3*H*-xanthen-3-one (**27a**)
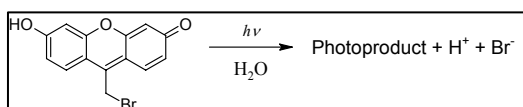
9-(Bromomethyl)-6-hydroxy-3*H*-xanthen-3-one was irradiated at $\lambda > 530$ nm and the progress of the photoreaction was followed by recording UV-VIS spectra at different irradiation times (Figure 43). UV-VIS monitoring of the reaction revealed a uniform and clean conversion, exhibiting several isosbestic points at $\lambda = 320, 342, 389, 438$ and 510 nm.
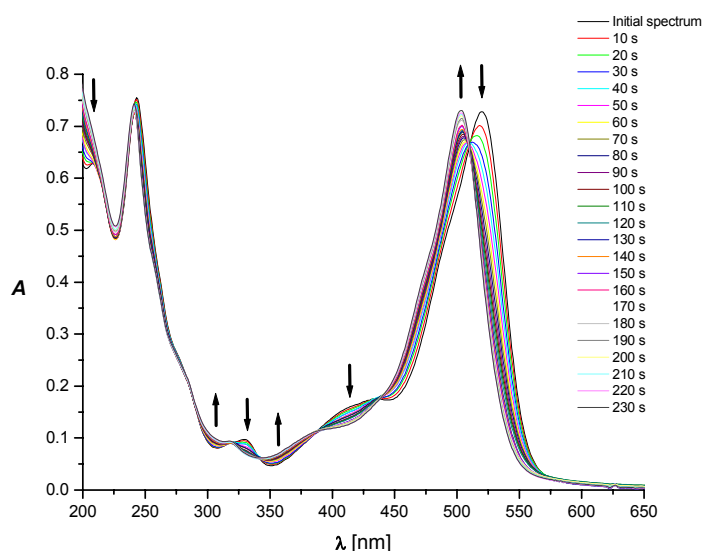
Figure 43: 9-(Bromomethyl)-6-hydroxy-3*H*-xanthen-3-one (**27a**) irradiated at $\lambda > 530$ nm in water pH = 7 (phosphate buffer, I = 0.1M). Arrows indicate the changes of absorbance during the irradiation period.

3.9.2. Photorelease of Diethyl Phosphate from Diethyl (6-hydroxy-3-oxo-3*H*-xanthen-9-yl)methyl phosphate (27c)
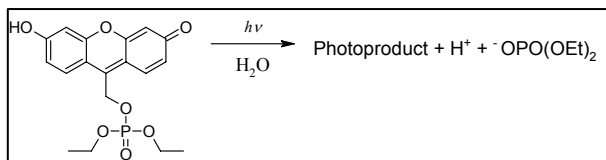
The absorption changes for **27c** were qualitatively the same as in the case of **27a** and suggested a clean photolytic conversion (isosbestic points at λ = 391, 515 and 557 nm) of **27c** to the photoproduct (λ_{max}= 504 nm) and diethyl phosphoric acid.
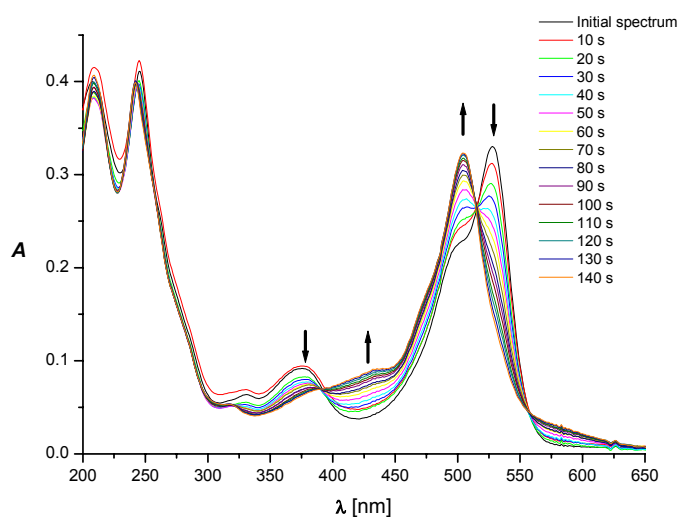
Figure 44: Diethyl (6-hydroxy-3-oxo-3*H*-xanthen-9-yl)methyl phosphate (**27c**) irradiated at λ > 530 nm in water pH= 7 (phosphate buffer, I = 0.1M). Arrows indicate the changes of absorbance during the irradiation period.

3.9.3. Photorelease of Acetic Acid from (6-Hydroxy-3-oxo-3*H*-xanthen-9-yl)methyl acetate (27b)
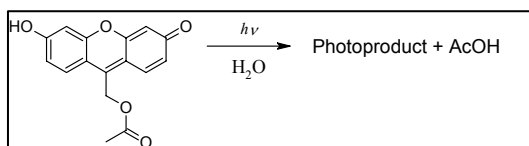
The initial progress of the irradiation of **27b** is shown in Figure 45. The reaction did not appear to be uniform and fast as in the case of **27a** and **27c**. This fact suggests an inefficient liberation of acetic acid.
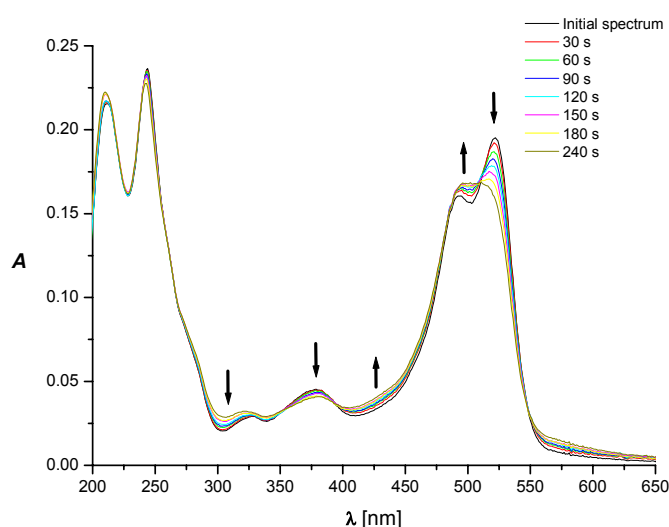
Figure 45: (6-hydroxy-3-oxo-3*H*-xanthen-9-yl)methyl acetate (**27b**) irradiated at $\lambda > 530$ nm in water pH = 7 (phosphate buffer, I = 0.1M). Arrows indicate the changes of absorbance during the irradiation period.

3.10. Outlook

In order to understand the events that occur between the absorption of light by the (6-hydroxy-3-oxo-3*H*-xanthen-9-yl)methyl group and the emergence of the unfettered substrate, further investigations have to be done. For example, the reactive excited state should be determined and kinetic analysis are necessary to ascertain how fast the caged compounds are released by using laser flash photolysis. In addition, reaction quantum yields and stability tests have to be accomplished and as well as the identification of the photoproduct represents a future target.

4. Summary

The aim of this work was to synthesize a new photoremovable protecting group (PPG) for carboxylic acids and phosphates that absorbs strongly in the visible region, because most of the PPG require ultraviolet (UV) light for deprotection, which may be harmful for the biological environment. The caged substrates, the caged compound should be soluble in buffered aqueous solution (pH ~ 7) and furthermore the photoproduct should not absorb light at the wavelength of irradiation of the PPG.

Based on the photochemistry of the efficient photolabile 7-hydroxycoumarinyl-4-ylmethyl (HCM) group, efforts were undertaken to extend this chromophoric system (−), by synthesizing the following two analogues.

HCM-group

Analogue A: R= COOH
Analogue B: R= H
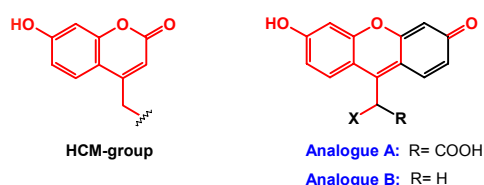
For both analogues, three derivatives (X = Br, OPO(OEt)$_2$ and OAc) should be synthesized. Finally, the acidity constants of the hydroxy group as well as preliminary photochemical properties should be determined.

All attempts to synthesize analogue A, which should have an enhanced solubility in comparison to B, were unsuccessful. Efficient syntheses of the three derivatives of analogue B were achieved by using an overall seven-step synthetic route. The key compound (X = OH, R = H) can be obtained by two different routes from readily available starting materials. Subsequent functional group interconversion, followed by deprotection and oxidation yielded the desired derivatives in overall yields of 44 – 96 %. The acidity constants were determined by spectrophotometric titrations. The photorelease of these derivatives was elucidated by employing irradiation experiments.

Investigations of the acidity constants afforded an overall pK_a of the neutral form of approximately 6.1. Consequently, the derivatives are largely monodeprotonated (ca. 80%) at pH = 7.0 and therefore they display sufficient solubility. Advantageous is their high extinction coefficient at around λ = 520 nm (ε ~ 23000) in aqueous buffered solutions (pH = 7.0), allowing for irradiation with visible light, harmless for the biological

environment. Preliminary observations showed that these solutions are stable for several hours, in the dark.

9-(Bromomethyl)-6-hydroxy-3*H*-xanthen-3-one   and   diethyl-(6-hydroxy-3-oxo-3*H*-xanthen-9-yl)methyl phosphate show a clean photolytic conversion to the photoproduct (λ_{max} = 504 nm) and the released acids (HBr and HOPO(OEt)$_2$) and therefore they should be applicable for producing rapid pH jumps or for caging ATP or caged cyclic nucleotides (cAMP, cGMP, etc.).

Irradiation experiments on (6-hydroxy-3-oxo-3*H*-xanthen-9-yl)methyl acetate indicated that the photorelease of acetic acid is not a clean and uniform reaction. Thus, poor leaving groups can not be efficiently released by this phototrigger.

5. Experimental

Solvents were of analytical quality and melting points are uncorrected. Drying of acetonitrile and acetone was performed by conventional means. Assignments of ^{1}H and ^{13}C NMR signals were achieved using 1D (^{1}H, ^{13}C, DEPT135, APT) and 2D experiments (COSY, HSQC, HMQC, HMBC) under standard instrument parameters and were performed either on a 400 MHz (1D), 500 MHz (2D) or 600 MHz (2D) instrument. As internal standards for NMR spectroscopy incompletely deuterated solvents were used (for ^{1}H NMR: *CDCl$_3$* (7.27 ppm), *CD$_2$Cl$_2$* (5.32 ppm), *DMSO-d$_6$* (2.50 ppm) and *CF$_3$COOD* (11.50 ppm); for ^{13}C NMR: *CDCl$_3$* (77.23 ppm), *CD$_2$Cl$_2$* (54.00 ppm), *DMSO*-d$_6$ (39.51 ppm) and *CF$_3$COOD* (164.2 ppm). Indication of multiplicity: s…singlet, d…doublet, t…triplet, q…quartet, and m…multiplet. All novel compounds were judged to be pure (>97%) by means of their ^{1}H NMR spectra and chromatography. TLC or PLC was performed on TLC aluminium sheets or PLC glass plates (silica gel 60 F$_{254}$, Merck) and preparative column chromatography on silica gel 60 (0.063-0.200 mm, Merck) using columns ranging from 1 to 5 cm in diameter depending on the scale.

Instruments:

Evaporation equipment:

- Rotavapor Büchi R 200 with Büchi B-490 water bath
- *Vaccuubrand* Diaphragm vacuum pump Type MZ 2
- High vacuum pump RS-4, *Brand*

IR spectrometer:

- *Shimadzu* FTIR 8400S

Melting point unit:

- Electrothermal Model 1A-8101 digital capillary melting point apparatus

NMR spectrometers:

- Bruker AVANCE 400 (400 MHz)
- Bruker DRX500 (500 MHz)
- Bruker DRX600 (600 MHz)

2D experiments (COSY, HSQC, HMBC and HMQC) were performed by Dr. Daniel Häussinger at the Institute for Organic Chemistry at the University of Basel.

Mass spectrometers:

- VG70-250 and Finnigan MAT 312

Mass spectra were carried out by Dr. H. Nadig at the Institute for Organic Chemistry at the University of Basel. The ion generation was achieved by electron impact (EI) or bombardment with fast xenon atoms (FAB). Nitrobenzyl alcohol was used as matrix and sodium chloride as additive.

The data are given in mass units per charge (m/z) and the intensities of the signals are indicated in percent of base peak in brackets.

- LCQ-Mass spectrometer System Finnigan MAT (ESI/MS)

- MALDI- Mass spectrometer Voyager-DE-PRO
     p-nitroaniline was used as matrix
     Mode of operation: Reflector
     Accelerating voltage: 20000V
     Grid voltage: 75%
     Extraction delay time: 50 ns
     Laser repetition time: 20 Hz

Elemental Analysis:

The instruments were Leco CHN-900 (C-, H-detection) and Leco RO-478 (O-detection). The elemental analyses were carried out by W. Kirsch at the Institute for Organic Chemistry at the University of Basel. The data are indicated in mass percents.

pH-meter and Dosimat:

- *Metrohm* 654 *pH*-meter with Metrohm LL micro pH glass electrode (Biotrode)
- *Metrohm* 725 Dosimat equipped with an 806-exchange unit (10-cm^3 cylinder)

Ultrasonic:

- *Telsonic* Ultrasonics TPC-15

UV/Vis spectrometers:

- *Agilent* 8453 UV-Vis spectrophotometer
- *Perkin-Elmer* Lamda 9 UV-Vis spectrophotometer

Chemicals:

Abbreviation:	c. p.	chemically pure
	d.	dried
	p.	pure
	p. a.	pro analysis
	p. s.	pro synthesis
	u.	ultra

Name	Formula	M / g · mol^{-1}	Quality	Supplier
Acetic anhydride	$C_4H_6O_3$	102.09	p. a., >99%	Fluka
Acetone	C_3H_6O	58.08	c. p.	Schweizerhall Chemie AG
Acetonitrile	C_2H_3N	41.05	HPLC grade	Scharlau
Ammonia	NH_3	17.03	32%, p.	Merck
Ammonium acetate	$C_2H_7NO_2$	77.08	p. a., ≥99.0%	Fluka
Argon	Ar	39.95	4.6	Linde
Benzene	C_6H_6	78.12	p., absolute	Fluka
Borane tetrahydrofuran solution	$C_4H_{11}BO$	85.94	p. s.; 1 M	Merck
Boron tribromide solution	BBr_3	250.52	p., 1 M in CH_2Cl_2	Fluka
Calcium sulfate hemihydrate (Sikkon)	$CaSO_4$ $0.5 \cdot H_2O$	145.15	98%	Sigma-Aldrich
Chloroform	$CHCl_3$	119.38	p., >97%	Fluka
Chloroform-d$_3$ (CDCl$_3$)	$CDCl_3$	---	99.95%	Uetikon
Dichlordicyanoquinone (DDQ)	$C_8Cl_2N_2O_2$	227.01	p. s.	Merck
Dichloromethane	CH_2Cl_2	84.93	p., absolute	Fluka
Dichloromethane	CH_2Cl_2	84.93	p.	Schweizerhall Chemie AG
Dichloromethane-d$_2$ (CD$_2$CL$_2$)	CD_2Cl_2	84.93	99.9%	Cambridge Iso. Lab.
Diethyl chlorophosphate	$C_4H_{10}ClO_3P$	172.55	p., >97%	Fluka
Diethyl ether	$C_4H_{10}O$	74.12	p.	Schweizerhall Chemie AG

4-Dimethylaminopyridine (DMAP)	$C_7H_{10}N_2$	122.08	p., >97%	Fluka
N,N-Dimethyl formamide-d$_7$ (*DMF*-d$_7$)	C_3D_7NO	79.13	99.5%	Armar
Dimethyl sulfoxide (*DMSO*)	C_2H_6OS	78.13	p. s.	Merck
Dimethyl sulfoxide-d$_6$ (*DMSO*-d$_6$)	C_2D_6OS	78.13	99.98%	Cambridge Iso. Lab.
Dimethylsulfate (*DMS*)	$C_2H_6O_4S$	126.13	p. a.	Fluka
1,4-Dioxane	$C_4H_8O_2$	88.11	p., absolute	Fluka
Ethanol	C_2H_6O	46.08	p., absolute	Fluka
Ethanol	C_2H_6O	46.08	p.	Schweizerhall Chemie AG
Ethyl acetate	$C_4H_8O_2$	88.11	p.	Schweizerhall Chemie AG
Glacial acetic acid	$C_2H_4O_2$	60.05	p. a.	Merck
n-Hexane	$C_{16}H_{14}$	86.18	HPLC-grade	Scharlau
Hydrobromic acid	HBr	80.92	p. a., 62%	Fluka
Hydrochloric acid	HCl	36.46	36-38%	Merck
Hydrogen peroxide	H_2O_2	34.01	p. a., 30%	Fluka
Magnesium sulfate anhydrous	$MgSO_4$	120.37	p., >97%	Fluka
Phosphorus pentoxide	P_2O_5	141.94	p., >97%	Fluka
Potassium carbonate anhydrous	K_2CO_3	138.21	p. a., >99%	Fluka
Propan-2-ol	C_3H_8O	60.1	HPLC-grade	Biosolve
Pyridine	C_5H_5N	79.1	p. a., d.	Riedel-de-Häen
Resorcinol	$C_6H_6O_2$	110.11	p. s.	Merck

Sodium	Na	22.99	---	Merck
Sodium acetate anhydrous	CH_3COONa	82.03	u.	Fluka
Sodium carbonate	Na_2CO_3	105.99	p.	Fluka
Sodium chloride	NaCl	58.44	p. a.	Merck
Sodium dihydrogenphosphate hydrate	H_4NaO_5P	137.99	p.a., $\geq99.0\%$	Fluka
Sodium hydrogencarbonate	$NaHCO_3$	84.01	p.	Fluka
Sodium hydrogenphosphate dihydrate	$H_5Na_2O_6P$	177.96	p.a., $\geq99.0\%$	Fluka
Sodium hydroxide	NaOH	39.99	p. a.	Fluka
Sodium sulfate anhydrous	Na_2SO_4	142.04	d.	Fluka
Tetrabromomethane	CBr_4	331.63	p., >97%	Fluka
Tetrahydrofuran	C_4H_8O	70.11	p., absolute	Acros
2,2′,4,4′-Tetrahydroxybenzophenone	$C_{13}H_{10}O_5$	246.22	97%	Aldrich
Toluene	C_7H_8	92.14	p., absolute	Fluka
Trifluoroacetic acid	CF_3COOD	115.03	99.5 %	Aldrich
Triethylamine	$C_6H_{15}N$	101.19	p. a., 99.5%	Fluka
Trimethylaluminum solution	C_3H_9Al	72.09	p., 2 M in toluene	Fluka
Triphenylphosphine	$C_{18}H_{15}P$	262.3	p., >99%	Fluka

Synthesis:

5.1. Synthesis of 3,6-Dihydroxy-9-methylxanthenium bromide (20, $C_{14}H_{11}BrO_3$)

(18)	(19)	(20)
$C_6H_6O_2$	$C_4H_6O_3$	$C_{14}H_{11}BrO_3$
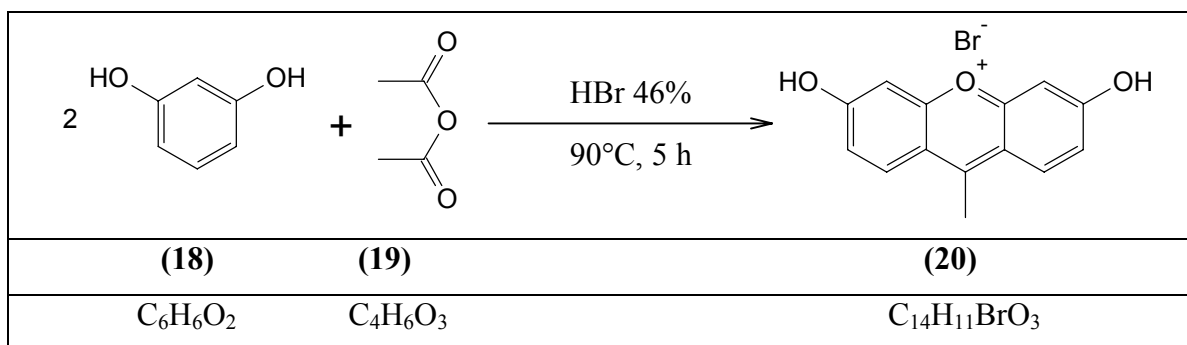
To an ice-cold, stirred solution of 28 ml acetic anhydride (294 mmol) **19**, was added 6.7 cm^3 of hydrobromic acid (46%, 57 mmol) dropwise over a period of 20 min. To this reaction mixture was added 11.00 g resorcinol **18** (100 mmol). After the addition, the water-ice bath was removed and the flask was heated to 90°C for 5 h whereupon it became a red solution with a red precipitate. Afterwards the mixture was cooled by a water-ice bath and filtered over a suction filter. The filter cake was washed thrice with ice-cold glacial acetic acid, as well with ice-cold propan-2-ol and the remaining solid was dried under vacuum over phosphorus pentoxide to yield 4.86 g (31.6%) **20** as orange solid.

M. p.: gives decomp. >250°C.

^{1}H NMR (600 MHz, δ, CF_3COOD, 25°C)**:** 8.40 (d, 2H, J=9.3Hz, *H1* and *H8*), 7.45 (dd, 2H, J=2.2Hz, J=9.3Hz, *H2* u. *H7*), 7.42 (d, 2H, J=2.2Hz, *H4* and *H5*), 3.25 (s, 3H, C*H₃*) ppm.

N*O*ESY (*DMSO*-d$_6$, 25°C)**:** *H1* and *H8* ↔ C*H₃*.

COSY (*DMSO*-d$_6$, 25°C)**:** *H1* and *H8* ↔ *H2* and *H7*, *H2* and *H7* ↔ *H4* and *H5*.

^{13}C-NMR (125 MHz, δ, CF_3COOD, 25°C)**:** 171.9 (C4a, C4b), 170.6 (C9), 161.4 (C3, C6), 132.8 (C1, C8), 122.4 (C2, C7), 119.8 (C8a, C8b), 105.0 (C4, C5), 16.7 (CH$_3$) ppm.

HMQC (*CF$_3$COOD*, 25°C)**:** *H1* and *H8* $\leftrightarrow$ C1 and C8, *H2* and *H7* $\leftrightarrow$ C2 and C7, *H4* and *H5* $\leftrightarrow$ C4 and C5, C*H$_3$* $\leftrightarrow$ CH$_3$.

HMBC (*CF$_3$COOD*, 25°C)**:** *H1* and *H8* $\rightarrow$ C3, C4a, C4b, C6, C8a and C8b, *H2* and *H7* $\rightarrow$ C4, C5, C4a, C4b, C8a and C8b, *H4* and *H5* $\rightarrow$ C2, C3, C4a, C4b, C6, C7, C8a and C8b, C*H$_3$* $\rightarrow$ C9, C8a and C8b.

Elemental Analysis: Found: C (54.49%) H (3.62%)

Calculated: C (54.75%) H (3.61%)

EI-MS (70 eV, 250°C)**:** *m/z* = 226.2 ([M]$^-$) 100 %, 227.21 ([M]) 14.04%, 228.2 ([M-H]$^+$) 1.58%, 229.2 ([M-H]$^{2+}$) 0.11%.

IR: $\bar{\nu}$ = 2916, 2721, 2582, 2359, 1721, 1632, 1599, 1551, 1530, 1474, 1469, 1461, 1410, 1356, 1310, 1269, 1228, 1206, 1168, 1124, 866, 838, 821, 702, 648 cm^{-1}.

UV-Vis (1M HCl)**:** λ_{max} = 205 (46), 226 (69), 249 (51), 291 (8), 426 (100) nm (rel. int.).

5.2. Synthesis of 6-Hydroxy-9-methyl-3*H*-xanthen-3-one (21a, C$_{14}$H$_{10}$O$_3$)

(20)	**(21a)**
C$_{14}$H$_{11}$BrO$_3$	C$_{14}$H$_{10}$O$_3$
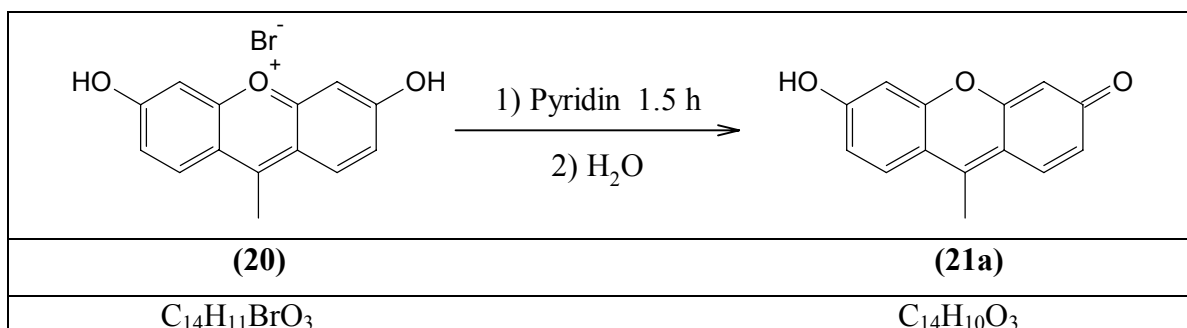
4.52 g (1.47 mmol) 3,6-dihydroxy-9-methylxanthenium bromide (**20**) was dissolved in 80 cm^3 dry pyridine on an ultrasonic bath and was put aside for 1.5 h. To this orange solution

was added about 400 cm^3 of distilled H_2O under slow stirring until the precipitation was completed. The solid was filtered over a suction strainer, washed five times with distilled H_2O and dried under vacuum over phosphorus pentoxide to yield 3.08 g (92.5%) **21a** as crimson solid.

M. p.: gives decomp. >170°C.

TLC: R_f = 0.41 ($CHCl_3$:CH_3OH = 20:1).

^{1}H NMR (400 MHz, δ, DMSO-d$_6$, 25°C)**:** 9.92 (s, 2H, OH), 7.65 (d, 2H, J=8.7Hz, *H1* and *H8*), 6.60 (dd, 2H, J=2.4Hz, J=8.7Hz, *H2* and *H7*), 6.49 (d, 2H, J=2.4Hz, *H4* and *H5*), 5.25 (s, 2H, =CH$_2$) ppm.

DEPT135 (125 MHz, δ, DMSO-d$_6$, 25°C)**:** 125.2 (+), 112.0 (+), 102.3 (+), 95.3(-).

^{13}C NMR (125 MHz, δ, DMSO-d$_6$, 25°C)**:** 158.1 (C6, C3), 150.8 (C4a, C4b), 131.0 (C9), 125.2 (C1, C8), 112.1 (C8a, C8b), 112.0 (C2, C7), 102.3 (C4, C5), 95.3 (=CH$_2$) ppm.

Elemental Analysis: Found: C (72.09%) H (4.52%) O (23.39%)

Calculated: C (74.33%) H (4.46%) O (21.22%)

ESI-MS: (CH_3OH + 2% NH_3, $\gamma \sim$ 0.1 mg·cm^{-3}, negative ion mode): m/z = 225.3 ([M]$^-$) 100%, 226.3 ([M]) 15.8%, 450.8 ([M$_2$]$^{2-}$) 35.2%, 451.9 ([M$_2$]$^-$) 9.9%.

IR: $\overline{\nu}$ = 3257, 2359, 2336, 1558, 1447, 1387, 1315, 1268, 1251, 1198, 1178, 1109, 1040, 927, 839, 814, 806, 778, 654 cm^{-1}.

UV-Vis (C_2H_5OH, c = 1.55 ·10^{-5} mol ·dm^{-3})**:** λ_{max} = 211 (25456), 232 (30733), 274 (9570), 497 (26312) nm (ε / dm^3 ·mol^{-1} ·cm^{-1}).

UV-Vis (0.1M NaOH): λ_{max} = 238 (60), 279 (14), 312 (9), 481 (100) nm (rel. int.).

5.3. Synthesis of 9-Methyl-9*H*-xanthene-3,6-diol (23, C$_{14}$H$_{10}$O$_3$)

(21a)	**(23)**
C$_{14}$H$_{10}$O$_3$	C$_{14}$H$_{12}$O$_3$
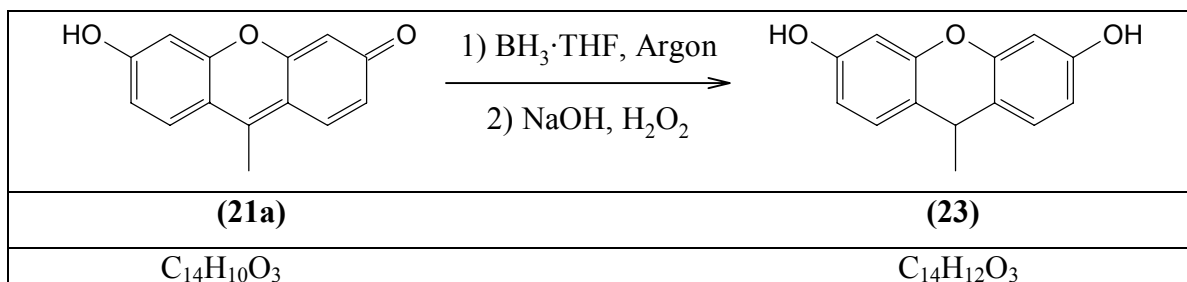
To an ice-cold, stirred solution of 0.8377g (3.7 mmol) 6-hydroxy-9-methyl-3*H*-xanthen-3-one (**21a**) in 10 cm^3 THF, was added BH$_3$-THF complex (8.0 cm^3 of 1.0 M solution in THF, 8.0 mmol) over a period of 20 minutes. The reaction mixture was stirred for 4 h at room temperature, cooled in a water-ice bath, and carefully treated with 2 cm^3 of a 10% solution of water in THF followed by addition of 12.8 cm^3 of a 3 M solution of aqueous sodium hydroxide (36 mmol) and 10 cm^3 of 30% hydrogen peroxide solution (96 mmol). The resulting mixture was stirred for 1.5 h at room temperature, poured into water, neutralized with 4 M hydrochloric acid and extracted with diethyl ether. The combined organic layers were washed with water, dried with Na$_2$SO$_4$ and filtered. The etheric solution was treated with hexane after which the formed precipitate was filtered and dried under vacuum over silica gel to yield 0.7142 g (79 %) **23** as pale yellow solid.

M. p.: gives decomp. >150°C.

1H-NMR (400 MHz, δ, *DMSO*-d$_6$, 25°C)**:** 9.46 (s, 2H, OH), 7.08 (d, 2H, J=8.3Hz, *H1* and *H8*), 6.50 (dd, 2H, J=2.4Hz, J=8.3Hz, *H2* and *H7*), 6.41 (d, 2H, J=2.3Hz, *H4* and *H5*), 3.89 (q, 1H, J=6.8Hz, *H9*), 1.30 (d, 3H, J=6.9Hz, C*H$_3$*-) ppm.

^{13}C NMR (125 MHz, δ, *DMSO*-d$_6$, 25°C)**:** 156.6 (C6, C3), 150.9 (C4a, C4b), 129.1 (C1, C8), 116.6 (C8a, C8b), 110.8 (C2, C7), 102.3 (C4, C5), 30.6 (C9), 27.6 (CH$_3$-) ppm.

DEPT135 (125 MHz, δ, *DMSO*-d$_6$, 25°C)**:** 129.1 (+), 110.8 (+), 102.3 (+), 30.6 (+), 27.6 (+).

COSY (*DMSO*-d$_6$, 25°C)**:** *H1* and *H8* $\leftrightarrow$ *H2* and *H7*, *H2* and *H7* $\leftrightarrow$ *H4* and *H5*, *H9* $\leftrightarrow$ C*H$_3$*-.

ESI-MS: (CH$_3$OH + 2% NH$_3$, $\gamma \sim$ 0.1 mg·cm^{-3}, negative ion mode): *m/z* = 226.2 ([M]$^{2-}$) 5%, 227.1 ([M]$^-$) 100%, 228.12 ([M])14.4%, 454.7 ([M$_2$]$^{2-}$) 54.2%, 455.8 ([M$_2$]$^-$) 13.1%.

IR: $\overline{V}$ = 3307, 2970, 2955, 2948, 2931, 2926, 2853, 2359, 2339, 1748, 1607, 1506, 1472, 1456, 1448, 1435, 1419, 1399, 1395, 1365, 1304, 1289, 1230, 1217, 1167, 1162, 1145, 1104, 995, 847, 805, 796, 668, 620 cm^{-1}.

UV-Vis (C$_2$H$_5$OH)**:** λ_{max} = 211 (100), 279 (11) nm (rel. int.).

5.4. Synthesis of 3,6-Dihydroxy-9*H*-xanthen-9-one (2, C$_{13}$H$_8$O$_4$)

(1)	(2)
C$_{13}$H$_{10}$O$_5$	C$_{13}$H$_8$O$_4$
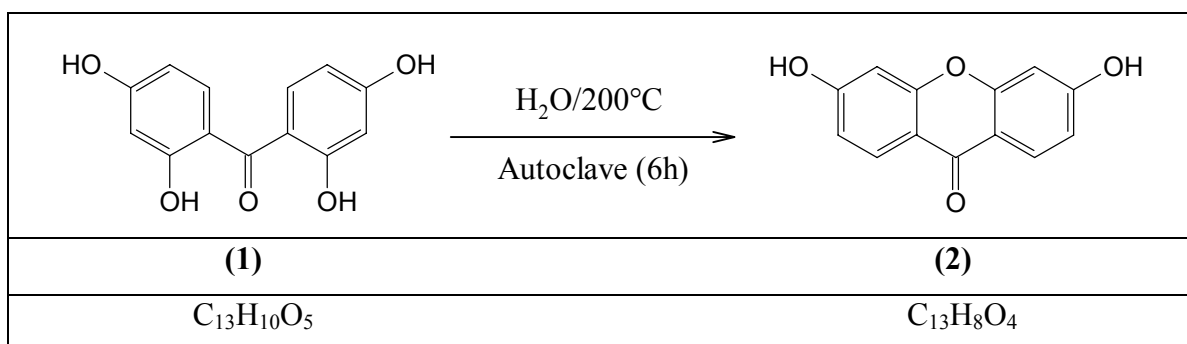
A stirred suspension of 4.00 g (16.3 mmol) 2,2′,4,4′-tetrahydroxybenzophenone (**1**) in 24 cm^3 H$_2$O dist. (1.33 mmol) was heated to 200°C in an autoclave for 6 hours. On cooling 3,6-dihydroxy-9*H*-xanthen-9-one was obtained in clusters of needles. It was filtered, washed thrice with hot distilled H$_2$O and recrystallised from an ethanol-acetone mixture (2/1). The remaining pale orange needles were filtered and dried under vacuum over silica gel to yield 3.3651 g (91 %) **2**.

M. p.: gives decomp. >330°C.

TLC: R_f = 0.87 (CHCl$_3$:CH$_3$OH = 2:1), R_f = 0.43 (CHCl$_3$:CH$_3$OH = 7:1).

¹H NMR (400 MHz, δ, DMSO-d$_6$, 25°C)**:** 10.82 (s, 2H, OH), 7.98 (d, 2H, J=8.7Hz, *H1* and *H8*), 6.86 (dd, 2H, J=2.1Hz, J=8.7Hz, *H2* and *H7*), 6.82 (d, 2H, J=2.0Hz, *H4* and *H5*) ppm.

¹³C-NMR (125 MHz, δ, DMSO-d$_6$, 25°C)**:** 173.8 (C9), 163.2 (C6, C3), 157.3 (C4a, C4b), 127.6 (C1, C8), 113.9 (C8a, C8b), 113.5 (C2, C7), 102.0 (C4, C5) ppm.

Elemental Analysis: Found: C (67.81%) H (3.7%) O (28.49%)

                 Calculated: C (68.42%) H (3.53%) O (28.04%)

ESI-MS: (CH$_3$OH + 2% NH$_3$, $\gamma \sim 0.1$ mg·cm^{-3}, negative ion mode): m/z = 227.2 ([M]$^-$) 100%, 228.25 ([M]) 12.8%, 454.7 ([M$_2$]$^{2-}$) 33.9%, 455.8 ([M$_2$]$^-$) 8.1%.

IR: $\bar{\nu}$ = 3382, 3095, 1629, 1611, 1575, 1454, 1393, 1352, 1324, 1291, 1273, 1254, 1245, 1243, 1169, 1115, 1104, 986, 847, 831, 790, 693, 665, 635 cm^{-1}.

UV-Vis (C$_2$H$_5$OH, c = 1.46·10^{-6} mol ·dm^{-3})**:** λ_{max} = 209 (29114), 239 (42507), 267 (11354), 280 (8053), 312 (24365), 321 (23613) nm (ε / dm^3 ·mol^{-1} ·cm^{-1}).

5.5. Synthesis of 9*H*-Xanthene-3,6-diol (3, C$_{13}$H$_{10}$O$_3$)

(2)	(3)
C$_{13}$H$_8$O$_4$	C$_{13}$H$_{10}$O$_3$
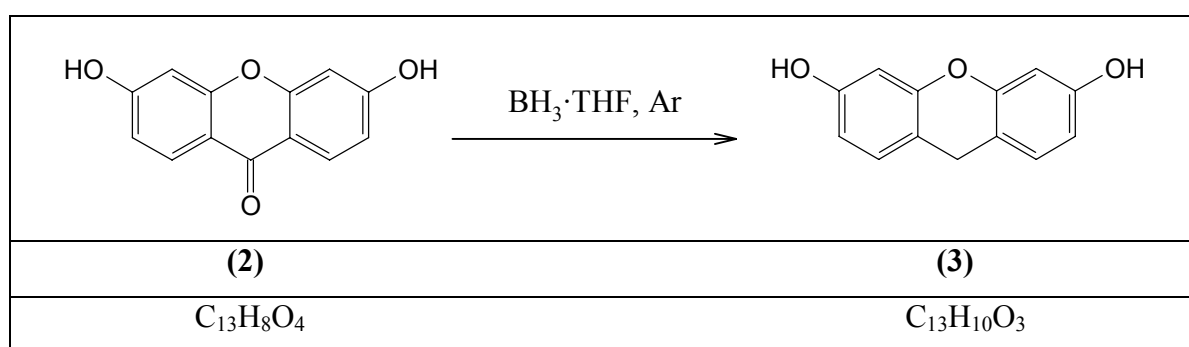
To a stirred suspension of 0.5778 g (2.5 mmol) 3,6-dihydroxy-9*H*-xanthen-9-one (**2**) in 60 cm^3 absolute THF was added 10 cm^3 of borane-tetrahydrofuran complex (1.0 M in THF) at room temperature under nitrogen. After stirring for 2.5 h at room temperature, the reaction mixture became a clear yellow solution. The solvent was removed and 10 cm^3 of 1.0 M HCl was added. The yellow solid product was filtered, washed three times with distilled

H_2O and dried under vacuum over phosphorus pentoxide to yield 0.5229 g (96.4%) **3** as yellow-orange solid.

M. p.: gives decomp. >185°C.

TLC: R_f = 0.41 (CHCl$_3$:CH$_3$OH = 7:1).

^{1}H NMR (400 MHz, δ, DMSO-d$_6$, 25°C)**:** 9.44 (s, 2H, OH), 6.99 (d, 2H, J=8.2Hz, *H1* and *H8*), 6.48 (dd, 2H, J=2.4Hz, J=8.2Hz, *H2* and *H7*), 6.41 (d, 2H, J=2.3Hz, *H4* and *H5*) ppm.

DEPT135 (125 MHz, δ, DMSO-d$_6$, 25°C)**:** 129.5 (+), 110.6 (+), 102.5 (+), 25.5(-).

^{13}C NMR (125 MHz, δ, DMSO-d$_6$, 25°C)**:** 156.4 (C6, C3), 151.4 (C4a, C4b), 129.2 (C1, C8), 110.4 (C8a, C8b), 110.3 (C2, C7), 102.5 (C4, C5), 25.5 (C9) ppm.

Elemental Analysis: Found: C (70.32%) H (4.86%) O (24.82%)

Calculated: C (72.89%) H (4.70%) O (22.41%).

ESI-MS: (CH$_3$OH + 2% NH$_3$, γ ~ 0.1 mg·cm^{-3}, negative ion mode): m/z = 212.2 ([M]$^{2-}$) 5%, 213.2 ([M]$^-$) 100%, 214.2 ([M]) 12.2%, 426.9 ([M$_2$]$^{2-}$) 53.5%, 427.9 ([M$_2$]$^-$) 13.8%.

IR: $\overline{V}$ = 3294, 1632, 1621, 1610, 1593, 1504, 1474, 1469, 1461, 1361, 1299, 1263, 1228, 1167, 1143, 1106, 994, 842, 835, 819, 800, 793, 740, 683, 640, 626, 617, 611 cm^{-1}.

UV-Vis (C$_2$H$_5$OH, c = 1.32 ·10^{-5} mol ·dm^{-3})**:** λ_{max} = 212 (57563), 282 (6476) nm (ε / dm^3 ·mol^{-1} ·cm^{-1}).

5.6. Synthesis of 6-Hydroxy-3*H*-xanthen-3-one (4, C₁₃H₈O₃)

(3)	**(4)**
$C_{13}H_{10}O_3$	$C_{13}H_8O_3$
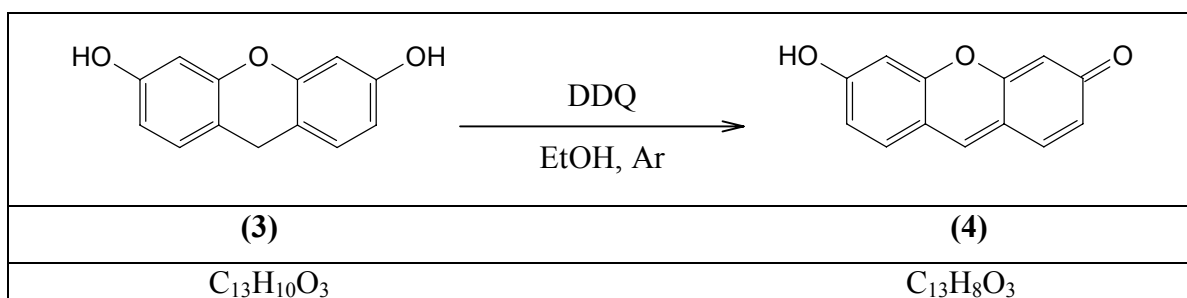
To a stirred solution of 0.4049 g (1.9 mmol) 9*H*-xanthene-3,6-diol (**3**) in 12 cm³ of absolute ethanol at room temperature was added 0.5150 g (2.3 mmol) 2,3-dichloro-5,6-dicyano-1,4-benzoquinone (DDQ). The solution was stirred for 8 h at room temperature under argon. The accumulated precipitate was filtered, washed three times with absolute ethanol and dried under vacuum over silica gel to yield 0.3650 g (91%) **4** as orange-brownish powder.

M. p.: gives decomp. >230°C.

TLC: R_f = 0.22 (CHCl₃:CH₃OH = 10:1).

¹H NMR (400 MHz, δ, *DMF*-d₇, 25°C)**:** 8.36 (s, 1H), 7.73 (d, 2H, J=9.0Hz), 6.81 (d, 2H, J=9.0Hz), 6.63 (s, 2H) ppm.

MALDI-MS: (negative mode)**:** m/z = 210.999, 211.119, 212.010.
MALDI-MS: (positive mode)**:** m/z = 213.027, 213.733, 214.0330, 215.044.
**ESI-MS:** (CH₃OH + 2% NH₃, $\gamma \sim$ 0.1 mg·cm⁻³, negative ion mode): m/z = 211.2 ([M]⁻) 100%, 212.2 ([M]) 11.7%, 422.8 ([M₂]²⁻) 35.3%, 423.8 ([M₂]⁻) 8.7%.

IR: $\overline{\nu}$ = 3070, 1650, 1608, 1581, 1526, 1466, 1447, 1407, 1300, 1247, 1198, 1158, 1103, 1058, 839, 821, 655, 638 cm⁻¹.

UV-Vis (C₂H₅OH)**:** λ_{max} = 210 (100), 229 (97), 273 (sh, 386), 453 (sh, 54), 486 (sh, 70) 504 (82) nm (rel. int.).
UV-Vis (DMF)**:** λ_{max} = 276 (41), 488 (sh, 74) 521 (100) nm (rel. int.).
UV-Vis (0.1M NaOH)**:** λ_{max} = 215 (66), 238 (56), 279 (13), 489 (100) nm (rel. int.).

UV-Vis (water, pH = 7.0, phosphate buffer, I = 0.1 M, c = $1.51 \cdot 10^{-5}$ mol·dm^{-3})**:** λ_{max} = 197 (16836), 238 (24145), 489 (43038) nm (ε / dm^3 ·mol^{-1} ·cm^{-1}).

5.7. Synthesis of 9-Cyano-3-hydroxy-6-fluorone (5, C$_{11}$H$_7$NO$_3$)

(4)	(5)
C$_{13}$H$_8$O$_3$	C$_{14}$H$_7$NO$_3$
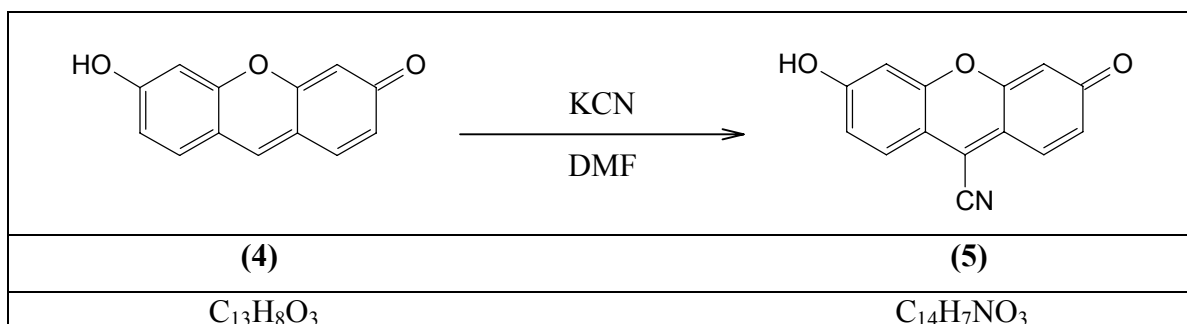
To a stirred solution of 0.2122 g (1.0 mmol) 6-hydroxy-3*H*-xanthen-3-one (**4**) in 5 cm^3 of dry DMF at room temperature was added 0.1330 g (2.0 mmol) potassium cyanide (KCN). The reaction was monitored by the visible absorption spectrum until the starting material was completely consumed. The reaction solution was treated with hexane/dichloromethane = 4/1 after which the formed precipitate was filtered, dried, treated with 5% hydrochloric acid, washed with water and dried under vacuum over silica gel to yield 0.2359 g. The crude product was purified by preparative TLC (SiO$_2$, CHCl$_3$:CH$_3$OH = 7:1) to yield 0.1594 g (67%) **5** as dark brown solid.

M. p.: gives decomp. >250°C.

TLC: R_f = 0.52 (CHCl$_3$:CH$_3$OH = 7:1).

^{1}H NMR (400 MHz, δ, DMSO-d$_6$, 25°C)**:** 7.88 (s, 1H), 7.31 (d, 2H, J=9.2Hz), 6.33 (dd, 2H, J=9.2Hz, J=1.9Hz), 5.99 (d, 2H, J=1.9Hz) ppm.

IR: $\overline{\nu}$ = 3203, 2359, 2331 (CN), 1642, 1615, 1596, 1574, 1543, 1507, 1503, 1481, 1470, 1432, 1410, 1397, 1358, 1341, 1313, 1213, 1169, 1097, 910, 842, 658, 628, 613 cm^{-1}.

UV-Vis (DMF, reaction control)**:** λ_{max} = 273 (19), 566 (46), 619 (10) nm (rel. int.).

5.8. Synthesis of 6-Methoxy-3-oxo-3*H*-xanthene-9-carbonitrile (6, C₁₅H₉NO₃)

(5)	**(6)**
C₁₄H₇NO₃	C₁₅H₉NO₃
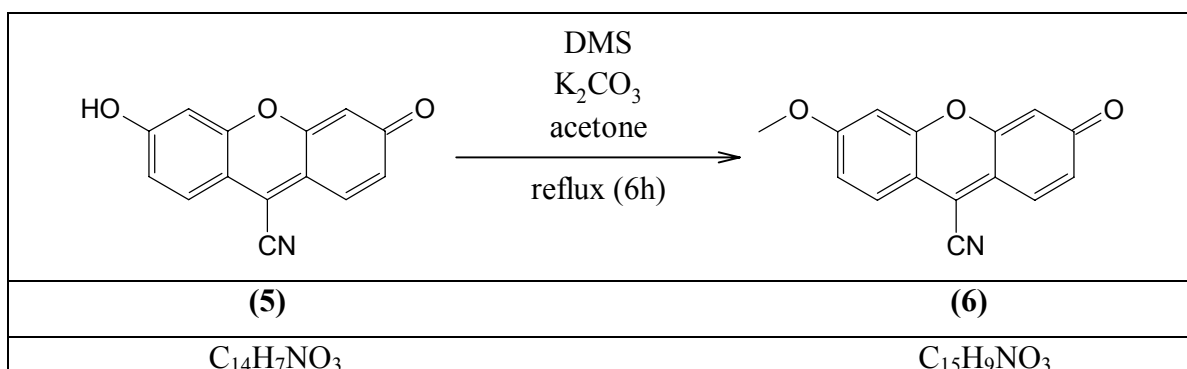
To a stirred suspension of 0.9549 g (4.0 mmol) 9-cyano-3-hydroxy-6-fluorone **5** and 4.2816 g (3.1 mmol) potassium carbonate anhydrous in 100 cm³ absolute acetone, 5.9850 g (50 mmol) dimethylsulfate (*DMS*) was added dropwise. The solution was stirred at room temperature for 30 min and refluxed for 6 h. Whilst cooling with a water-ice bath, 54 cm³ of an ammonia solution (28%) was added dropwise and then stirred for 1 hour at room temperature. By adding distilled H₂O to the mixture the precipitation of the white solid was completed. The precipitate was filtered off, washed three times with distilled H₂O and the remaining solid was dried under vacuum over silica gel to yield 0.4381 g (43%) **6** as red solid. Compound **6** displays extreme poor solubility in all common deuterated solvents, therefore it was impossible to record any NMR spectrum.

M. p.: gives decomp. >230°C.

TLC: R_f = 0.28 (CHCl₃:CH₃OH = 7:1).

EI-MS (70 eV, 150°C)**:** m/z = 251.0 ([M]) 100 %, 252.0 ([M-H]⁺) 31.48 %, 253.0 ([M-H]²⁺) 7.33 %, 254.0 ([M-H]³⁺) 1.30 %.

IR: $\overline{\nu}$ = 2230 (CN), 1646, 1608, 1596, 1568, 1553, 1525, 1501, 1470, 1445, 1438, 1414, 1382, 1351, 1335, 1295, 1264, 1212 (CH₃O-), 1201, 1137, 1108, 1029, 1015, 966, 913, 893, 867, 855, 821, 678, 651, 626, 615 cm⁻¹.

UV-Vis (DMF)**:** λ_{max} = 266 (49), 389 (b, 90) 488 (100) nm (rel. int.).

5.9. Synthesis of 3-Hydroxy-6-methoxy-9H-xanthen-9-one (9, $C_{13}H_8O_3$)

(6)	(9)
$C_{15}H_9NO_3$	$C_{14}H_{10}O_4$
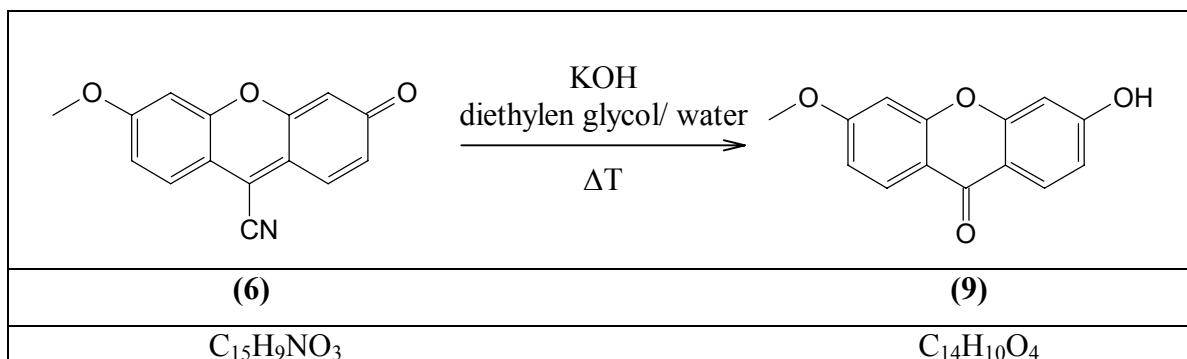
To a stirred solution of 0.1755 g (0.7 mmol) 6-methoxy-3-oxo-3H-xanthene-9-carbonitrile (6) in 6 cm^3 of diethylene glycol and 0.5 cm^3 water at room temperature was added 0.10 g KOH (1.8 mmol). The reaction mixture was refluxed for 5 h, cooled to room temperature and diluted with 12 cm^3 water. Whilst cooling with a water-ice bath, 20% sulphuric acid was added dropwise until the precipitation is completed. The brown precipitate was filtered, washed twice with water and dried under vacuum over silica gel to yield 0.1249 g (73.8%) 9 as beige solid.

M. p.: 303.9-305.1°C (Ref.[66]: 304-305°C)

1H-NMR (600 MHz, δ, DMSO-d$_6$, 25°C)**:** 10.87 (s, 1H, OH), 8.04 (d, 1H, J=8.8Hz, $H8$), 8.00 (d, 1H, J=8.7Hz, $H1$), 7.10 (d, 1H, J=2.1Hz, $H5$), 7.00 (dd, 1H, J=2.3Hz, J=8.8Hz, $H7$), 6.89 (dd, 1H, J=2.1Hz, J=8.7Hz $H2$), 6.84 (d, 1H, J=2.0Hz, $H4$), 3.91 (s, 3H, CH$_3$O-) ppm.

^{13}C-NMR (125 MHz, δ, DMSO-d$_6$, 25°C)**:** 173.8 (C9); 164.31 (C6), 163.5 (C3), 157.5 (C4a), 157.4 (C4b), 127.8 (C1), 127.3 (C8), 114.9 (C8a), 113.9 (C8b), 113.8 (C2), 113.1 (7), 102.0 (C4), 100.5 (C5) ppm.

N*O*ESY (DMSO-d$_6$, 25°C)**:** *OH* ↔ *H2* and *H4*, CH$_3$O- ↔ *H5* and *H7*.

COSY (DMSO-d$_6$, 25°C)**:** *H8* ↔ *H7*, *H7* ↔ *H5*, *H1* ↔ *H2*, *H2* ↔ *H4*.

HMQC (*DMSO*-d$_6$, 25°C)**:** *H1* ↔ *C*1, *H8* ↔ *C*8, *H2* ↔ *C*2, *H7* ↔ *C*7, *H4* ↔ *C4*, *H5* ↔ *C*5, 6-O*CH$_3$* ↔ 6-O*CH$_3$*.

HMBC (*DMSO*-d$_6$, 25°C)**:** *H1* → C9, C3 and C4a, *H8* → C9, C6 and C4b, *H4* → C2, C3, C4, C4a and C8b, *H5*→ C4b, C5, C6, C7 and C8a, *H2* → C4 and C8b, *H7* → C5 and C8a, O*H* → C3, C2 and C4, CH$_3$O- → C6.

EI-MS (70 eV, 250°C)**:** *m/z* = 242.1 ([M]) 100 %, 243.1 ([M-H]$^+$) 12.94 %, 244.1 ([M-H]$^{2+}$) 1.56 %.

ESI-MS: (CH$_3$OH/H$_2$O = 1/1, γ ~ 0.1 mg·cm^{-3}, negative ion mode): *m/z* = 241.2 ([M-H]$^+$) 52.3%, 242.3 ([M]) 8.8%, 482.6 ([M$_2$-2H]$^{2-}$) 100%, 483.7 ([M$_2$-H]$^-$) 20.7%.

IR: $\bar{\nu}$ = 3203, 1620 (C=O), 1597, 1583, 1564, 1456, 1442, 1339, 1299, 1277, 1250, 1213, 1200 (CH$_3$O-), 1173, 1156, 1113, 1105, 1024, 985, 845, 832, 793, 768, 714, 693, 685, 670, 642, 632, 625, 621, 610 cm^{-1}.

5.10. Synthesis of 3,6-Dimethoxy-9*H*-xanthen-9-one (10, C$_{15}$H$_{12}$O$_4$)

(2)	(10)
C$_{13}$H$_8$O$_4$	C$_{15}$H$_{12}$O$_4$
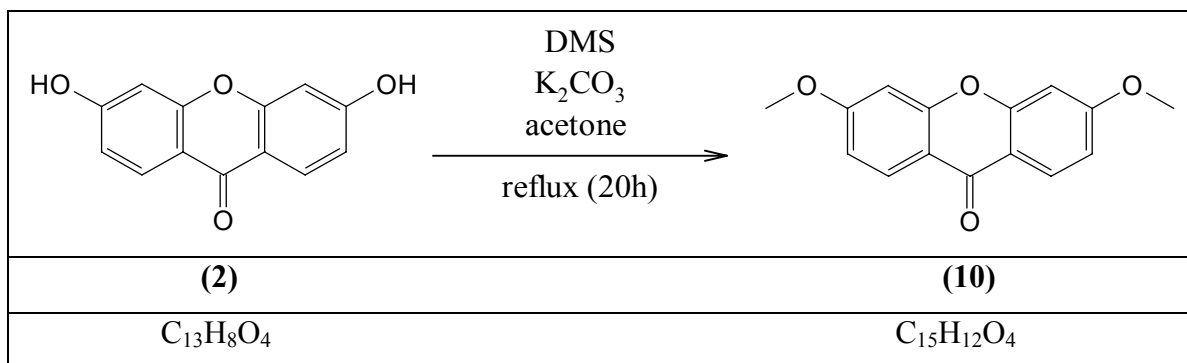
To a stirred suspension of 1.5100 g (6.6 mmol) 3,6-dihydroxy-9*H*-xanthen-9-one (**2**) and 5.9269 g (42.9 mmol) potassium carbonate anhydrous in 110 cm^3 absolute acetone, 15 g (118.6 mmol) dimethylsulfate (*DMS*) was added dropwise. The solution was stirred at room temperature for 30 min and refluxed for 20 h. Whilst cooling with a water-ice bath, 75 cm^3 of an ammonia solution (32%) was added dropwise and then stirred for 1 hour at room temperature. By adding distilled H$_2$O to the mixture the precipitation of the white solid was completed. The precipitate was filtered off, washed three times with distilled

H$_2$O and the remaining solid was dried under vacuum over silica gel to yield 1.5765 g (93%) **10** as white felted needles.

M. p.: 184.5 - 186°C (Ref.[93,94]:187 - 188°C).

TLC: R_f = 0.82 (CHCl$_3$:CH$_3$OH = 20:1).

^{1}H NMR (500 MHz, δ, CD_2Cl_2, 25°C)**:** 8.13 (d, 2H, J=8.8Hz, *H1* and *H8*), 6.90 (ddd, 2H, J=8.8Hz, J=2.4Hz, J=0.7 Hz, *H2* and *H7*), 6.84 (dd, 2H, J=2.4Hz, J=1.0 Hz, *H4* and *H5*), 3.90 (s, 6H, O-CH$_3$) ppm.

^{13}C NMR (125 MHz, δ, CD_2Cl_2, 25°C)**:** 175.3 (C9), 165.0 (C6, C3), 158.3 (C4a, C4b), 128.1 (C1, C8), 116.1 (C8a, C8b), 113.1 (C2, C7), 100.5 (C4, C5), 56.2 (O-CH$_3$) ppm.

HMQC (*CD$_2$Cl$_2$*, 25°C)**:** *H1* ↔ C1, *H8* ↔ C8, *H2* ↔ C2, *H7* ↔ C7, *H4* ↔ C*4*, *H5* ↔ C5, 6-OC*H$_3$* ↔ 6-OCH$_3$, 3-OC*H$_3$* ↔ 3-OCH$_3$.

HMBC (*CD$_2$Cl$_2$*, 25°C)**:** *H1* and *H8* → C3, C6, C4a, C4b and C9, *H2* and *H7* → C8a, C8b, C4 and C5, *H4* and *H5* → C3, C6, C4a, C4b, C8a, C8b, C2 and C7, C*H$_3$*O- → C3 and C6.

Elemental Analysis: Found: C (70.18%) H (4.75%) O (25.07%)

Calculated: C (70.31%) H (4.72%) O (24.97%)

EI-MS (70 eV, 150°C)**:** *m/z* = 256.1 ([M]) 100 %, 257.1 ([M-H]$^+$) 15.91%, 258.1 ([M-H]$^{2+}$) 1.79%, 259.1 ([M-H]$^{3+}$) 0.11%.
ESI-MS: (CH$_3$OH/H$_2$O = 1/1 + 5mM NH$_4$OAc, γ ~ 0.1 mg·cm^{-3}, positive ion mode): *m/z* = 257.1 ([M+H]$^+$) 100%, 258.1 ([M+2H]$^+$) 16.2%.

IR: $\bar{\nu}$ = 1612, 1501, 1428, 1357, 1302, 1257, 1211, 1157, 1099, 1018, 979, 925, 825, 763, 663 cm^{-1}.

UV-Vis (C$_2$H$_5$OH, c = 1.27 ·10^{-5} mol ·dm^{-3})**:** λ_{max} = 209 (26675), 240 (42988), 266 (10957), 307 (22655) nm (ε / dm^3 ·mol^{-1} ·cm^{-1}).
UV-Vis (CH$_2$Cl$_2$): λ_{max} = 242 (100), 266 (68), 302 (50) nm (rel. int.).

5.11. Synthesis of 3,6-Dimethoxy-9*H*-xanthene (12, C$_{15}$H$_{14}$O$_4$)

(10)	(12)
C$_{15}$H$_{12}$O$_4$	C$_{15}$H$_{14}$O$_3$
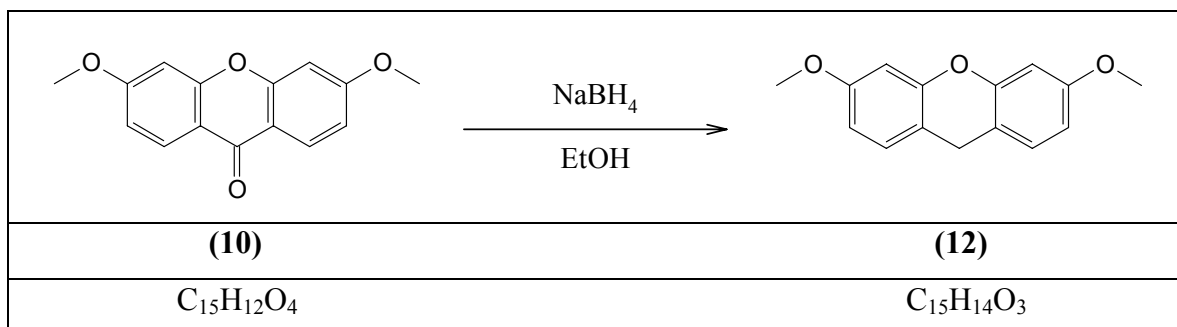
To a solution of 0.9918 g (3.9 mmol) 3,6-dimethoxy-9*H*-xanthen-9-one (**10**) in ethanol (100 cm^3) was added sodium borohydride 4.0807 g (108 mmol). The mixture was refluxed for 24 h. Ethanol was removed from the reaction mixture by evaporation and the resulting residue was treated with aqueous acetic acid (80ml, 20%) to decompose the excess of sodium borohydride, followed by extraction with methylenchloride and washing with H$_2$O. The extract was dried (Na$_2$SO$_4$), filtered, and evaporated to dryness to give a pale yellow solid, which was purified by preparative TLC (SiO$_2$, toluene/hexane = 9/1) to yield 0.6313 g (67.3 %) **12** as white solid.

M. p.: 107 - 108°C

TLC: R_f = 0.75 (toluene/hexane = 9/1).

^{1}H NMR (500 MHz, *δ*, CD$_2$Cl$_2$, 25°C)**:** 7.06 (dt, 2H, J=8.3Hz, J=1.0Hz, *H1* and *H8*), 6.60 (dd, 2H, J=8.3Hz, J=2.5Hz, *H2* and *H7*), 6.57 (d, 2H, J=2.5Hz, *H4* and *H5*), 3.90 (s, 2H, *H9*), 3.78 (s, 6H, -O-C*H$_3$*) ppm.

^{13}C NMR (125 MHz, *δ*, CD$_2$Cl$_2$, 25°C)**:** 159.6 (C3), 152.6 (C4a, C4b), 129.8 (C1, C8), 113.0 (C8a, C8b), 109.8 (C2, C7), 101.7 (C4, C5), 55.7 (O-CH$_3$), 26.6 (C9) ppm.

HMQC (*CD$_2$Cl$_2$*, 25°C)**:** *H1* ↔ *C*1, *H8* ↔ *C*8, *H2* ↔ *C*2, *H7* ↔ *C*7, *H4* ↔ *C4*, *H5* ↔ *C*5, 6-OC*H$_3$* ↔ 6-OC*H$_3$*, 3-OC*H$_3$* ↔ 3-OC*H$_3$*, *H9* ↔ *C9*.

HMBC (*CD$_2$Cl$_2$*, 25°C): *H1* and *H8* → C3, C6, C4a, C4b and C9, *H2* and *H7* → C8a, C8b, C4 and C5, *H4* and *H5* → C3, C6, C4a, C4b, C8a, C8b, C2 and C7, C*H$_3$*O- → C3 and C6, *H9* → C4a and C4b

EI-MS (70 eV, 100°C): *m/z* = 241.0 ([M]) 100 %, 242.0 ([M-H]$^+$) 51.99%, 243.0 ([M-H]$^{2+}$) 7.59%, 244.0 ([M-H]$^{3+}$) 0.71%.

IR: $\overline{V}$ = 1634, 1610, 1576, 1509, 1499, 1462, 1446, 1437, 1420, 1323, 1307, 1276, 1255, 1207, 1183, 1163, 1148, 981, 966, 928, 841, 823, 813, 802, 731, 691, 631, 611 cm^{-1}.

5.12. Synthesis of 3,6-Dimethoxy-9-methylene-9*H*-xanthene (22a, C$_{16}$H$_{14}$O$_3$)

Method A:

(10)	(22a)
C$_{15}$H$_{12}$O$_4$	C$_{16}$H$_{14}$O$_3$
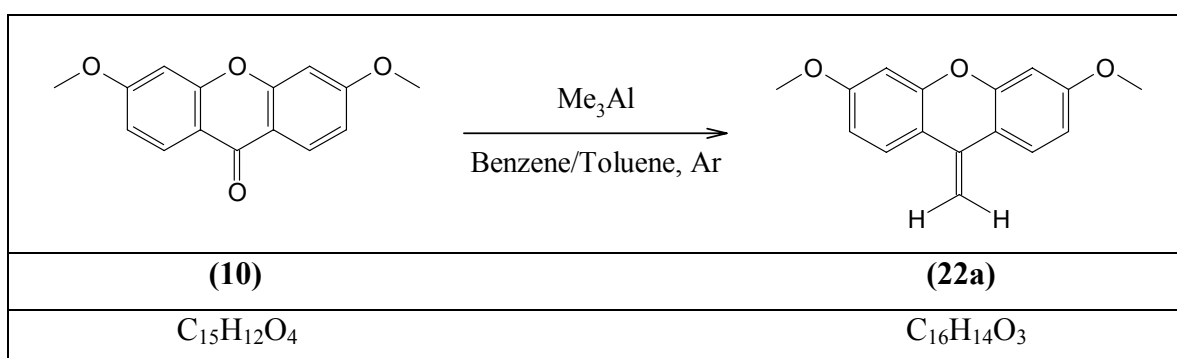
To a stirred suspension of 6.163 g (24.1 mmol) 3,6-dimethoxy-9*H*-xanthen-9-one (**10**) in mixture of 30 cm^3 benzene absolute and 20 cm^3 toluene absolute, 14 cm^3 (28 mmol) of a 2M trimethylaluminum solution was added dropwise under argon at 25°C. After addition the suspension became yellow and was warmed up to 50°C, whereupon it became homogeneous. The temperature was allowed to fall to 25 - 30°C, and then 28.5 cm^3 of the trimethylaluminum solution (57 mmol) was added at the rate required for steady methane evolution. The reaction was completed by heating the mixture at 65°C for 90 min. Afterwards the reaction was terminated by adding 0.1 M HCl under cooling with a water-ice bath. The mixture was extracted with CH$_2$Cl$_2$. The extract was dried (Na$_2$SO$_4$), filtered, and evaporated to dryness to yield 6.014 g (98 %) **22a** as yellow micro needles.

M. p.: 144.5 - 145.8°C (Ref.[79]:146-147°C).

TLC: R_f = 0.84 (CHCl$_3$:CH$_3$OH = 20:1).

1H-NMR (400 MHz, δ, CD_2Cl_2, 25°C)**:** 7.66 (d, 2H, J=8.8Hz, *H1* and *H8*) 6.72 (dd, 2H, J=2.6Hz, J=8.8Hz, *H2* and *H7*) 6.62 (d, 2H, J=2.6Hz, *H4* and *H5*) 5.29 (s, 2H, =CH$_2$) 3.83 (s, 6H, O-CH$_3$) ppm.

1H-NMR (400 MHz, δ, *DMSO*-d$_6$, 25°C)**:** 7.78 (d, 2H, J=8.9Hz, *H1* and *H8*) 6.78 (dd, 2H, J=2.6Hz, J=8.8Hz, *H2* and *H7*) 6.72 (d, 2H, J=2.6Hz, *H4* and *H5*) 5.39 (s, 2H, =CH$_2$) 3.80 (s, 6H, O-CH$_3$) ppm.

DEPT135 (125 MHz, δ, *DMSO*-d$_6$, 25°C)**:** 125.2 (+), 111.3 (+), 100.8 (+), 97.2 (-), 55.4 (+).

^{13}C NMR (125 MHz, δ, *DMSO*-d$_6$, 25°C)**:** 160.4 (C6, C3), 150.7 (C4a, C4b), 130.5 (C9), 125.2 (C1, C8), 113.3 (C8a, C8b), 111.3 (C2, C7), 100.8 (C4, C5), 97.2 (=CH$_2$), 55.4 (O-CH$_3$) ppm.

EI-MS (70 eV, 100°C)**:** m/z: 254.1 (100.0%), 255.10 (17.14 %), 256.10 (2.83 %), 257.10 (0.23 %).

Elemental Analysis: Found: C (75.55%) H (5.59%) O (18.86%)
                        Calculated: C (75.57%) H (5.55%) O (18.88%)

IR: $\overline{\nu}$ = 1625, 1619, 1599, 1567, 1467, 1462, 1440, 1425, 1386, 1330, 1265, 1247, 1207, 1171, 1160, 1109, 1098, 1078, 1028, 983, 946, 925, 838, 818, 783, 636 cm^{-1}.

UV-Vis (C_2H_5OH, c = 8.71 $\cdot 10^{-6}$ mol $\cdot$dm^{-3})**:** λ_{max} = 220 (27674), 231 (32601), 273 (3233) nm (ε / dm^3 $\cdot$mol^{-1} $\cdot$cm^{-1}).
UV-Vis (CHCl$_3$)**:** λ_{max} = 242 (100), 272 (46), 302 (27), 339 (21) nm (rel. int.).

Method B:

(21a)	**(22a)**
$C_{14}H_{10}O_3$	$C_{16}H_{14}O_3$
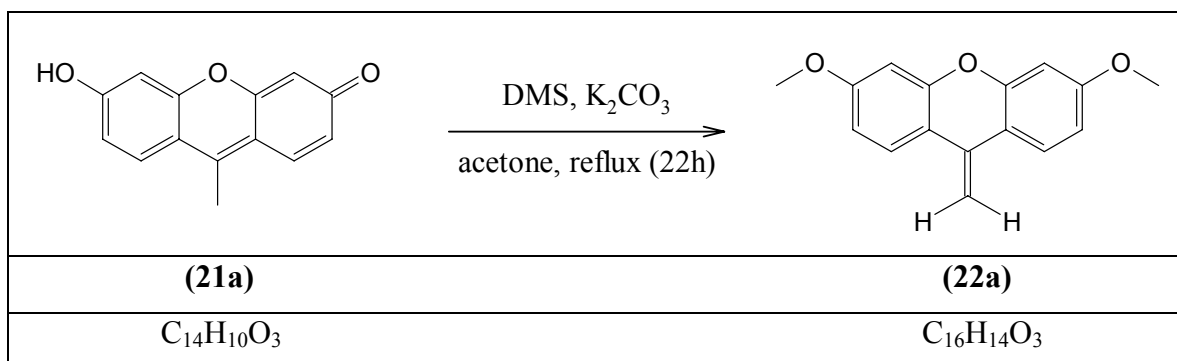
To a stirred suspension of 2.0082 g (8.9 mmol) 9-methylene-9*H*-xanthene-3,6-diol (**21a**) and 7.9960 g (58 mmol) potassium carbonate anhydrous in 150 cm^3 absolute acetone, 15 g (179 mmol) dimethylsulfate (*DMS*) was added dropwise. After addition the solution was stirred at room temperature for 30 min and then refluxed for 22 h. Under cooling with a water-ice bath 117 cm^3 of an aqueous ammonia solution (32%) was added dropwise and then stirred for additional 30 min at 25°C. By adding distilled H_2O to the mixture the precipitation of the solid was completed. After this, the precipitate was filtered off and washed three times with distilled H_2O and the remaining solid was dried under vacuum over phosphorus pentoxide and purified by extraction with n-hexane in an Soxhlet apparatus to yield 1.9369 g (86%) **22a** as yellow needles.

M. p., TLC, IR, UV-Vis, MS and NMR spectra of the product were identical with that obtained by *method A*.

5.13. Synthesis of (3,6-Dimethoxy-9*H*-xanthen-9-yl)methanol (24a, C₁₆H₁₆O₄)

(22a)	**(24a)**
$C_{16}H_{14}O_3$	$C_{16}H_{16}O_4$
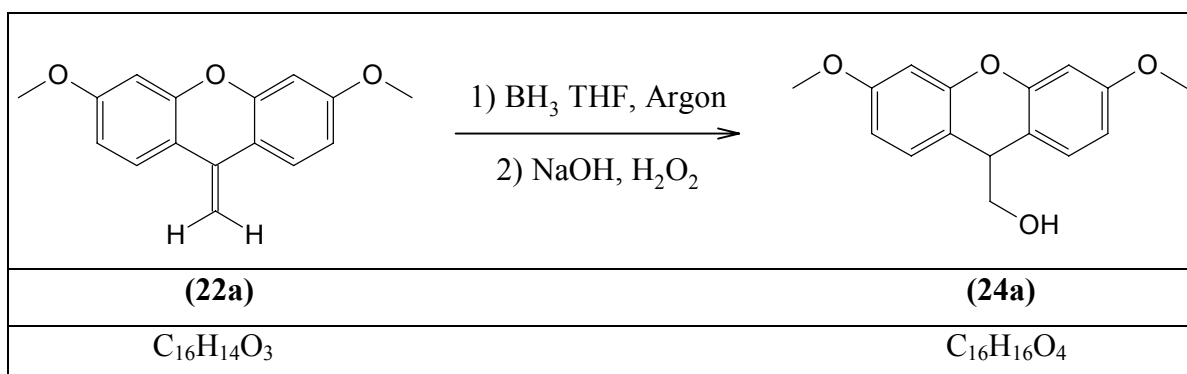
To an ice-cold, stirred solution of 1.0063 g (4.0 mmol) 3,6-dimethoxy-9-methylene-9*H*-xanthene (**22a**) in THF, was added BH₃-THF complex (8.5 cm³ of 1.0 M solution in THF, 8.5 mmol) over a period of 20 minutes. The reaction mixture was stirred for 4 h at room temperature, cooled by using a water-ice bath, and carefully treated with 2 cm³ of a 10% solution of water in THF followed by addition of 12.8 cm³ of a 3.0 M solution of aqueous sodium hydroxide (38.4 mmol) and 10.6 cm³ of 30% hydrogen peroxide solution (102 mmol). The resulting mixture was stirred for 1.5 h at room temperature, poured into water, neutralized with 4 M hydrochloric acid and extracted with diethyl ether. The combined organic layers were washed with water, dried with Na₂SO₄, filtered, evaporated to dryness to give a pale yellow solid, which was purified by column chromatography (SiO₂, CHCl₃/MeOH = 20/1) to yield 0.9574 g (88.8%) **24a** as white solid.

M. p.: 83.9 - 85.0°C

TLC: R_f = 0.64 (CHCl₃:CH₃OH = 20:1).

1H-NMR (600 MHz, δ, *DMSO*-d₆, 25°C)**:** 7.23 (d, 2H, J=8.5Hz, *H1* and *H8*), 6.68 (dd, 2H, J=2.6Hz, J=8.4Hz, *H2* and *H7*), 6.63 (d, 2H, J=2.5Hz, *H4* and *H5*), 4.81 (t, 1H, J=5.3Hz, OH), 3.86 (t, 1H, J=6.1Hz, *H9*), 3.86 (s, 6H, O-CH₃), 3.43 (t₍dd₎, 2H, J=5.7Hz, -C*H₂*-) ppm.

COSY (*DMSO*-d$_6$, 25°C)**:** *H1* and *H8* ↔ *H2* and *H7*, *H2* and *H7* ↔ *H4* and *H5*, *OH* ↔ -C**H$_2$**-OH, -C**H**-CH$_2$-OH ↔ -CH-C**H$_2$**-OH.

DEPT135 (125 MHz, δ, *DMSO*-d$_6$, 25°C)**:** 109.4 (+), 100.8 (+), 100.8 (+), 68.2 (-), 55.2 (+), 39.7 (+).

HMQC (*DMSO*-d$_6$, 25°C)**:** *H1* and *H8* ↔ C1 and C8, *H2* and *H7* ↔ C2 and C7, *H4* and *H5* ↔ C4 and C5, *H9* ↔ C9, -C**H$_2$**-OH ↔ -**C**H$_2$-OH, -OC**H$_3$** ↔ -O**C**H$_3$.

^{13}C NMR (125 MHz, δ, *DMSO*-d$_6$, 25°C)**:** 158.8 (C6, C3), 152.0 (C4a, C4b), 130.2 (C1, C8), 114.9 (C8a, C8b), 109.4 (C2, C7), 100.8 (C4, C5), 68.2 (-CH$_2$-OH), 55.2 (O-CH$_3$), 39.7 (C9) ppm.

Elemental Analysis: Found: C (70.63%) H (6.06%) O (23.31%)

Calculated: C (70.58%) H (5.92%) O (23.50%)

ESI-MS: (CH$_3$OH:H$_2$O = 1:1 + 5mmol NH$_4$OAc, $\gamma \sim 0.1$ mg·cm^{-3}, positive ion mode): m/z = 255.1 ([M-OH]$^+$) 32.4%, 272.1 ([M]) 3.1%, 273.0 ([M+H]$^+$) 100%, 289.7 ([M+NH$_4$]$^+$) 3.9%, 561.5 ([M$_2$+NH$_4$]$^+$) 33.4%.

IR: $\overline{\nu}$ = 3299, 3053, 2941, 2921, 2875, 2831, 1633, 1614, 1574, 1500, 1462, 1435, 1425, 1325, 1276, 1259, 1205, 1184, 1161, 1149, 1097, 1053, 1034, 1022, 983, 976, 925, 824, 815, 638, 617 cm^{-1}.

UV-Vis (C$_2$H$_5$OH, c = 1.19 ·10^{-5} mol ·dm^{-3})**:** λ_{max} = 212 (46351), 278 (304) nm (ε / dm^3 ·mol^{-1} ·cm^{-1}).
UV-Vis (CHCl$_3$)**:** λ_{max} = 241 (100), 279 (82) nm (rel. int.).

5.14. Synthesis of 9-(Bromomethyl)-3,6-dimethoxy-9*H*-xanthene (25a, C₁₆H₁₅BrO₃)

(24a)	**(25a)**
C₁₆H₁₆O₄	C₁₆H₁₅BrO₃
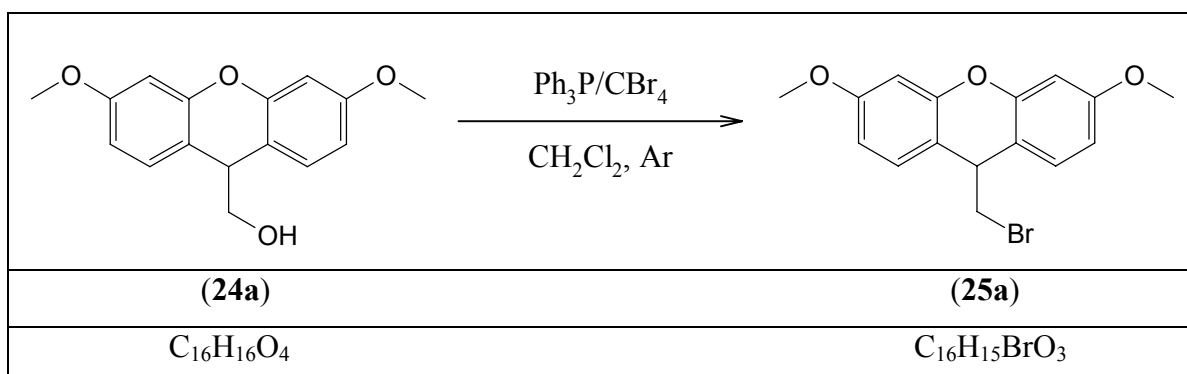
A solution of 0.5055 g (1.86 mmol) (3,6-dimethoxy-9*H*-xanthen-9-yl)methanol (**24a**) in 12.0 cm^3 dichloromethane, 0.5917 g (2.25 mmol) triphenylphosphine (Ph$_3$P) and 1.6322 g (4.92 mmol) carbon tetrabromide (CBr$_4$) was added. After being stirred at room temperature under argon for 10 h, the reaction mixture was sequentially washed twice in each case with saturated sodium hydrogencarbonate solution and brine. The organic layer was dried over Na$_2$SO$_4$, filtered and evaporated to dryness. The residue was purified by column chromatography (SiO$_2$, CHCl$_3$/MeOH = 20/1) to yield 0.6058 g (97.4%) **25a** as a yellow greenish solid.

M. p.: 134.3 - 135.3°C.

TLC: R_f = 0.88 (CHCl$_3$:CH$_3$OH = 20:1).

1H-NMR (400 MHz, δ, *DMSO*-d$_6$, 25°C)**:** 7.31 (d, 2H, J=8.6Hz, *H1* and *H8*), 6.70 (dd, 2H, J=2.6Hz, J=8.5Hz, *H2* and *H7*), 6.63 (d, 1H, J=2.6Hz, *H4* and *H5*), 4.49 (t, 1H, J=4.0Hz, *H9*), 3.78 (d, 2H, J=4.1Hz, -C*H*$_2$-Br), 3.75 (s, 6H, O-CH$_3$) ppm.

COSY (*DMSO*-d$_6$, 25°C)**:** *H1* and *H8* ↔ *H2* and *H7*, -C*H*-CH$_2$-Br ↔ -CH-C*H*$_2$-Br.

DEPT135 (125 MHz, δ, *DMSO*-d$_6$, 25°C)**:** 129.7 (+), 109.9 (+), 100.7 (+), 55.2 (+), 44.3 (-), 37.4 (+) ppm.

^{13}C NMR (125 MHz, δ, DMSO-d$_6$, 25°C)**:** 159.2 (C6, C3), 152.1 (C4a, C4b), 129.7 (C1, C8), 113.7 (C8a, C8b), 109.9 (C2, C7), 100.7 (C4, C5), 55.2 (O-CH$_3$), 44.3 (-CH$_2$-Br), 37.4 (C9) ppm.

Elemental Analysis: Found: C (57.37%) H (4.75%)

Calculated: C (57.33%) H (4.51%)

FAB: m/z (rel. intensity) = 334.0 ([M], 22.3%), 334.9 (100%), 335.9 (31.1%), 336.9 (68.1%), 338.0 (13.4%), 339.0 (3.9%), 340.0 (6.3%).

IR: $\overline{\nu}$ = 2359, 2336, 1656, 1631, 1604, 1566, 1551, 1502, 1469, 1462, 1437, 1422, 1327, 1291, 1257 (CH$_2$), 1201, 1185, 1168, 1149, 1097, 1029, 980, 845, 830, 821, 806, 800, 788, 668 (C-Br), 626, 618 cm^{-1}.

UV-Vis (CHCl$_3$)**:** λ_{max} = 241 (100), 278 (59) nm (rel. int.).

5.15. Synthesis of 9-(Bromomethyl)-9*H*-xanthene-3,6-diol (26a, C$_{14}$H$_{11}$BrO$_3$)

(25a)	**(26a)**
C$_{16}$H$_{15}$BrO$_3$	C$_{14}$H$_{11}$BrO$_3$
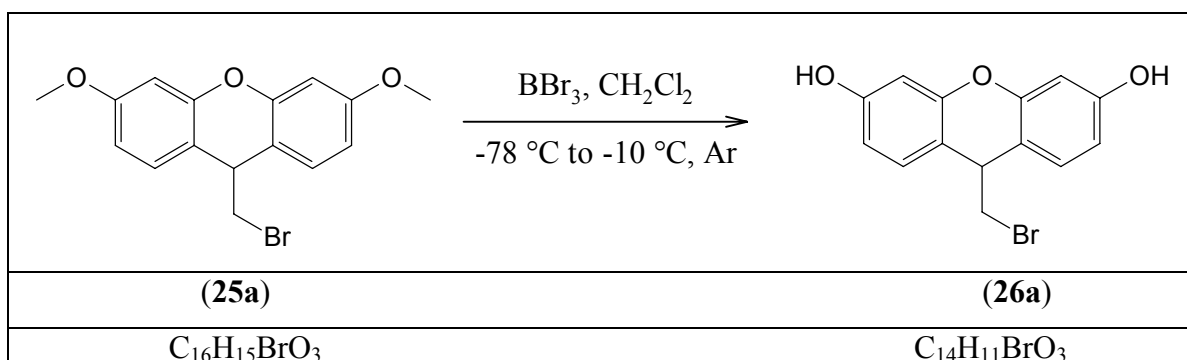
0.8173 g (2.4 mmol) 9-(bromomethyl)-3,6-dimethoxy-9*H*-xanthene (**25a**) was dissolved in 22 cm^3 absolute CH$_2$Cl$_2$ and cooled to -78°C under a positive argon pressure. A 1 M solution of boron tribromide (BBr$_3$) (10 cm^3) was added through a septum with a syringe dropwise. After stirring and warming up during 24 h, the reaction mixture was quenched at around -10°C with 10 cm^3 distilled water and extracted thrice with EtOAc. The combined organic layers were washed with brine, dried over Na$_2$SO$_4$, filtered and evaporated to

dryness. The remaining solid was dried under vacuum over silica gel to yield 0.7428 g (99.2%) **26a** as ochre powder.

M. p.: gives decomp. >120°C.

TLC: R_f = 0.46 (CHCl$_3$:CH$_3$OH = 7:1).

1H-NMR (400 MHz, δ, DMSO-d$_6$, 25°C)**:** 9.57 (s, 2H, OH), 7.16 (d, 2H, J=8.4Hz, *H1* and *H8*), 6.51 (dd, 2H, J=2.4Hz, J=8.3Hz, *H2* and *H7*), 6.42 (d, 1H, J=2.4Hz, *H4* and *H5*), 4.34 (t, 1H, J=4.2Hz, *H9*), 3.70 (d, 2H, J=4.3Hz, -C*H$_2$*-Br) ppm.

COSY (*DMSO*-d$_6$, 25°C)**:** *H1* and *H8* ↔ *H2* and *H7*, *H2* and *H7* ↔ *H4* and *H5*, H*9* ↔ -C*H$_2$*-Br.

^{13}C-NMR (125 MHz, δ, DMSO-d$_6$, 25°C)**:** 157.3 (C3, C6), 152.1 (C4a, C4b), 129.6 (C1, C8), 112.3 (C8a, C8b), 110.9 (C2, C7), 102.2 (C4, C5), 44.3 (-CH$_2$-Br), 37.6 (C9) ppm.

HMQC (*DMSO*-d$_6$, 25°C)**:** *H1* and *H8* ↔ C1 and C8, *H2* and *H7* ↔ C2 and C7, *H4* and *H5* ↔ C4 and C5, *H9* ↔ C9, -C*H$_2$*-Br ↔ -*C*H$_2$-Br.

HMBC (*DMSO*-d$_6$, 25°C)**:** *H1* and *H8* → C3, C6, C4a, C4b and C9, *H2* and *H7* → C3, C6, C8a, C8b, C4 and C5, *H4* and *H5* → C3, C6, C4a, C4b, C8a, C8b, C2 and C7, *H9* → C4a, C4b, C8a, C8b, C2 and C7, -C*H$_2$*-Br- → C9, C8a and C8b.

Elemental Analysis: Found: C (54.84%) H (3.99%)
                          Calculated: C (54.75%) H (3.62%)

MALDI-MS: (positive mode): *m/z* = 304.358, 305.073, 307.084.
ESI-MS: (CH$_3$OH/H$_2$O = 1/1 + 5mM NH$_4$OAc, γ ~ 0.1 mg·cm^{-3}, positive ion mode): *m/z* = 305.0 (^{77}Br: [M+H]$^+$) 30%, 306 ([M]) 6.0%, 307.0 ([M+H]$^+$) 32.6%, 308.0 ([M+2H]$^+$) 5.5%.

IR: $\bar{\nu}$ = 3348, 3217, 2360, 2341, 1612, 12589, 1504, 1450, 1296, 1265 (CH$_2$), 1172, 1095, 987, 933, 840, 756, 648 (C-Br) cm^{-1}.

UV-Vis (CH$_3$OH, c = 1.22·10^{-5} mol·dm^{-3}): λ_{max} = 203 (54772), 211 (54502), 279 (14032) nm (ε / dm^3 ·mol^{-1} ·cm^{-1}).

5.16. Synthesis of 9-(Bromomethyl)-6-hydroxy-3*H*-xanthen-3-one (27a, C$_{14}$H$_9$BrO$_3$)

Method A:

(26a)	(27a)
C$_{14}$H$_{11}$BrO$_3$	C$_{14}$H$_9$BrO$_3$
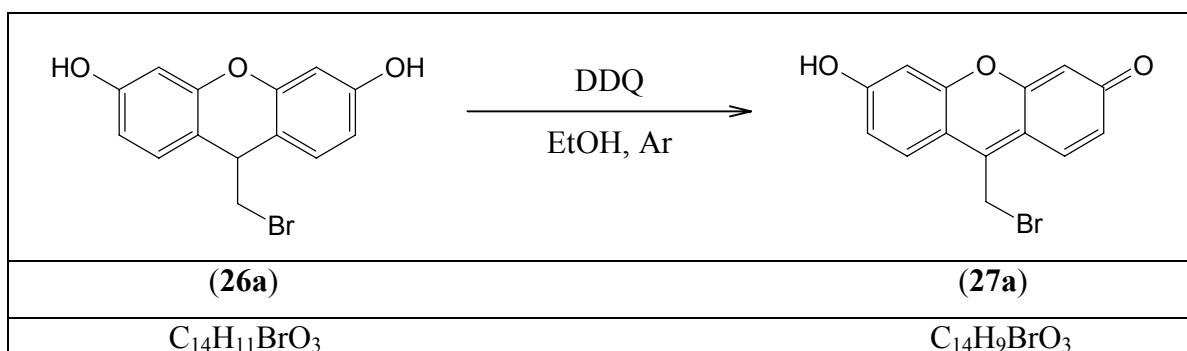
To a solution of 0.3002 g (1 mmol) 9-(bromomethyl)-9*H*-xanthene-3,6-diol (**26a**) in 3 cm^3 absolute ethanol at room temperature 0.2671 g (1.2 mmol) 2,3-dichlo-5,6-dicyano-1,4-benzochinone (DDQ) was added. The reaction mixture was stirred for 1 h at room temperature under argon. The red precipitate was filtered, washed with cold ethanol and dried under vacuum over silica gel and paraffin to yield 0.1421 g (47.6%) **27a** as red-brownish powder.

M. p., TLC, IR, MS and NMR spectra of the product were identical with that obtained by *method B*.

Method B:

(26a)	(27a)
$C_{14}H_{11}BrO_3$	$C_{14}H_9BrO_3$
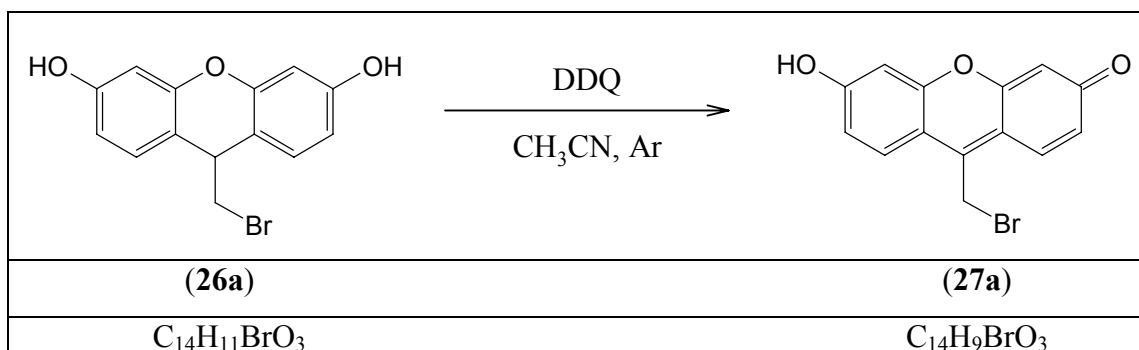
To a solution of 61.3 mg (0.2 mmol) 9-(bromomethyl)-9H-xanthene-3,6-diol **26a** in 2.7 cm^3 absolute acetonitrile at room temperature 54.3 mg (0.24 mmol) 2,3-dichlo-5,6-dicyano-1,4-benzochinone (DDQ) was added. The reaction mixture was stirred for 1.75 h at room temperature under argon. The red precipitate was filtered, washed with acetonitrile and dried under vacuum over silica gel and paraffin to yield 57.8 mg (95%) **27a** as crimson powder.

M. p.: gives decomp. >105°C.

TLC: R_f = 0.44 (CHCl$_3$:CH$_3$OH = 7:1).
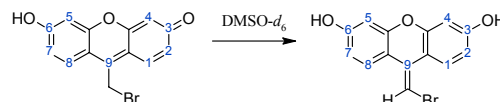
^{1}H NMR (400 MHz, δ, DMSO-d$_6$, 25°C): 10.04 (d, 2H, J=59.9Hz, OH), 8.32 (d, 1H, J=8.8Hz, *H1*), 7.51 (d, 1H, J=8.7Hz, *H8*), 6.68 (dd, 1H, J=2.5Hz, J=8.8Hz, *H2*), 6.67 (s, 1H, =C*H*-Br), 6.60 (m, 2H, J=2.444 Hz, J=2.340 Hz, J=2.4 Hz, *H7* and *H4*), 6.53 (d, 1H, J=2.4Hz, *H5*) ppm.

N*O*ESY (*DMSO*-d$_6$, 25°C): *H8* ↔ 9-(=C*H*-Br), *H1* ↔ 9-(=C*H*-Br).

COSY (*DMSO*-d$_6$, 25°C): *H8* ↔ *H7*, *H7* ↔ *H5*, *H1* ↔ *H2*, *H2* ↔ *H4*.

^{13}C NMR (125 MHz, δ, DMSO-d$_6$, 25°C): 158.9 (C3), 158.6 (C6), 152.6 (C4a), 150.5 (C4b), 128.1 (C9), 127.8 (C1), 124.8 (C8), 113.8 (C8a), 113.85 (C8b), 112.0 (C7), 110.4 (C2), 102.0 (C5), 102.3 (C4), 94.2 (=CH-Br) ppm.

HMQC (*DMSO*-d$_6$, 25°C)**:** *H8* ↔ C8, *H7* ↔ C7, *H5* ↔ C5, *H1* ↔ C1, *H2* ↔ C2,

H4 ↔ C4, =C*H*-Br ↔ =CH-Br.

HMBC (*DMSO*-d$_6$, 25°C)**:** *H1* → C3, C9 and C4a, *H2*→ C4 and C8b, *H4* → C2 and C8b,

H8 → C6, C9 and C8a, *H7* → C5 and C8a, *H5* → C7 and C8a.

MALDI-MS: (positive mode): *m/z* = 304.31, 305.030.

ESI-MS: (CH$_3$OH:H$_2$O = 1:1 + 5mmol NH$_4$OAc, γ ~ 0.1 mg·cm^{-3}, positive ion mode):

m/z = 305.0 ([M+H]$^+$) 100%, 305.9 ([M+2H]$^+$) 17.2%, 307.0 ([M+3H]$^+$) 90.3%, 308.0

([M+4H]$^+$) 12.6%.

IR: $\bar{\nu}$ = 2970, 2359, 2334, 1736 (C=O), 1364, 1601, 1575, 1568, 1456, 1418, 1404, 1318,

1267 (CH$_2$), 1209, 1188, 1129, 1118, 1083, 1048, 931, 848, 826, 815, 771, 764, 668, 653

(C-Br), 633 cm^{-1}.

UV-Vis (water, pH = 7.0, phosphate buffer, I = 0.1M, *c* = 7.54 ·10^{-6} mol ·dm^{-3})**:** λ_{max} = 214

243 (100), 330 (20), 519 (97) nm (rel. int.).

5.17. Synthesis of (3,6-Dimethoxy-9*H*-xanthen-9-yl)methyl acetate (25b, C$_{18}$H$_{18}$O$_5$)

(24a)	(25b)
C$_{16}$H$_{14}$O$_3$	C$_{18}$H$_{18}$O$_5$
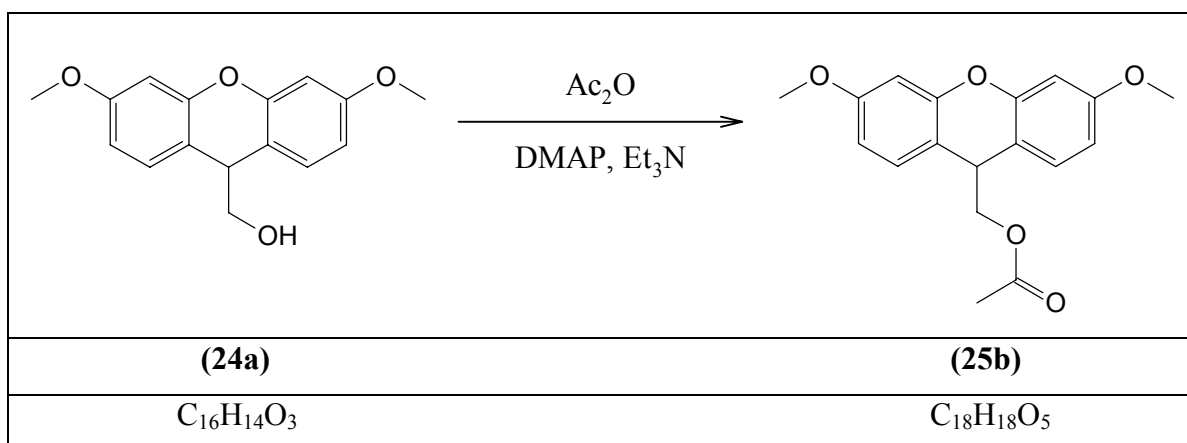
A mixture of 0.3356 g (1.9 mmol) (3,6-dimethoxy-9*H*-xanthen-9-yl)methanol (**24a**), 0.8
cm^3 (5.7 mmol) triethylamine (Et$_3$N), 0.0179 g (0.15 mmol) 4-dimethylaminopyridine

(DMAP) and 0.7 cm^3 (7.4 mmol) acetic anhydride was kept at room temperature for 14 h under argon. The reaction mixture was then distributed between diethyl ether and 2M hydrochloric acid. The organic layer was washed twice with saturated sodium hydrogencarbonate solution and once with distilled water, dried (Na$_2$SO$_4$), filtered, and evaporated to dryness to give a slightly brownish oil, which was purified by thin layer chromatography (SiO$_2$, CHCl$_3$/EtOAc = 30/1) to yield 0.3802 g (98.1%) **25b** as slightly yellow oil, which hardly crystallizes do give a pale yellow solid.

TLC: R_f = 0.61 (CHCl$_3$/EtOAc =3 0/1), R_f = 0.86 (CHCl$_3$:CH$_3$OH = 20:1)

1H-NMR (400 MHz, δ, *DMSO*-d$_6$, 25°C)**:** 7.26 (d, 2H, J=8.5Hz, *H1* and *H8*), 6.71 (dd, 2H, J=2.6Hz, J=8.4Hz, *H2* and *H7*), 6.67 (d, 2H, J=2.5Hz, *H4* and *H5*), 4.20 (t, 1H, J=5.8Hz, *H9*), 4.06 (d, 2H, J=5.9Hz, -C*H$_2$*-O-), 3.76 (s, 6H, O-C*H$_3$*), 1.90 (s, 3H, C*H$_3$*-CO-) ppm.

COSY (*DMSO*-d$_6$, 25°C)**:** *H1* and *H8* ↔ *H2* and *H7*, *H2* and *H7* ↔ *H4* and *H5*, -C*H*-CH$_2$-OAc ↔ -CH-C*H$_2$*-OAc.

DEPT135 (125 MHz, δ, *DMSO*-d$_6$, 25°C)**:** 129.9 (+), 109.9 (+), 101.0 (+), 68.9 (-), 55.2 (+), 36.1 (+), 20.5 (+) ppm.

^{13}C NMR (125 MHz, δ, *DMSO*-d$_6$, 25°C)**:** 169.9 (CH$_3$-**C**O-) 159.22 (C3, C6), 152.2 (C4a, C4b), 129.9 (C1, C8), 113.2 (C8a, C8b), 109.9 (C2, C7), 101.0 (C4, C5), 68.9 (-CH-**C**H$_2$-O-), 55.2 (-O**C**H$_3$), 36.1 (-**C**H-CH$_2$-O-), 20.5 (**C**H$_3$-CO-) ppm.

Elemental Analysis: Found: C (68.26%) H (5.96%) O (25.78%)

　　　　　　　　　　Calculated: C (68.78%) H (5.77%) O (25.45%)

MALDI-MS: (negative mode): *m/z* = 313.358, 314.341.

FAB: *m/z* (rel. intensity) = 314.0 ([M]) 3.08%, 315.1 ([M+H]$^+$) 9.56%, 316.1 ([M+H]$^{2+}$) 2.24%, 317.0 ([M+H]$^{3+}$) 0.67%.

IR: $\overline{\nu}$ = 3000, 2943, 2908, 2836, 2365, 1735 (C=O), 1693, 1650, 1631, 1612, 1599, 1573, 1499, 1462, 1436, 1425, 1377, 1358, 1327, 1286, 1250 (O-CH$_2$), 1224, 1195, 1160, 1120, 1100, 1028, 974, 926, 830, 806, 736, 716, 659, 645 cm^{-1}.

UV-Vis (CHCl$_3$)**:** λ_{max} = 241 (100), 278 (67) nm (rel. int.).

5.18. Synthesis of (3,6-Dihydroxy-9*H*-xanthen-9-yl)methyl acetate (26b, C$_{16}$H$_{14}$O$_5$)

(25b)	(26b)
C$_{18}$H$_{18}$O$_5$	C$_{16}$H$_{14}$O$_5$
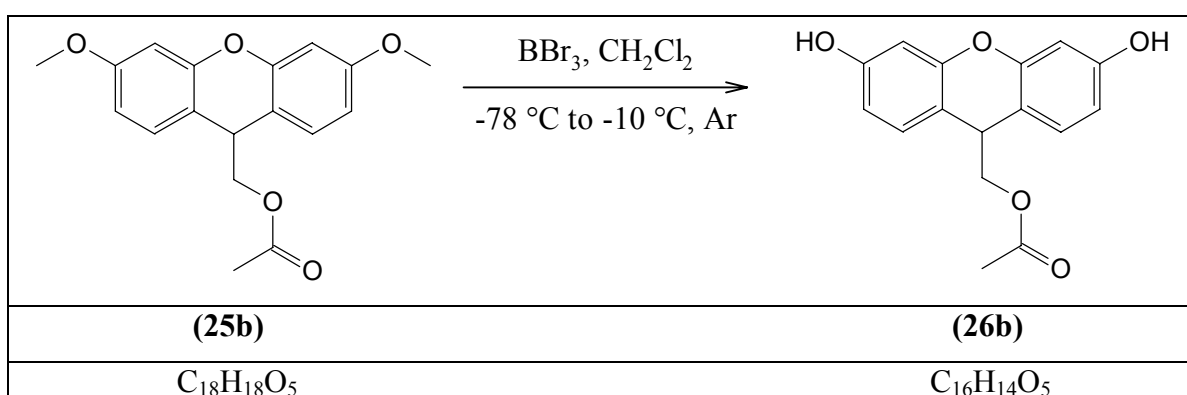
0.4795 g (1.5 mmol) (3,6-dimethoxy-9*H*-xanthen-9-yl)methyl acetate (**25b**) was dissolved in 14 cm^3 absolute CH$_2$Cl$_2$ and cooled to -78°C under a positive argon pressure. A 1M solution of boron tribromide (BBr$_3$) (7.8 cm^3) was added dropwise. After stirring and warming up during 24 h, the reaction mixture was quenched at -10°C with 10 cm^3 distilled water and extracted thrice with EtOAc. The combined organic layers were washed with brine, dried over Na$_2$SO$_4$, filtered and evaporated to dryness. The remaining solid was dried under vacuum over silica gel to yield 0.4258 g (97%) **26b** as a beige powder.

M. p.: gives decomp. >150°C.

TLC: R_f = 0.48 (CHCl$_3$:CH$_3$OH = 7:1).

1H-NMR (600 MHz, δ, DMSO-d$_6$, 25°C)**:** 9.56 (s, 2H, O*H*), 7.11 (d, 2H, J=8.3Hz, *H1* and *H8*), 6.52 (dd, 2H, J=2.1Hz, J=8.2Hz, *H2* and *H7*), 6.46 (d, 2H, J=2.0Hz, *H4* and *H5*), 4.07 (t, 1H, J=5.9Hz, *H9*), 4.00 (d, 2H, J=6.0Hz, -C*H$_2$*-OAc), 1.92 (s, 3H, C*H$_3$*-CO-) ppm.

COSY (*DMSO*-d$_6$, 25°C)**:** *H1* and *H8* ↔ *H2* and *H7*, *H2* and *H7* ↔ *H4* and *H5*, *H9* ↔ -C**H₂**-OAc.

¹³C NMR (125 MHz, δ, *DMSO*-d$_6$, 25°C)**:** 169.7 (CH$_3$-**C**O-), 157.1(C6, C3), 152.0 (C4a, C4b), 129.7 (C1, C8), 111.6 (C8a, C8b), 110.7 (C2, C7), 102.3 (C4, C5), 68.9 (-**C**H$_2$-OAc), 36.0 (C9), 20.4 (**C**H$_3$-CO-) ppm.

HMQC (*DMSO*-d$_6$, 25°C)**:** *H1* and *H8* ↔ C1 and C8, *H2* and *H7* ↔ C2 and C7, *H4* and *H5* ↔ C4 and C5, *H9* ↔ C9, -C**H₂**-OAc ↔-**C**H$_2$-OAc, C**H₃**-CO- ↔ **C**H$_3$-CO-.

HMBC (*DMSO*-d$_6$, 25°C)**:** *H1* and *H8* → C3, C6, C4a, C4b and C9, *H2* and *H7* →C3, C6, C8a, C8b, C4 and C5, *H4* and *H5* → C3, C6, C4a, C4b, C8a, C8b, C2 and C7, *H9* → C4a, C4b, C8a, C8b, C1, C8 and -**C**H$_2$-OAc-, -C**H₂**-OAc- → C9, C8a, C8b and CH$_3$-**C**O-, C**H₃**-CO- → **C**H$_3$-**C**O-.

Elemental Analysis: Found: C (66.01%) H (5.13%) O (28.86%)

Calculated: C (67.13%) H (4.93%) O (27.94%)

ESI-MS: (CH$_3$OH:H$_2$O = 1:1 + 5mmol NH$_4$OAc, γ ~ 0.1 mg·cm^{-3}, negative ion mode): *m/z* = 285.0 ([M]⁻)100%, 286 ([M]) 16%.

IR: $\overline{\nu}$ = 3353, 2359, 2341, 1739 (C=O), 1725, 1700, 1608, 1558, 1506, 1456, 1446, 1374, 1358, 1280, 1272, 1256, 1239 (O-CH$_2$), 1226, 1217, 1209, 1166, 1148, 1109, 1036, 989, 955, 840, 668, 660 cm^{-1}.

UV-Vis (C$_2$H$_5$OH, c = 1.16·10^{-5} mol·dm^{-3})**:** λ_{max} = 211 (48389), 278 (4724) nm (ε / dm^3 ·mol^{-1} ·cm^{-1}).

5.19. Synthesis of (6-Hydroxy-3-oxo-3*H*-xanthen-9-yl)methyl acetate (27b, C$_{16}$H$_{12}$O$_5$)

(26b)	(27b)
C$_{16}$H$_{14}$O$_5$	C$_{16}$H$_{12}$O$_5$
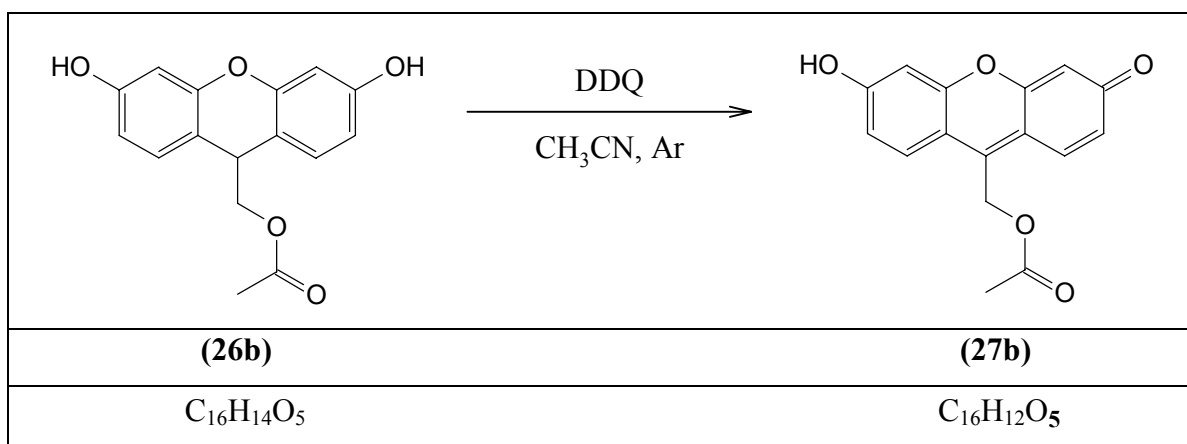
To a solution of 50.7 mg (0.18 mmol) (3,6-dihydroxy-9*H*-xanthen-9-yl)methyl acetate (**26b**) in 2 cm^3 absolute acetonitrile at room temperature 48.1 mg (0.21 mmol) 2,3-dichlor-5,6-dicyano-1,4-benzochinone (DDQ) was added. The reaction mixture was stirred for 1 h at room temperature under argon. The brown precipitate was filtered, washed with acetonitrile and dried under vacuum over silica gel and paraffin to yield 40.3 mg (80.0%) **27b** as dark brown powder.

M. p.: gives decomp. >190°C.

TLC: R_f = 0.10 (CHCl$_3$:CH$_3$OH = 4:1).
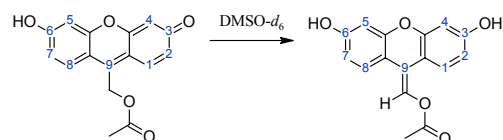
^{1}H NMR (600 MHz, δ, *DMSO*-d$_6$, 25°C): 9.67 (s, 2H, OH), 7.57 (dd, 2H, J=8.5Hz, J=17.1Hz, *H1* and *H8*), 6.63 (m, 2H, *H2* and *H7*), 6.47 (dd, 2H, J=2.3Hz, J=4.8Hz, *H4* and *H5*), 6.24 (s, 1H, =C*H*-OAc), 1.94 (s, 3H, C*H*$_3$-CO-) ppm.

N*O*ESY (*DMSO*-d$_6$, 25°C)**:** *H8* ↔ 9-(=C*H*-OAc), *H1* ↔ 9-(=CH-***OAc***).

COSY (*DMSO*-d$_6$, 25°C)**:** *H8* ↔ *H7*, *H7* ↔ *H5*, *H1* ↔ *H2*, *H2* ↔ *H4*.

¹³C NMR (125 MHz, δ, *DMSO*-d$_6$, 25°C)**:** 169.4 (CH$_3$-**C**O-), 158.1 (C6), 157.9 (C3), 151.7 (C4b), 151.4 (C4a), 129.3 (C1), 128.6 (C8), 114.1 (C8a), 112.9 (C8b), 110.5 (C7), 109.8 (C2), 101.2 (C4 and C5), 98.7 (=**C**H-OAc), 67.6 (C9), 20.2 (**C**H$_3$-CO-) ppm.

HMQC (*DMSO*-d$_6$, 25°C)**:** *H8* ↔ C8, *H7* ↔ C7, *H5* ↔ C5, *H1* ↔ C1, *H2* ↔ C2, *H4* ↔ C4, =C**H**-OAc ↔ =CH-OAc, C**H$_3$**-CO- ↔ CH$_3$-CO-.

HMBC (*DMSO*-d$_6$, 25°C)**:** *H1* → C2, C3, C9 and C4a, *H2*→ C2, C4 and C8b, *H4* → C2, C3, C4a and C8b, *H8* → C6, C7, C9 and C4a, *H7* → C5 and C8a, *H5* → C3, C4b, C6, C7 and C8a, =C**H**-OAc → CH$_3$-**C**O-, C**H$_3$**-CO- → CH$_3$-**C**O-.

MALDI-MS**:** (positive mode): *m/z* = 284.115, 285.124, 286.135, 287.208.

ESI-MS: (CH$_3$OH:H$_2$O = 1:1 + 5mmol NH$_4$OAc, γ ~ 0.1 mg·cm^{-3}, positive ion mode): *m/z* = 285.1 ([M+H]$^+$) , 286.1 ([M+2H]$^+$), 287.2 ([M+3H]$^+$).

IR: $\bar{\nu}$ = 2513, 2360, 2331, 2229, 2221, 1755 (C=O), 1643, 1593, 1556, 1446, 1402, 1272, 1253, 1199, 1176, 1114, 1068, 1041, 991, 946, 927, 839, 818, 650, 613, 590 cm^{-1}.

UV-Vis (water, pH = 7.0, phosphate buffer, I = 0.1 M)**:** λ_{max} = 2143 (85), 244 (100), 377 (21), 496 (sh, 66), 522 (88) nm (rel. int.).

5.20. Synthesis of (3,6-Dimethoxy-9*H*-xanthen-9-yl)methyl diethyl phosphate (25c, C$_{20}$H$_{25}$O$_7$P)

(24a)	(25c)
C$_{16}$H$_{16}$O$_4$	C$_{20}$H$_{25}$O$_7$P
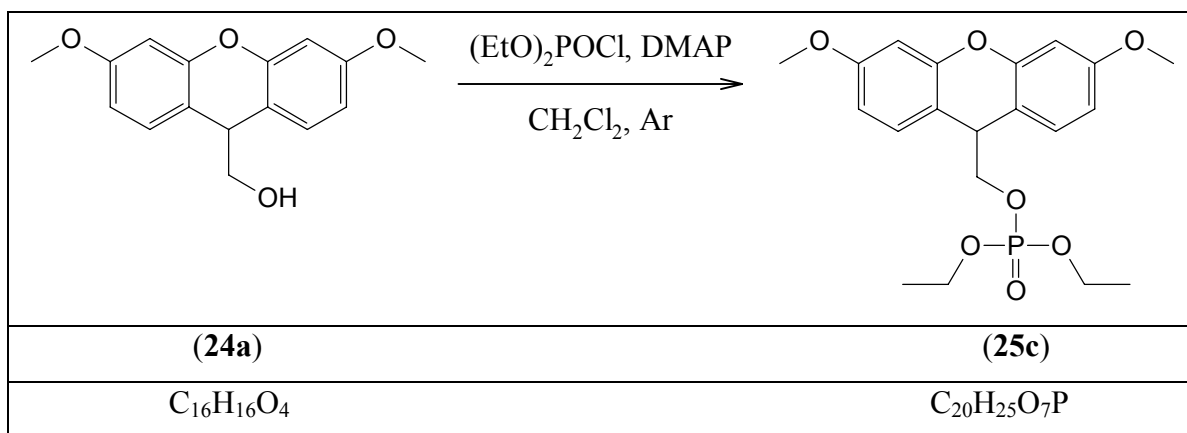
To a solution containing 0.5082 g (1.87 mmol) (3,6-dimethoxy-9*H*-xanthen-9-yl)methanol (**24a**) and 0.2730 g (2.23 mmol) 4-Dimethylaminopyridine (DMAP) dissolved in 18.5 cm^3 dichloromethane absolute 0.32 cm^3 (2.20 mmol) diethyl chlorophosphate was added. The solution was stirred at room temperature under argon for 24 h and quenched by the addition of distilled water (17 cm^3). The solution was then extracted thrice with EtOAc. The combined organic layers were washed twice with brine, dried over anhydrous Na$_2$SO$_4$, filtered and evaporated to dryness. The remaining yellow oil was purified by thin layer chromatography (SiO$_2$, hexane/EtOAc = 60/40) to yield 0.4190 g (55.0%) **25c** as slightly yellow oil.

TLC: R_f = 0.06 (n-hexane/EtOAc = 60/40), R_f = 0.78 (CHCl$_3$:CH$_3$OH = 20:1).

¹H NMR (400 MHz, δ, *DMSO*-d$_6$, 25°C): 7.30 (d, 2H, J=8.6Hz, *H1* and *H8*), 6.73 (dd, 2H, J=2.6Hz, J=8.5Hz, *H2* and *H7*), 6.67 (d, 2H, J=2.5Hz, *H4* and *H5*), 4.24 (dt, 1H, J=1.5Hz, J=4.5Hz, *H9*), 4.02 (t, 2H, J=4.9Hz, CH-C***H***$_2$-O-), 3.76 (s, 6H, -OC***H***$_3$), 3.72 (m, 4H, -O-C***H***$_2$-CH$_3$), 1.07 (dt, 6H, J=0.8Hz, J=7.1Hz, -O-CH$_2$-C***H***$_3$) ppm.

¹H NMR (600 MHz, δ, *CD$_2$Cl$_2$*, 25°C): 7.21 (d, 2H, J=8.4Hz, *H1* and *H8*), 6.68 (dd, 2H, J=2.6Hz, J=8.4Hz, *H2* and *H7*), 6.64 (d, 2H, J=2.5Hz, *H4* and *H5*), 4.18 (t, 1H, J=5.9Hz, *H9*), 4.01 (t, 2H, J=5.9Hz, CH-C***H***$_2$-O-), 3.87 (m, 4H, -O-C***H***$_2$-CH$_3$), 3.80 (s, 6H, -OC***H***$_3$), 1.19 (dt, 6H, J=0.9Hz, J=7.1Hz, -O-CH$_2$-C***H***$_3$) ppm.

N*O*ESY (*CD$_2$Cl$_2$*, 25°C)**:** *H1* and *H8* ↔ *H9* and C9-C*H$_2$*, *H4* and *H5* ↔ 3,6-C*H$_3$*O-, *H2* and *H7* ↔ 3,6-OC*H$_3$*.

COSY (*CD$_2$Cl$_2$*, 25°C)**:** *H1* and *H8* ↔ *H2* and *H7*, *H9* ↔ C9-C*H$_2$*, -O-CH$_2$-*C**H$_3$*** ↔ -O-*C**H$_2$***-CH$_3$.

^{13}C NMR (125 MHz, *δ, CD$_2$Cl$_2$*, 25°C)**:** 160.5 (C3, C6), 153.5 (C4a, C4b), 130.5 (C1, C8), 113.6 (C8a, C8b), 110.3 (C2, C7), 101.7 (C4, C5), 72.6 (-CH-**C**H$_2$-O-), 64.0 (-O-**C**H$_2$-CH$_3$), 55.8 (-O**C**H$_3$), 38.7 (-**C**H-CH$_2$-O-), 16.2 (-O-CH$_2$-**C**H$_3$) ppm.

HMQC (*CD$_2$Cl$_2$*, 25°C)**:** *H1* and *H8* ↔ C1 and C8, *H2* and *H7* ↔ C2 and *C7*, *H4* and *H5* ↔ C4 and C5, *H9* ↔ C9, CH-C*H$_2$*-O- ↔ CH-**C**H$_2$-O-, -O-C*H$_2$*-CH$_3$ ↔ -O-**C**H$_2$-CH$_3$, -OC*H$_3$* ↔ -O**C**H$_3$, -CH$_2$-C*H$_3$* ↔ -O-CH$_2$-**C**H$_3$.

HMBC (*CD$_2$Cl$_2$*, 25°C)**:** *H1* and *H8* → C3, C6, C4a, C4b, C4, C5 and C9, *H2* and *H7* → C3, C6, C8a, C8b, C4 and C5, *H4* and *H5* → C3, C6, C4a, C4b, C8a, C8b, C2 and C7, *H9* → C1, C8, C4a, C4b, C8a, C8b and -CH-C*H$_2$*-O-, -CH-C*H$_2$*-O- → C9, C8a and C8b, -O-C*H$_2$*-CH$_3$ → -O-CH$_2$-**C**H$_3$, -O-CH$_2$-C*H$_3$* → -O-CH$_2$-CH$_3$, -OC*H$_3$* → -O**C**H$_3$.

^{31}P NMR (162 MHz**, 25°C)**:** -1.468 ppm.

Elemental Analysis: Found: C (57.90%) H (6.25%) O (35.85%)

Calculated: C (58.82%) H (6.17%) O (35.01%)

FAB: *m/z* (rel. intensity) = 406.1 ([M]$^{2-}$) 0.74%, 407.1([M]$^-$) 4.66%, 408.1([M]) 1.34%, 409.1([M+H]$^+$) 3.85%, 410.1([M+H]$^{2+}$) 1.02%.

MALDI-MS: (positive mode): *m/z* = 406.978, 407.977, 408.979.

IR: $\overline{\nu}$ = 2980, 2940, 2906, 2836, 2360, 2332, 1733, 1634, 1614, 1599, 1574, 1500, 1464, 1437, 1427, 1394, 1369, 1326, 1258 (P=O), 1202, 1196, 1162 (P-O-C), 1121, 1101, 1014 (P-O-C), 971 (P-O-C), 891, 830, 800, 733 cm^{-1}.

UV-Vis (CHCl$_3$)**:** λ_{max} = 241 (100), 278 (62) nm (rel. int.).

5.21. Synthesis of (3,6-Dihydroxy-9*H*-xanthen-9-yl)methyl diethyl phosphate (26c, C$_{18}$H$_{21}$O$_7$P)

Attempt 1:

(25c)	R=H (26c) R= CH$_3$ (26d)
C$_{20}$H$_{25}$O$_7$P	R= H, C$_{18}$H$_{21}$O$_7$P R= CH$_3$, C$_{19}$H$_{23}$O$_7$P
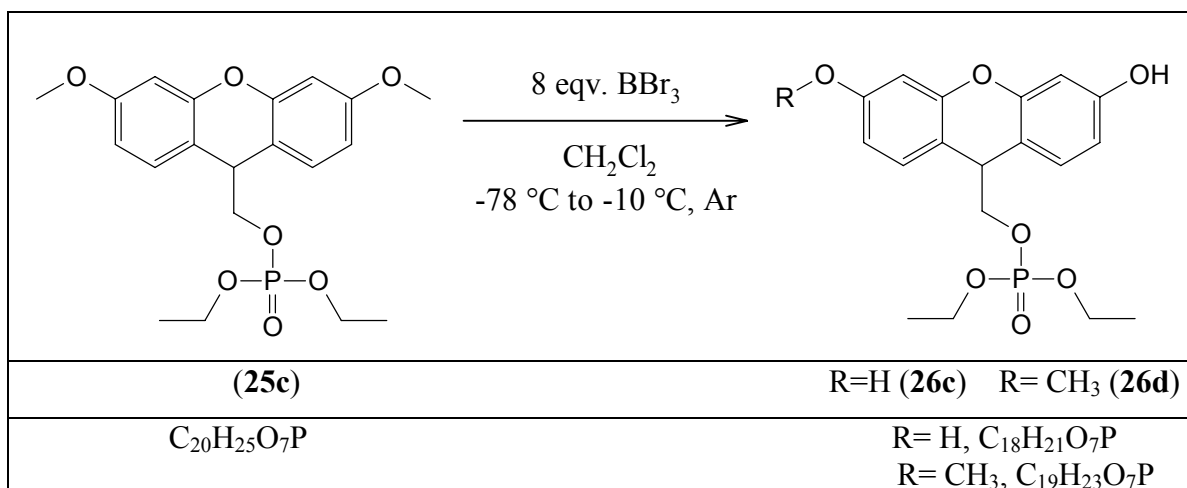
46.2 mg (0.1 mmol) (3,6-dimethoxy-9*H*-xanthen-9-yl)methyl diethyl phosphate (**25c**) was dissolved in 4 cm^3 absolute CH$_2$Cl$_2$ and cooled to -78°C under a positive argon pressure. A 1 M solution of boron tribromide (BBr$_3$) (0.8 cm^3, 8 equivalents) was added dropwise whilst stirring. After stirring and warming up during 24 h, the reaction mixture was quenched at -10°C with distilled 2 cm^3 water and extracted thrice with EtOAc. The combined organic layers were washed with brine, dried over Na$_2$SO$_4$, filtered and evaporated to dryness. The remaining yellow solid was separated by PLC with CHCl$_3$/MeOH = 7/1 as mobile phase to give 28.3 mg (65.8%) (3,6-dihydroxy-9*H*-xanthen-9-yl)methyl diethyl phosphate (**26c**) as beige powder and 9.5 mg (21.3%) diethyl (3-hydroxy-6-methoxy-9*H*-xanthen-9-yl)methyl phosphate (**26d**) as yellow oil.

NMR-data for (3,6-dihydroxy-9*H*-xanthen-9-yl)methyl diethyl phosphate (**26c**) vide page 123.

Diethyl (3-hydroxy-6-methoxy-9*H*-xanthen-9-yl)methyl phosphate (**26d**):

TLC: R_f = 0.70 (CHCl$_3$:CH$_3$OH = 7:1)

1H-NMR (400 MHz, δ, *DMSO*-d$_6$, 25°C)**:** 9.63 (s, 1H, *OH*), 7.28 (d, 1H, J=8.5Hz, *H8*), 7.17 (d, 1H, J=8.5Hz, *H1*), 6.71 (dd, 1H, J=2.6Hz, J=8.4Hz, *H7*), 6.67 (d, 1H, J=2.5Hz, *H5*), 6.55 (dd, 1H, J=2.4Hz, J=8.3Hz, *H2*), 6.47 (d, 1H, J=2.4Hz, *H4*), 4.18 (dt, 1H, J=1.3Hz, J=4.7Hz, *H9*), 3.98 (m, 2H, J=1.4Hz, J=5.1Hz, CH-C*H$_2$*-O-), 3.75 (s, 3H, C*H$_3$*O-), 3.73 (m, 4H, -O-C*H$_2$*-CH$_3$), 1.08 (ddt, 6H, J=0.9Hz, J=1.3Hz, J=7.1Hz, -O-CH$_2$-C*H$_3$*) ppm.

COSY (*DMSO*-d$_6$, 25°C)**:** *H1* $\leftrightarrow$ *H2*, *H2* $\leftrightarrow$ *H4*, *H8* $\leftrightarrow$ *H7*, *H7* $\leftrightarrow$ *H5*, *H9* $\leftrightarrow$ CH-C*H$_2$*-O-, -O-CH$_2$-C*H$_3$* $\leftrightarrow$ -O-C*H$_2$*-CH$_3$.

N*O*ESY (*DMSO*-d$_6$, 25°C)**:** *H2* $\leftrightarrow$ O*H*, *H4* $\leftrightarrow$ O*H*.

^{13}C NMR (125 MHz, δ, *DMSO*-d$_6$, 25°C)**:** 159.2 (C6), 157.4 (C3), 152.4 (C4b), 152.2 (C4a), 129.87 and 129.80 (C1 and C8), 112.9 (C8a), 111.08 (C8b), 111.00 (C2), 109.8 (C7), 102.3 (C4), 100.9 (C5), 72.36 and 72.30 (CH-**C**H$_2$-O-, diastereotopic), 62.95 and 62.89 (O-**C**H$_2$-CH$_3$, diastereotopic), 55.2 (CH$_3$O-), 37.13 and 37.05 (C9, diastereotopic), 15.75 (O-CH$_2$-**C**H$_3$), 15.69 (O-CH$_2$-**C**H$_3$) ppm.

APT (*DMSO*-d$_6$, 25°C)**:** 159.2 (-), 157.4 (-), 152.4 (-), 152.2 (-), 129.87 and 129.80 (+), 112.9 (-), 111.08 (-), 111.00 (+), 109.8 (+), 102.3 (+), 100.9 (+), 72.36 and 72.30 (-), 62.95 and 62.89 (-), 55.2 (+), 37.13 and 37.05 (+), 15.75 (+), 15.69 (+) ppm.

DEPT135 (*DMSO*-d$_6$, 25°C)**:** 129.87 and 129.80 (+), 111.00 (+), 109.8 (+), 102.3 (+), 100.9 (+), 72.36 and 72.30 (-), 62.95 and 62.89 (-), 55.2 (+), 37.13 and 37.05 (+), 15.75 (+), 15.69 (+) ppm.

HMQC (*DMSO*-d$_6$, 25°C)**:** *H1* $\leftrightarrow$ C1, *H2* $\leftrightarrow$ C2, *H4* $\leftrightarrow$ C4, *H8* $\leftrightarrow$ C8, *H7* $\leftrightarrow$ C7, *H5* $\leftrightarrow$ C5, *H9* $\leftrightarrow$ C9, CH-C*H$_2$*-O- $\leftrightarrow$ CH-**C**H$_2$-O-, -O-C*H$_2$*-CH$_3$ $\leftrightarrow$ -O-**C**H$_2$-CH$_3$, -CH$_2$-C*H$_3$* $\leftrightarrow$ -O-CH$_2$-**C**H$_3$, C*H$_3$*O- $\leftrightarrow$ **C**H$_3$O-.

HMBC (*DMSO*-d$_6$, 25°C)**:** *H1* → C3, C4a and C9, *H2* → C3, C4b and C8b, *H4* → C2, C3, C4a and C8b, *H5* → C4b, C7, C6 and C8a, *H7* → C5, C6 and C8a, *H8* → C4b, C6 and C9, *CH$_3$O-* → C6, *H9* → C8a, C8b ,C1, C8 and CH-C*H$_2$*-O-, CH-C*H$_2$*-O- → C9, C8a and C8b, O-C*H$_2$*-CH$_3$ → -O-CH$_2$-CH$_3$, -O-CH$_2$-C*H$_3$* → -O-**C**H$_2$-CH$_3$.

^{31}P NMR (162 MHz, 25°C)**:** -4.582 ppm.

ESI-MS: (CH$_3$OH:H$_2$O = 1:1 + 5mmol NH$_4$OAc, $\gamma \sim$ 0.1 mg·cm^{-3}, positive ion mode): m/z = 241.1 ([M-OP=O(OEt)$_2$]$^+$) 100%, 394.7 ([M]) 46.4%, 411.7 ([M+NH$_4$]$^+$) 22.6%, 788.8 ([M$_2$]) 17.2%.

IR: $\overline{\nu}$ = 3203, 2981, 2908, 2835, 1633, 1612, 1606, 1581, 1502, 1462, 1441, 1394, 1369, 1304, 1258 (P=O), 1286, 1230, 1191, 1163 (P-O-C), 1101, 1101, 1078, 1014 (P-O-C), 979 (P-O-C), 8961, 848, 833, 815, 744, 644 cm^{-1}.

Attempt 2:

(25c)	(26c)
C$_{20}$H$_{25}$O$_7$P	C$_{18}$H$_{21}$O$_7$P
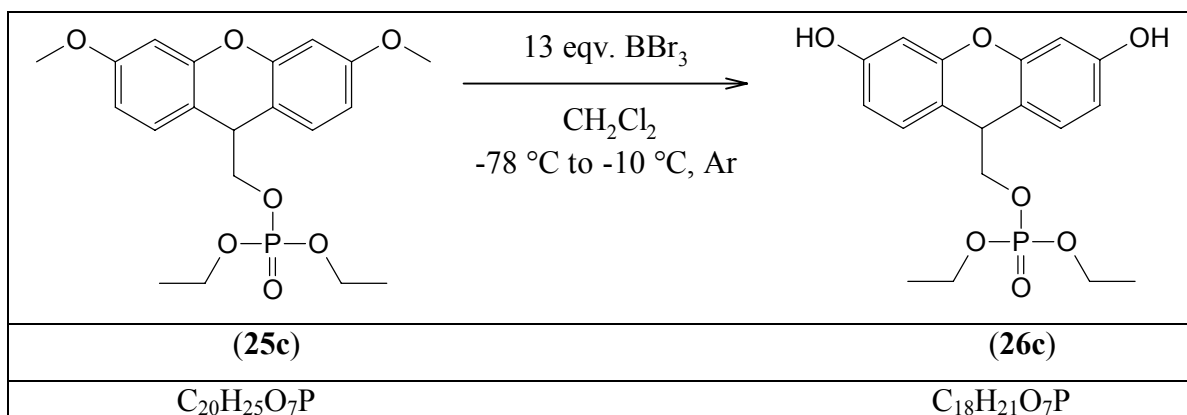
107.2 mg (0.26 mmol) (3,6-dimethoxy-9*H*-xanthen-9-yl)methyl diethyl phosphate (**25c**) was dissolved in 9.5 cm^3 absolute CH$_2$Cl$_2$ and cooled to -78°C under a positive argon pressure. A 1 M solution of boron tribromide (BBr$_3$) (3.5 cm^3, 13 equivalents) was added dropwise whilst stirring. After stirring and warming up during 24 h, the reaction mixture was quenched at around -10°C with distilled 10 cm^3 water and extracted thrice with EtOAc. The combined organic layers were washed with brine, dried over Na$_2$SO$_4$, filtered and evaporated to dryness. The remaining solid was dried under vacuum over silica gel to yield 100 mg (99%) **26c** as a beige powder.

M. p.: gives decomp. >135°C.

TLC: R_f = 0.51 (CHCl$_3$:CH$_3$OH = 7:1).

^{1}H NMR (400 MHz, δ, *DMSO*-d$_6$, 25°C)**:** 9.56 (s, 2H, OH), 7.15 (d, 2H, J=8.4Hz, *H1* and *H8*), 6.53 (dd, 2H, J=2.2Hz, J=8.3Hz, *H2* and *H7*), 6.45 (d, 2H, J=2.2Hz, *H4* and *H5*), 4.12 (t, 1H, J=4.3Hz, *H9*), 3.94 (t, 2H, J=5.2Hz, CH-C*H$_2$*-O-), 3.74 (m, 4H, -O-C*H$_2$*-CH$_3$), 1.09 (t, 6H, J=7.1Hz, -O-CH$_2$-C*H$_3$*) ppm.

COSY (*DMSO*-d$_6$, 25°C)**:** *H1* and *H8* $\leftrightarrow$ *H2* and *H7*, *H2* and *H7* $\leftrightarrow$ *H4* and *H5*, *H9* $\leftrightarrow$ C9-C*H$_2$*, -O-CH$_2$-C*H$_3$* $\leftrightarrow$ -O-C*H$_2$*-CH$_3$.

^{13}C NMR (125 MHz, δ, *DMSO*-d$_6$, 25°C)**:** 157.3 (C3, C6), 152.3 (C4a, C4b), 129.8 (C1, C8), 111.3 (C8a, C8b), 110.8 (C2, C7), 102.3 (C4, C5), 72.2 (CH-**C**H$_2$-O-), 62.93 and 62.87 (-O-**C**H$_2$-CH$_3$, diastereotopic), 37.1 (**C**H-CH$_2$-O-), 15.76 and 15.70 (-O-CH$_2$-**C**H$_3$) ppm.

HMQC (*DMSO*-d$_6$, 25°C)**:** *H1* and *H8* $\leftrightarrow$ C1 and C8, *H2* and *H7* $\leftrightarrow$ C2 and C7, *H4* and *H5* $\leftrightarrow$ C4 and C5, *H9* $\leftrightarrow$ C9, CH-C*H$_2$*-O- $\leftrightarrow$ CH-**C**H$_2$-O-, -O-C*H$_2$*-CH$_3$ $\leftrightarrow$ -O-**C**H$_2$-CH$_3$, -CH$_2$-C*H$_3$* $\leftrightarrow$ -O-CH$_2$-**C**H$_3$.

HMBC (*DMSO*-d$_6$, 25°C)**:** *H1* and *H8* $\rightarrow$ C3, C6, C4a, C4b, C4, C5 and C9, *H2* and *H7* $\rightarrow$ C3, C6, C8a, C8b, C4 and C5, *H4* and *H5* $\rightarrow$ C3, C6, C4a, C4b, C8a, C8b, C2 and C7, *H9* $\rightarrow$ C8a, C8b and CH-**C**H$_2$-O-, CH-C*H$_2$*-O- $\rightarrow$ C9, C8a and C8b, -O-C*H$_2$*-CH$_3$ $\rightarrow$ -O-CH$_2$-**C**H$_3$, -O-CH$_2$-C*H$_3$* $\rightarrow$ -O-**C**H$_2$-CH$_3$.

^{31}P NMR (162 MHz**,** 25°C)**:** -4.768 ppm.

Elemental Analysis: Found: C (56.90%) H (5.77%)

Calculated: C (56.84%) H (5.57%)

ESI-MS: (CH$_3$OH:H$_2$O = 1:1 + 5 mmol NH$_4$OAc, $\gamma \sim$ 0.1 mg·cm^{-3}, positive ion mode): m/z = 380.7 ([M]), 381.7 ([M+H]$^+$), 382.7 ([M+H]$^{2+}$).

IR: $\overline{\nu}$ = 3296, 2960, 2925, 2873, 2853, 2357, 2332, 1736, 1612, 1589, 1502, 1487, 1458, 1365, 1309, 1285, 1262, 1227 (P=O), 1208, 1198, 1174, 1147, 1098, 1069, 1032 (P-O-C), 984 (P-O-C), 859, 851, 820, 801, 778, 668, 651 cm^{-1}.

UV-Vis (CH_3OH, c = 1.20 $\cdot 10^{-5}$ mol $\cdot dm^{-3}$)**:** λ_{max} = 211 (34708), 279 (4208) nm (ε / dm^3 $\cdot mol^{-1}$ $\cdot cm^{-1}$).

5.22. Synthesis of Diethyl (6-hydroxy-3-oxo-3*H*-xanthen-9-yl)methyl phosphate (27c, $C_{18}H_{19}O_7P$)

(26c)	(27c)
$C_{18}H_{21}O_7P$	$C_{18}H_{19}O_7P$
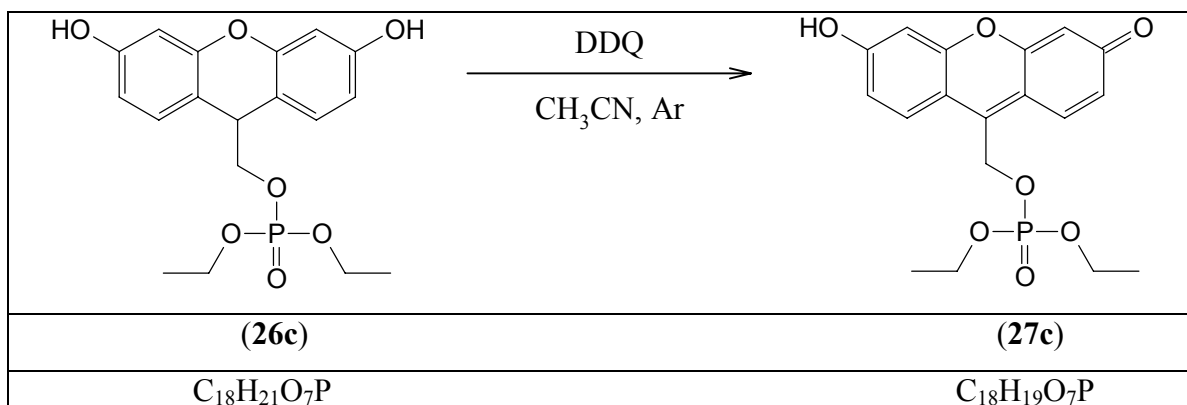
To a solution of 31.3 mg (0.08 mmol) (3,6-dihydroxy-9*H*-xanthen-9-yl)methyl diethyl phosphate (**26c**) in 2 cm^3 absolute acetonitrile at room temperature 23.3 mg (0.1 mmol) 2,3-dichlo-5,6-dicyano-1,4-benzochinone (DDQ) was added. The reaction mixture was stirred for 1 h at room temperature under argon. The red precipitate was filtered, washed with acetonitrile and dried under vacuum over silica gel and paraffin to yield 25.1 mg (80.6%) **27c** as orange powder.

M. p.: gives decomp. >170°C.

TLC: R_f = 0.08 ($CHCl_3$:CH_3OH = 4:1).
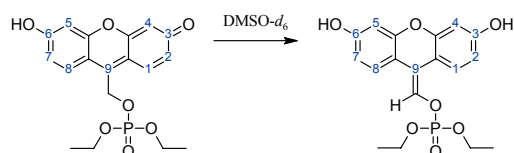
¹H NMR (600 MHz, δ, *DMSO*-d$_6$, 25°C)**:** 9.66 (s, 2H, OH), 7.54 (dd, 2H, J=8.5Hz, J=21.8Hz, *H1* and *H8*), 6.63 (dt, 2H, J=2.2Hz, J=8.7Hz, *H2* and *H7*), 6.47 (dd, 2H, J=2.4Hz, J=3.8Hz, *H4* and *H5*), 5.89 (d, 1H, $^3J_{P-H}$ =7.1Hz, =C*H*-O-),

3.94 (m, 2H, -O-C$\textbf{\textit{H}}_2$-CH$_3$, diastereotopic), 3.74 (m, 2H, -O-C$\textbf{\textit{H}}_2$-CH$_3$, diastereotopic), 1.17 (t, 3H, J=7.0Hz, -O-CH$_2$-C$\textbf{\textit{H}}_3$), 1.04 (t, 3H, J=7.0Hz, -O-CH$_2$-C$\textbf{\textit{H}}_3$) ppm.

N$\textbf{\textit{O}}$ESY (*DMSO*-d$_6$, 25°C)**:** *H8* ↔ 9-(=C*H*-O-).

COSY (*DMSO*-d$_6$, 25°C)**:** *H8* ↔ *H7, H7* ↔ *H5, H1* ↔ *H2, H2* ↔ *H4*.

^{13}**C NMR** (125 MHz, δ, *DMSO*-d$_6$, 25°C)**:** 158.0 (*C*3), 157.9 (*C*6), 151.6 (*C*4a), 151.4 (*C*4b), 129.3 (*C*1), 128.5 (*C*9), 114.1 (*C*8a), 112.5 (*C*8b), 110.42 (*C*2), 110.38 (*C*7), 101.3 (*C*5), 101.1 (*C*4), 67.9 (=$\textbf{\textit{C}}$H-O-), 63.4 (-O-$\textbf{\textit{C}}$H$_2$-CH$_3$), 15.4 (-O-CH$_2$-$\textbf{\textit{C}}$H$_3$) ppm.

HMQC (*DMSO*-d$_6$, 25°C)**:** *H8* ↔ *C*8, *H7/2* ↔ *C*7/2, *H5/4* ↔ *C*5/4, *H1* ↔ *C*1, =C$\textbf{\textit{H}}$-O- ↔ =CH-O-, -O-C$\textbf{\textit{H}}_2$-CH$_3$ ↔ -O-CH$_2$-CH$_3$, -O-CH$_2$-C$\textbf{\textit{H}}_3$ ↔, -O-CH$_2$-CH$_3$.

HMBC (*DMSO*-d$_6$, 25°C)**:** *H1* → *C*3, *C*9 and *C*4a, *H2*→ *C*4 and *C*8b, *H4/5* → *C*2/7, *C*3/6, *C*4a/4b, *C*8a and *C*8b, *H8* → *C*6, *C*9 and *C*4b, *H7* → *C*5 and *C*8a, =CH-O- → *C*8a and *C*8b.

^{31}**P NMR (**162 MHz, 25°C)**:** -2.92 ppm.

ESI-MS: (CH$_3$OH:H$_2$O = 1:1 + 5mmol NH$_4$OAc, γ ~ 0.1 mg·cm^{-3}, positive ion mode): *m/z* = 378.0 ([M]) 100%, 379.1 ([M+H]$^+$) 60.6%, 380.1 ([M+2H]$^+$) 12.5%.

MALDI-MS: (negative mode): *m/z* = 376,370, 377.384, 378.387, 379.379, 380.393, 381.391, 382.243

IR: $\overline{\nu}$ = 3151, 2712, 2586, 2367, 2336, 1722 (C=O), 1599, 1561, 1552, 1480, 1463, 1424, 1413, 1384, 1361, 1323, 1266, 1240 (P=O), 1152, 1125, 1090, 1039 (P-O-C), 992, 954 (P-O-C), 925, 863, 793, 641 cm^{-1}.

UV-Vis (water, pH = 7.0, phosphate buffer, I = 0.1 M): λ_{max} = 214 (80), 245 (100), 332 (14), 527 (84) nm (rel. int.).

5.23. Investigations:

5.23.1. Spectrophotometric Determination of pK_a Values

Data Acquisition:

The absorption spectra were recorded with a Perkin-Elmer Lambda 9 spectrophotometer. The temperature was upholded within 25 ± 0.3°C with a thermostated cell holder. A quartz cell of 1cm path length and 2 cm width with a volumetric capacity of 8 ml was used. The microprocessor-controlled Metrohm LL micro pH glass electrode (Biotrode) was thermostated at 25°C for at least 24 h prior to use and calibrated with standard Metrohm buffer solutions (pH 4, 7) before every set of measurements. A baseline was recorded with H_2O before each set of experiments. 40 µl portions of the titrant were added directly to the quartz cell inside the spectrophotometer using Metrohm 725 Dosimat equipped with an 806-exchange unit (10 cm^3 cylinder). A magnetic stirrer inside the cell ensured rapid mixing of added titrant. Subsequent to each addition of titrant, a spectrum was acquired after the time required to keep the drift of the pH electrode within 0.01 pH units per minute. Approximately 100 spectra and pH readings were collected during each titration. The titrations were conducted at constant ionic strength I = 0.1M. The resulting acidity constants are, therefore, dissociation quotients $K_{a,c}$ at I = 0.1M.

The protonation of the compounds were measured by addition of 0.1M HCl containing 0.1M KCl for keeping the ionic strength constant to a solution of the compound in 0.1M AcONa, pH 1.9 – 7.4. AcONa was dissolved in doubly distilled, CO_2 free H_2O. The absorption of this buffer is negligible above 240 nm.

Data Analysis:

The spectra were corrected for dilution and analyzed with the help of the program SPECFIT [95], which performs a factor analysis and allows to calculate acidity constants as optimized model parameters, with their standard errors, from multiwavelength spectrophotometric data by nonlinear least-squares fitting to the appropriate model function. Nonlinear fitting of three independent runs gave the averaged pK_a's of every compound.

5.23.2. Irradiation

Solutions were irradiated in a quartz UV-cell with a Hanau medium pressure mercury lamp. A band-pass filter was used to isolate the desired excitation wavelength (546 nm). The solutions had concentrations in the range from 10^{-5} to 10^{-6} M and were continuously stirred. Absorption spectra were recorded on an *Agilent* 8453 UV-Vis spectrophotometer.

5.23.3. Computational Calculation

All the geometries were fully optimized using the semiempirical method PM3 (parameterization method 3) and the HOMO-LUMO orbital surface plots were also calculated by PM3 (single point) using PC Spartan Pro software (version 1.0.5). All the calculations were performed under gas phase conditions.

6. References

1.   Cody, W.L., *Greene's Protective Groups in Organic Synthesis. Fourth Edition. By Peter G. M. Wuts and Theodora W. Greene. John Wiley & Sons, Inc., Hoboken, NJ. 2006. xvii + 1082 pp. 16 * 24 cm. ISBN 0-471-69754-0.*.

2.   Jarowicki, K. and P. Kocienski, *Protecting groups.* Journal of the Chemical Society, Perkin Transactions 1, 2001(18): p. 2109-2135.

3.   Barltrop, J.A. and P. Schofield, *Photosensitive protecting groups.* Tetrahedron Letters, 1962: p. 697-9.

4.   Kaplan, J.H., B. Forbush, 3rd, and J.F. Hoffman, *Rapid photolytic release of adenosine 5'-triphosphate from a protected analogue: utilization by the Na:K pump of human red blood cell ghosts.* Biochemistry, 1978. 17(10): p. 1929-35.

5.   Pelliccioli Anna, P. and J. Wirz, *Photoremovable protecting groups: reaction mechanisms and applications.* Photochemical & photobiological sciences: Official journal of the European Photochemistry Association and the European Society for Photobiology, 2002. 1(7): p. 441-58.

6.   Goeldner, M.G., Richard, *Dynamic Studies in Biology* Handbook/Reference Book, 2005. 1. Edition: p. 557 Pages.

7.   Adams, S.R. and R.Y. Tsien, *Controlling cell chemistry with caged compounds.* Annual Review of Physiology, 1993. 55: p. 755-84.

8.   Marriott, G., *Caged Compounds. [In: Methods Enzymol., 1998; 291].* 1998. 529 pp.

9.   Gurney, A.M. and H.A. Lester, *Light-flash physiology with synthetic photosensitive compounds.* Physiological Reviews, 1987. 67(2): p. 583-617.

10.   Mayer, G. and A. Heckel, *Biologically active molecules with a \"Light switch\".* Angewandte Chemie, International Edition, 2006. 45(30): p. 4900-4921.

11.   Nerbonne, J.M., *Caged compounds: tools for illuminating neuronal responses and connections.* Current Opinion in Neurobiology, 1996. 6(3): p. 379-386.

12.   McCray, J.A. and D.R. Trentham, *Properties and uses of photoreactive caged compounds.* Annual Review of Biophysics and Biophysical Chemistry, 1989. 18: p. 239-70.

13.   Giovannardi, S., L. Lando, and A. Peres, *Flash photolysis of caged compounds: casting light on physiological processes.* News in Physiological Sciences, 1998. 13(Oct.): p. 251-255.

14.   Pillai, V.N.R., *Photoremovable protecting groups in organic synthesis.* Synthesis, 1980(1): p. 1-26.

15.   Bochet, C.G., *Photolabile protecting groups and linkers.* Journal of the Chemical Society, Perkin Transactions 1, 2002(2): p. 125-142.

16.   Barltrop, J.A., P.J. Plant, and P. Schofield, *Photosensitive protective groups.* Chemical Communications (London), 1966(22): p. 822-3.

17.   Il'ichev Yuri, V., A. Schworer Markus, and J. Wirz, *Photochemical reaction mechanisms of 2-nitrobenzyl compounds: methyl ethers and caged ATP.* Journal of the American Chemical Society, 2004. 126(14): p. 4581-95.

18.   Abbruzzetti, S., et al., *Kinetics of Proton Release after Flash Photolysis of 1-(2-Nitrophenyl)ethyl Sulfate (Caged Sulfate) in Aqueous Solution.* J. Am. Chem. Soc., 2005. 127(27): p. 9865-9874.

19.   McCray, J.A., et al., *A New Approach to Time-Resolved Studies of ATP-Requiring Biological Systems: Laser Flash Photolysis of Caged ATP.* PNAS, 1980. 77(12): p. 7237-7241.

20.   Adams, S.R., J.P.Y. Kao, and R.Y. Tsien, *Biologically useful chelators that take up calcium(2+) upon illumination.* Journal of the American Chemical Society, 1989. 111(20): p. 7957-68.

21.   Blanc, A. and C.G. Bochet, *Bis(o-nitrophenyl)ethanediol: A Practical Photolabile Protecting Group for Ketones and Aldehydes.* Journal of Organic Chemistry, 2003. 68(3): p. 1138-1141.

22.   Pirrung, M.C., et al., *Pentadienylnitrobenzyl and Pentadienylnitropiperonyl Photochemically Removable Protecting Groups.* Journal of Organic Chemistry, 1999. 64(14): p. 5042-5047.

23.   Sheehan, J.C., R.M. Wilson, and A.W. Oxford, *Photolysis of methoxy-substituted benzoin esters. Photosensitive protecting group for carboxylic acids.* Journal of the American Chemical Society, 1971. 93(26): p. 7222-8.

24.   Shi, Y., J.E.T. Corrie, and P. Wan, *Mechanism of 3',5'-Dimethoxybenzoin Ester Photochemistry: Heterolytic Cleavage Intramolecularly Assisted by the Dimethoxybenzene Ring Is the Primary Photochemical Step.* Journal of Organic Chemistry, 1997. 62(24): p. 8278-8279.

25.   Rock, R.S. and S.I. Chan, *Preparation of a Water-Soluble \"Cage\" Based on 3',5'-Dimethoxybenzoin.* Journal of the American Chemical Society, 1998. 120(41): p. 10766-10767.

26.   Rajesh, C.S., R.S. Givens, and J. Wirz, *Kinetics and Mechanism of Phosphate Photorelease from Benzoin Diethyl Phosphate: Evidence for Adiabatic Fission to an a-Keto Cation in the Triplet State.* Journal of the American Chemical Society, 2000. 122(4): p. 611-618.

27.   Stowell, M.H.B., et al., *Efficient synthesis of photolabile alkoxy benzoin protecting groups.* Tetrahedron Letters, 1996. 37(3): p. 307-10.

28.   Sheehan, J.C. and K. Umezawa, *Phenacyl photosensitive blocking groups.* Journal of Organic Chemistry, 1973. 38(21): p. 3771-4.

29.   Anderson, J.C. and C.B. Reese, *Photo-induced rearrangement involving aryl participation.* Tetrahedron Letters, 1962: p. 1-4.

30.   Givens, R.S. and C.-H. Park, *Hydroxyphenacyl ATP: a new phototrigger. V.* Tetrahedron Letters, 1996. 37(35): p. 6259-6262.

31.   Givens, R.S., et al., *New Phototriggers 9: p-Hydroxyphenacyl as a C-Terminal Photoremovable Protecting Group for Oligopeptides.* Journal of the American Chemical Society, 2000. 122(12): p. 2687-2697.

32.   Conrad, P.G., II, et al., *p-Hydroxyphenacyl Phototriggers: The Reactive Excited State of Phosphate Photorelease.* Journal of the American Chemical Society, 2000. 122(38): p. 9346-9347.

33.   Klan, P., M. Zabadal, and D. Heger, *2,5-Dimethylphenacyl as a New Photoreleasable Protecting Group for Carboxylic Acids.* Organic Letters, 2000. 2(11): p. 1569-1571.

34.   Klan, P., et al., *2,5-Dimethylphenacyl esters: A photoremovable protecting group for phosphates and sulfonic acids.* Photochemical & Photobiological Sciences, 2002. 1(11): p. 920-923.

35.   Shaginian, A., et al., *Light-Directed Radial Combinatorial Chemistry: Orthogonal Safety-Catch Protecting Groups for the Synthesis of Small Molecule Microarrays.* Journal of the American Chemical Society, 2004. 126(51): p. 16704-16705.

36.   Givens, R.S. and B. Matuszewski, *Photochemistry of phosphate esters: an efficient method for the generation of electrophiles.* Journal of the American Chemical Society, 1984. 106(22): p. 6860-1.

37. Schade, B., et al., *Deactivation Behavior and Excited-State Properties of (Coumarin-4-yl)methyl Derivatives. 1. Photocleavage of (7-Methoxycoumarin-4-yl)methyl-Caged Acids with Fluorescence Enhancement.* Journal of Organic Chemistry, 1999. 64(25): p. 9109-9117.

38. Kim, H.C., et al., *Two-photon-induced cycloreversion reaction of coumarin photodimers.* Chemical Physics Letters, 2003. 372(5,6): p. 899-903.

39. Furuta, T., et al., *Brominated 7-hydroxycoumarin-4-ylmethyls: photolabile protecting groups with biologically useful cross-sections for two photon photolysis.* Proceedings of the National Academy of Sciences of the United States of America, 1999. 96(4): p. 1193-200.

40. Fedoryak, O.D. and T.M. Dore, *Brominated Hydroxyquinoline as a Photolabile Protecting Group with Sensitivity to Multiphoton Excitation.* Organic Letters, 2002. 4(20): p. 3419-3422.

41. Zhu, Y., et al., *8-Bromo-7-hydroxyquinoline as a Photoremovable Protecting Group for Physiological Use: Mechanism and Scope.* Journal of the American Chemical Society, 2006. 128(13): p. 4267-4276.

42. Lukeman, M. and C. Scaiano Juan, *Carbanion-mediated photocages: rapid and efficient photorelease with aqueous compatibility.* Journal of the American Chemical Society, 2005. 127(21): p. 7698-9.

43. Atemnkeng, W.N., et al., *1-[2-(2-Hydroxyalkyl)phenyl]ethanone: A New Photoremovable Protecting Group for Carboxylic Acids.* Organic Letters, 2003. 5(23): p. 4469-4471.

44. Coleman, M.P. and M.K. Boyd, *S-Pixyl Analogues as Photocleavable Protecting Groups for Nucleosides.* Journal of Organic Chemistry, 2002. 67(22): p. 7641-7648.

45. Furuta, T., Y. Hirayama, and M. Iwamura, *Anthraquinon-2-ylmethoxycarbonyl (Aqmoc): a new photochemically removable protecting group for alcohols.* Org Organic letters, 2001. 3(12): p. 1809-12.

46. Singh Anil, K. and K. Khade Prashant, *Synthesis and photochemical properties of nitro-naphthyl chromophore and the corresponding immunoglobulin bioconjugate.* Bioconjugate chemistry, 2002. 13(6): p. 1286-91.

47. Ma, C., et al., *Photochemical cleavage and release of carboxylic acids from alpha-keto amides.* Organic letters, 2003. 5(1): p. 71-4.

48. Haugland, R.P., *The Handbook — A Guide to Fluorescent Probes and Labeling Technologies* 1996. (10th Edition) http://probes.invitrogen.com/handbook/sections/0503.html.

49. Li, G. and L. Niu, *How Fast Does the GluR1Qflip Channel Open?* Journal of Biological Chemistry, 2004. 279(6): p. 3990-3997.

50. Kandler, K., L.C. Katz, and J.A. Kauer, *Focal photolysis of caged glutamate produces long-term depression of hippocampal glutamate receptors.* Nature Neuroscience, 1998. 1(2): p. 119-123.

51. Li, W.-h., et al., *Cell-permeant caged InsP3 ester shows that Ca2+ spike frequency can optimize gene expression.* Nature (London), 1998. 392(6679): p. 936-941.

52. Soeller, C., et al., *Application of two-photon flash photolysis to reveal intercellular communication and intracellular Ca2+ movements.* Journal of biomedical optics, 2003. 8(3): p. 418-27.

53. Svoboda, K., D.W. Tank, and W. Denk, *Direct measurement of coupling between dendritic spines and shafts.* Science (Washington, D. C.), 1996. 272(5262): p. 716-19.

54. Merrifield, R.B., *Solid phase peptide synthesis. I. The synthesis of a tetrapeptide.* Journal of the American Chemical Society, 1963. 85(14): p. 2149-54.

55. Endo, M., et al., *Design and synthesis of photochemically controllable caspase-3.* Angewandte Chemie, International Edition, 2004. 43(42): p. 5643-5645.

56. Hahn Michael, E. and W. Muir Tom, *Photocontrol of Smad2, a multiphosphorylated cell-signaling protein, through caging of activating phosphoserines.* Angewandte Chemie (International ed. in English), 2004. 43(43): p. 5800-3.

57. Hansen, K.C., et al., *A Method for Photoinitiating Protein Folding in a Nondenaturing Environment.* Journal of the American Chemical Society, 2000. 122(46): p. 11567-11568.

58. Fodor, S.P., et al., *Light-directed, spatially addressable parallel chemical synthesis.* Science FIELD Full Journal Title:Science, 1991. 251(4995): p. 767-73.

59. Goppert-Mayer, M., *Elementary processes with two quantum jumps.* Annalen der Physik (Berlin, Germany), 1931. 9: p. 273-94.

60. Kaiser, W. and C.G.B. Garrett, *Two-photon excitation in CaF2:Eu++.* Physical Review Letters, 1961. 7: p. 229-31.

61. Shen, T., *A study on 6-hydroxyfluorone using a modified PPP-CI method.* Dyes and Pigments, 1987. 8(5): p. 375-80.

62. Warren, S., *Organic Synthesis: The Disconnection Approach.* 1982. 391 pp.

63. Shi, J., X. Zhang, and D.C. Neckers, *Xanthenes: fluorone derivatives. I.* Journal of Organic Chemistry, 1992. 57(16): p. 4418-21.

64. Neckers, D.C. and J. Shi, *Preparation of fluorone and pyronine Y derivatives as fluorescers.* 1992, (Spectra Group Ltd. Inc., USA). Application: EP EP. p. 24 pp.

65. Neckers, D.C. and J. Shi, *Preparation of fluorone and pyronin-Y derivatives as photoinitiators and fluorescent dyes.* 1995, (Spectra Group Ltd., Inc., USA). Application: WO. p. 61 pp.

66. Neckers, D.C. and J. Shi, *Fluorone and pyronin Y derivatives.* 1995, (Spectra Group Limited, Inc., USA). Application: US US. p. 18 pp Cont -in-part of U S Ser No 881, 048, abandoned.

67. Baeyer, A., Chem Ber., 1871. 5: p. 255.

68. Sen, R.N. and N.N. Sinha, *Condensations of aldehydes with resorcinol and some other aromatic hydroxy compounds.* Journal of the American Chemical Society, 1923. 45: p. 2984-96.

69. Pope, F.G. and H. Howard, *Fluorones.* Journal of the Chemical Society, Transactions, 1910. 97: p. 1023-8.

70. Amat-Guerri, F., et al., *Structures of molecular and ionic forms of succinylfluorescein in solution and in the solid state.* Journal of Chemical Research, Synopses, 1988(6): p. 184-5.

71. Briggs, S. and F.G. Pope, *Succinylfluorescein and its derivatives.* Journal of the Chemical Society, Transactions, 1923. 123: p. 2934-43.

72. Amat-Guerri, F., et al., *Application of factor analysis to the study of the forms of succinylfluorescein present in buffer solutions in aqueous methanol.* Talanta, 1989. 36(6): p. 704-7.

73. Bhatt, M.V. and S.U. Kulkarni, *Cleavage of ethers.* Synthesis, 1983(4): p. 249-82.

74. Ranu, B.C. and S. Bhar, *Dealkylation of ethers. A review.* Organic Preparations and Procedures International, 1996. 28(4): p. 371-409.

75. Ornstein, P.L., et al., *2-Substituted (2SR)-2-Amino-2-((1SR,2SR)-2-carboxycycloprop-1-yl)glycines as Potent and Selective Antagonists of Group II*

Metabotropic Glutamate Receptors. 1. Effects of Alkyl, Arylalkyl, and Diarylalkyl Substitution. J. Med. Chem., 1998. 41(3): p. 346-357.

76.   Kulkarni, N.A., N.A. Kudav, and A.B. Kulkarni, *Sodium borohydride reduction of xanthones.* Indian Journal of Chemistry, 1975. 13(8): p. 856-7.

77.   Snieckus, V., *Directed ortho metalation. Tertiary amide and O-carbamate directors in synthetic strategies for polysubstituted aromatics.* Chemical Reviews (Washington, DC, United States), 1990. 90(6): p. 879-933.

78.   Nishino, H., et al., *Manganese(III)-mediated carbon-carbon bond formation in the reaction of xanthenes with active methylene compounds.* J. Org. Chem., 1992. 57(13): p. 3551-3557.

79.   Poronik, E.M., et al., *Substituted xanthylocyanines. 1. Dyes with 3,6-dimethoxyxanthylium nucleus.* Zhurnal Organichnoi ta Farmatsevtichnoi Khimii, 2004. 2(4): p. 38-42.

80.   Rochlin, E. and Z. Rappoport, *Stable simple enols. 31. Substituted xanthenylidene enols. The importance of b-Ar-C:C conjugation in the stabilization of aryl-substituted enols.* Journal of the American Chemical Society, 1992. 114(1): p. 230-41.

81.   Dradi, E. and G. Gatti, *Proton and carbon-13 nuclear magnetic resonance spectra of heteroaromatic carbocations. Xanthylium ions.* Journal of the American Chemical Society, 1975. 97(19): p. 5472-6.

82.   Evans, J.J., et al., *Reactions of 3,6-diethoxyxanthen-9-one with alkylaluminum compounds.* Australian Journal of Chemistry, 1975. 28(3): p. 519-23.

83.   Zimmerman, H.E. and E.E. Nesterov, *Quantitative Cavities and Reactivity in Stages of Crystal Lattices: Mechanistic and Exploratory Organic Photochemistry.* Journal of the American Chemical Society, 2002. 124(11): p. 2818-2830.

84.   Landvatter, S.W. and J.A. Katzenellenbogen, *Nonsteroidal estrogens: synthesis and estrogen receptor binding affinity of derivatives of (3R*,4S*)-3,4-bis(4-hydroxyphenyl)hexane (hexestrol) and (2R*,3S*)-2,3-bis(4-hydroxyphenyl)pentane (norhexestrol) functionalized on the side chain.* Journal of Medicinal Chemistry, 1982. 25(11): p. 1300-7.

85.   Ohno, M., et al., *Development of Dual-Acting Benzofurans for Thromboxane A2 Receptor Antagonist and Prostacyclin Receptor Agonist: Synthesis, Structure-Activity Relationship, and Evaluation of Benzofuran Derivatives.* Journal of Medicinal Chemistry, 2005. 48(16): p. 5279-5294.

86.   Hoefle, G., W. Steglich, and H. Vorbrueggen, *New synthetic methods. 25. 4-Dialkylaminopyridines as acylation catalysts. 4. Puridine syntheses. 1. 4-Dialkylaminopuridines as highly active acylation catalysts.* Angewandte Chemie, 1978. 90(8): p. 602-15.

87.   Neises, B. and W. Steglich, *4-Dialkylaminopyridines as acylation catalysts. 5. Simple method for the esterification of carboxylic acids.* Angewandte Chemie, 1978. 90(7): p. 556-7.

88.   Williamson, M.P. and C.E. Griffin, *Three- and four-bond phosphorus-31-proton coupling constants and geminal proton nonequivalence in ethyl esters of phosphorus acids.* J. Phys. Chem., 1968. 72(12): p. 4043-4047.

89.   Jennings, W.B., *Chemical shift nonequivalence in prochiral groups.* Chemical Reviews (Washington, DC, United States), 1975. 75(3): p. 307-22.

90.   McOmie, J.F.W., M.L. Watts, and D.E. West, *Demethylation of aryl methyl ethers by boron tribromide.* Tetrahedron, 1968. 24(5): p. 2289-2292.

91.   Shi, J., X.P. Zhang, and D.C. Neckers, *Xanthenes: fluorone derivatives II.* Tetrahedron Letters, 1993. 34(38): p. 6013-16.

92.   Gallagher, M.J. and I.D. Jenkins, *Stereochemical aspects of phosphorus chemistry.* Topics in Stereochemistry, 1968. 3: p. 1-96.
93.   Finnegan, R.A. and K.E. Merkel, *NMR solvent shift data for methoxylated xanthones.* Journal of Pharmaceutical Sciences, 1977. 66(6): p. 884-6.
94.   Westerman, P.W., et al., *Carbon-13 NMR study of naturally occurring xanthones.* Organic Magnetic Resonance, 1977. 9(11): p. 631-6.
95.   Gampp, H., et al., *Calculation of equilibrium constants from multiwavelength spectroscopic data - II SPECFIT: two user-friendly programs in BASIC and standard FORTRAN 77.* Talanta, 1985. 32(4): p. 257-64.

7. Appendix

Abbreviation Index

A	absorption
Φ	quantum yield
1PE	one-photon excitation
2D	two-dimensional
2-NB	2-nitrobenzyl group
2PE	two-photon excitation
3D	three-dimensional
5-HT	serotonin
ACh	acetylcholine
AOC	allyloxycarbonyl group
APT	attached proton test
Aqmoc	anthrachinon-2-ylmethoxy-group
ATP	adenosine triphosphate
BAPTA	(1,2-bis(2-aminophenoxy)ethane-*N,N,N′,N′*-tetraacetic acid
BCMB	3',5'-bis(carboxymethoxy)benzoin-group
b	broad
BH_3	borane
Bhc	bromo-7-hydroxycoumarin-4-yl-methyl group
BHQ	8-bromo-7-hydroxyquinoline-group
Bnz	benzoin group
Boc	*t*-butyloxycarbonyl-group
cAMP	cyclic Adenosine Monophosphate
cGMP	cyclic Guanosin Monophosphate
cNMP	cyclic Nucleotides Monophosphate
d	doublet (multiplicity in NMR spectroscopy)
δ	chemical shift
DA	dopamine
DAG	diacylglycerol
DANP	2-(dimethylamino)-5-nitrophenol-group
DDQ	2,3-dichloro-5,6-dicyanobenzoquinone
decomp.	decomposition
DEPT	distortionless enhancement by polarization transfer
DFT	density functional theory
DMAP	4-dimethylaminopyridine
DMB	3', 5'-dimethoxybenzoin-group
DMF	dimethyl formamide
DMG	direct metalation group
DMNB	dimethoxy-nitrobenzene
DMP	3,5-dimethylphenacyl-group
DMS	dimethyl sulphate
DMSO	dimethyl sulfoxide
DNA	deoxyribonucleic acid

ε	molar extinction coefficient
e.g.	*exempli gratia* (= for instance)
ECF	extracellular fluid
EDTA	ethylendiamine tetraacetic acid
EGTA	3,12-bis(carboxymethyl)-6,9-dioxa-3,12-diazatetradecanedioic acid disodium salt
EI	electron impact
ESI	electrospray ionisation
et al.	*et. alia* (= and others)
FAB	fast atom bombardment
FGI	functional group interconversion
Fig(s).	figure(s)
Fmoc	9-fluorenylmethyloxycarbonyl-group
FRAP	fluorescence recovery after photobleaching
γ	mass concentration
GABA	γ-aminobutyric acid
GM	1 Göppert-Mayer = $10\text{-}50$ cm^3 s photon^{-1}
GPCR	G-protein-coupled receptors
GTP	guanosin triphosphate
HAPE	1-[2-(2-hydroxyalkyl)phenyl]ethanone-group
HCM	7-hydroxycoumarin-4-yl-methyl-group
HFA	3-hydroxy-6-fluorone anion
HMBC	heteronuclear multiple bond correlation
HMQC	heteronuclear multiple quantum coherence
HOMO	highest occupied molecular orbital
HPLC	high performance liquid chromatography
HWE	Horner-Wadsworth-Emmons
IgG	immunoglobulin
in lieu of	instead of
InsP3	inositol trisphosphate
IR	infrared spectroscopy
IR	infrared radiation
KCN	potassium cyanide
KHMDS	potassium bis(trimethylsilyl)amide
λ	wavelength
LG	leaving group
LTD	long-term depression
LTP	long-term potentiation
LUMO	lowest unoccupied molecular orbital
m	multiplet (multiplicity in NMR spectroscopy)
M.p.	melting point
m/z	mass per charge
MALDI	matrix-assisted laser desorption/ionization
MES	2-(*N*-morpholino)ethanesulfonic acid
MS	mass spectroscopy
NA	norepinephrine
NaH	sodium hydride
NCST	none codon suppression technique
NDBF	nitrodibenzofurane
NMR	nuclear magnetic resonance

NOESY	nuclear Overhauser enhancement spectroscopy
NPE	nitrophenylethyl-group
NPP	2-(2-nitrophenyl)propyl group
NPPoc	(nitrophenylpropyloxy)carbonyl group
OA	oxyallyl valence isomer
Ox	oxidation
PAF	photoactivation of fluorescence
pH	pH-value
pHP	p-hydroxyphenacyl-group
pK_a	pK_a-value
PKC	protein kinase C
PM3	parameterized model number 3
q	quartet (multiplicity in NMR spectroscopy)
RASM	readily available starting materials
RC	ring closure
Red	reduction
rel. int.	relative intensity
R_f	retention factor
s	singlet (multiplicity in NMR spectroscopy) or second (unit of the time)
sh	shoulder
SD	standard deviation
SDD	spirodienedione
S-pixyl	9-phenylthioxanthyl-group
SPS	solid phase synthesis
t	triplet (multiplicity in NMR spectroscopy) or time
THF	tetrahydrofuran
TLC	thin layer chromatography
TM	target molecule
TMSCN	trimethylsilyl cyanide
TRIR	time-resolved infrared spectroscopy
t-RNA	transfer ribonucleic acid
UV/Vis	ultraviolet/visible
vide infra	see below
vide supra	see above
δ_μ	two-photon absorption cross section

CURRICULUM VITAE

Dipl.-Ing. Jürgen Wintner

Address:	Gmöserstrasse 23, A-4663 Laakirchen, Austria
Phone:	+41(0)612673847
	+43(0)69912187608
Email:	juergen.wintner@gmail.com
Date of Birth:	March 31, 1973
Place of Birth:	Gmunden, Upper Austria

Education:

November 1, 2003	Employment as Assistant at the University of Basel
March 1, 2003	Inscription at the University of Basel, Switzerland
November 22, 2002	University Diploma in Technical Chemistry ("Dipl.-Ing." similar to Master of Technology)
1994 - 2002	Studies of Technical Chemistry at the Johannes Kepler University in Linz, Upper Austria
October 93 - May 94	Military Service in Salzburg
June 24, 1993	High School Diploma in Chemical Engineering
1988 - 1993	Higher School for Chemical Engineering in Wels, Upper Austria
1987 - 1988	School for Chemical Engineering in Wels, Upper Austria
1983 - 1987	Secondary School in Laakirchen, Upper Austria
1979 - 1983	Primary School in Laakirchen, Upper Austria

Professional Experience:

Several Summer-Jobs in Chemical Plants and Laboratories   **1994 - 2002**

Others:

Regulatory Affairs Course at the Center of Pharmaceutical Sciences (Uni Basel - ETH Zürich)   **26 - 28.3.2006**

Pharmaceutical Development and Production Course at the Center of Pharmaceutical Sciences (Uni Basel - ETH Zürich)   **13 - 14 and 19 - 21.9.2006**

Quality and GMP Course at the Center of Pharmaceutical Sciences (Uni Basel - ETH Zürich)   **13 - 15 and 20 - 21.3.2006**

Projectmanagement at the Economical Faculty of the University Basel   **WS 2005/06**

Supramolecular and Superdupermolecular Control of Chemical Reactivity lecture by
Dr. Nicholas Turro, Ciba Spezialitätenchemie AG, Basel   **17.11. 2004**

3rd cycle Summer School in Physical Chemistry „Computational Chemistry", CH- Manno / Ticino   **20 - 24.10. 2004**

Advanced laboratory „Inorganic Chemistry" at the L. F. University Innsbruck
                                                                                       Dez. bis Jän. 2000/01

Additional Skills:	Windows 95/98/2000/XP, MS Office, Internet, Chemoffice, Scifinder, MDL Crossfire Commander, Gaussian, Hyperchem, MicrocalOrigin, Maple and Matlab

Interests:

Sport:	Skiing, Hiking and Mountain-Biking
Others:	Music, Cooking